

**Nuclear Waste Policy Act**  
(Section 113)

GEOENGINEERING

B

*Consultation Draft*



**Site Characterization  
Plan**

**Yucca Mountain Site, Nevada Research  
and Development Area, Nevada**

**Volume I**

PART A

January 1988

U.S. Department of Energy  
Office of Civilian Radioactive Waste Management  
Washington, DC 20585

8802190049 880131  
PDR WASTE PDR  
WM-11

Ac4  
51928

# CONSULTATION DRAFT

## Chapter 2

### GEOENGINEERING

#### INTRODUCTION

Chapter 2 summarizes the available information on the geoengineering properties that contribute to the demonstration that performance objectives and design criteria will be met. The performance objectives and design criteria for the geologic operations area are described in 10 CFR Part 60.

The Nevada Nuclear Waste Storage Investigations (NNWSI) Project has assembled an issues hierarchy, as defined in Sections 8.1 and 8.2, which provides a structured approach to defining information that must be obtained to demonstrate that the performance objectives will be met. The reader is referred to those sections for details about the issue hierarchy structure and content. The issues, and subsidiary information needs; and characterization programs and subsidiary investigations that contribute to individual issues, are described in detail in Section 8.3.

The list of specific issues that use geoengineering data as input is extensive. The relationship between the issues and specific geoengineering parameters is elucidated in Section 2.9.3. These parameters form the basis for discussion for most of the remainder of Chapter 2.

The behavior of tuff as an engineering material must be understood to design, license, construct, operate, and decommission a repository at Yucca Mountain. The uniqueness of a repository design (when compared with mines or tunnels) results from the addition of heat and radiation to the rock mass and from the need for long-time stability. The heat produces changes in the preexisting temperature field, which in turn changes the state of stress and possibly the distribution and flow of ground water within the rock mass. Two important tasks must be completed to understand the behavior of tuff:

1. Identify and understand the geotechnical phenomena, properties, and parameters important to the design and evaluation of a repository system.
2. Develop the data base for these required geotechnical phenomena, properties, and parameters to form the basis for technical decisions to be made in site evaluation, repository and waste package design, and performance assessment.

The remainder of this introduction is devoted to the following:

1. Delineating the quantities that must be known to evaluate thermal, mechanical, and hydrothermal phenomena.
2. Identifying the specific properties or measured values that are needed to make or to evaluate the required predictions.

## CONSULTATION DRAFT

3. Delineating the strategy being used for developing the data base of geotechnical properties.
4. Summarizing the philosophy of sample selection for laboratory testing.
5. Summarizing the status of the geotechnical measurement activities.
6. Identifying conceptual models for which the data provide input.

### REPOSITORY CONDITIONS TO BE EVALUATED

Demonstration that a repository will be in compliance with regulatory criteria must rely on analyses of the behavior of the repository system as a whole and its subsystems (e.g., the waste package). Such analyses must treat thermal, mechanical, hydrologic, and geochemical effects, and coupled effects in relation to the emplacement, retrieval, long-term isolation, and containment of the radioactive waste. The relationship between the regulatory criteria and repository design and the resulting definition of data needs are discussed in Section 6.1.1.

Input data necessary for performing the analyses will vary with the approach selected to resolve an issue (see Section 8.2 for a general discussion of the issue resolution strategy), the type of behavior being addressed (e.g., thermal or mechanical), the amount of detail or complexity in each analysis, and the scale of the problem both in space and in time. As the understanding of the system improves, data needs and analysis techniques may change or be refocused to increase the quality and relevance of analyses of system behavior.

The demonstration of compliance will require, among other things, a minimum ground-water travel time over some designated distance from the repository. Calculation of this travel time requires input data on the distribution and characterization of fractures (Chapter 1) and porosity (Sections 2.4.2.4 and 2.4.3) and the distribution and movement of water within the fractures and pores (Chapter 3). Knowledge of ground-water movement is also implicit in the determination of radionuclides release rates. The effects of variations in temperature and pressure on these data must then be estimated to calculate the effect that a waste repository will have on water movement and thus on radionuclide movement and release rates.

The stability of waste emplacement holes will play a role in the estimation of radionuclide releases through estimates of waste container integrity and containment capability. Thus, the potential for movement of rock surrounding the waste canister or for coupled hydrologic and thermal effects on waste container corrosion (Chapter 7) must be assessed; the data needs in this area are discussed in Section 8.3.4.2.

Demonstration of compliance with the retrievability requirement of a repository involves the retrievability of the waste, which in turn requires demonstration that mined openings and waste emplacement holes remain usable during construction, operation, caretaker period, and possibly waste

## CONSULTATION DRAFT

retrieval. This time period currently is estimated to be 84 yr (Flores, 1986). Such a demonstration requires knowledge of how the rock will respond to the presence of a combination of mined openings and waste-generated heat over long periods of time.

To quantify the effects of the heat generated by the waste, temperatures must be calculated. The resulting stresses and displacements in the rock must be calculated to assess the opening stability, waste container integrity, and the nature of fracture and porosity distribution as a function of time and location. This last consideration will also affect the development of a zone of material around the repository that has different fracture characteristics than those of the remainder of the rock mass. This is a consideration in the evaluation of the extent of the disturbed zone. The interaction between the repository, including the zone of material with different fracture characteristics, and the hydrologic system must be assessed to obtain realistic estimates of radionuclide releases.

The application of individual data needs are summarized in the following lists. No attempt has been made to set priorities for the various applications.

Analyses of rock temperature are needed:

1. To establish the acceptable gross thermal loading within the repository horizon, accounting for constraints on repository and waste container design (Section 8.3.4.2).
2. To evaluate the stability of pillars, waste emplacement holes, and mined openings (Section 8.3.1.15).
3. To determine the waste container environment (Chapter 7).
4. To establish the ventilation requirements (Chapter 6).
5. To evaluate the relative importance of different physical mechanisms of mechanical deformation (Sections 2.1.2.3.1.3 and 2.1.2.3.1.4).
6. To conduct tradeoff studies for such alternatives as horizontal versus vertical waste emplacement, ramp versus shaft as a means of underground access, age of the waste to be emplaced, the size of the waste package, the spacing of the canisters, and the spacing of the drifts (Section 8.3.4.2).
7. To evaluate the potential for thermally induced water movement (Section 2.7.2).

Stress and displacement analyses are needed:

1. To perform detailed analyses of room size, shape, spacing, and support requirements (Section 8.3.1.15).
2. To evaluate emplacement hole stability (including liner requirements, if any, for stability) (Section 8.3.4.2).

## CONSULTATION DRAFT

3. To determine the repository horizon spatial extent acceptable for waste emplacement (particularly with regard to lithophysae content and gross thermal loading) (Section 8.3.1.4, 8.3.1.15).
4. To evaluate shaft designs with respect to opening stability and liner loading (Section 8.3.1.15).
5. To evaluate the amounts and consequences of far-field displacements (Section 8.3.2.2).
6. To evaluate potential coupling between induced stresses and displacements and the movement of ground water (Section 8.3.4.2).

Analyses of the quantities and mechanisms of thermally induced water migration are needed:

1. To accurately calculate rock temperatures (Section 8.3.1.15).
2. To establish ventilation requirements (Chapter 6).
3. To define the waste container environment (Chapter 7).
4. To assess the impact of the thermal pulse on ground-water travel time and thus on radionuclide releases (Section 8.3.5.12).

Details of the relationships between the analyses mentioned previously and the design process are provided in Chapters 6 and 7.

### PROPERTIES AND INITIAL CONDITIONS TO BE MEASURED

This section discusses the properties and initial conditions that must be measured to predict temperatures, stresses, displacements, and thermally induced water movement and specifies the sections of this document that present relevant data. Although the discussion is divided into three categories (temperature, stress and displacement, and water migration), these categories are not totally independent. Coupled processes such as temperature effects on mechanical properties or the effects of water migration on temperature will be an integral part of the response of the rock mass to a repository.

The initial condition required for the calculation of temperature fields is the distribution of temperatures before waste emplacement. Such data are presented in Section 1.3.2.5. This preexisting temperature field will be altered by the construction and operation of the repository including the emplacement of heat-producing waste. The rock properties necessary to calculate the conduction of heat away from the waste are the thermal conductivity (Sections 2.4.2.1, 2.5.2, and 2.5.3), the heat capacity (Sections 2.4.2.2, 2.5.2, and 2.5.3), and the density (Sections 2.4.2.4, 2.5.2, and 2.5.3). Heat transfer also could occur by the convection of water in the pores and fractures, as discussed in Section 2.7.2.

## CONSULTATION DRAFT

The prediction of stresses and displacements around a repository first requires a knowledge of the mechanical behavior of the rock mass. Different deformation models require different properties as input. Treating the rock as an elastic material requires data on the elastic properties (e.g., Young's modulus and Poisson's ratio; Sections 2.1.2.2, 2.3.2, and 2.3.3) for the prediction of displacements. At elevated temperatures or over long times, the rock may exhibit inelastic deformation rather than the elastic behavior expected to predominate over short time intervals (Section 2.1.2.3.1.4). In addition, the strength of the rock (Section 2.1.2.3) may be exceeded in some locations, which would result in stresses and displacements different from those resulting from prefailure deformation.

Stresses in the rock will have as an initial condition the state of stress before the excavation of the repository and the emplacement of waste. Determination of this preexisting stress state is discussed in Sections 1.3.2.3 and 2.6. Stresses induced by the excavation and by the temperature field will be superimposed on this preexisting stress state; the magnitude of excavation and thermally induced stresses will depend on the spatial location and on the deformation behavior of the rock. In an elastic continuum model, thermal stresses will be a function of the elastic modulus and Poisson's ratio (Sections 2.1.2.2, 2.3.2, and 2.3.3), and of the coefficient of thermal expansion (Sections 2.4.2.3, 2.5.2, and 2.5.3).

The mechanical behavior of both the intact rock and the fractures contributes to the mechanical behavior of the rock mass. Thus, for a given model of rock deformation, the behavior of both components must be understood. Fracture properties are discussed in Section 2.2, intact rock properties in Section 2.1, and the mechanical behavior of the rock mass in Section 2.3.

The prediction of thermally induced water migration requires as an initial condition an understanding of water movement for preexisting temperature (and stress) conditions. Data pertaining to this topic are presented in Chapter 3. The response of the water to the thermal pulse is discussed in Section 2.7.2.

As mentioned earlier, temperatures, stresses, displacements, chemistry, and water movement are all coupled in a repository environment. The effects of this coupling on rock properties are included in discussions of individual properties. The effects of the chemical environment and radiation on the properties of the rock in the vicinity of the waste container are addressed in Chapter 7.

### DATA BASE DEVELOPMENT--HISTORY AND STRATEGY

A strategy for the development of the geoenvironmental properties data base needed for technical decisions has been developed and implemented in the NNWSI Project. The strategy relies primarily on data determined in laboratory tests that are then evaluated and later confirmed in field tests in G-Tunnel and in the exploratory shaft facility.

## CONSULTATION DRAFT

The laboratory data presently available consist of test results on core samples from the following locations (Figure 2-1):

1. Coreholes at Yucca Mountain (UE-25a#1, UE-25b#1, USW G-1, USW G-2, USW GU-3, and USW G-4).
2. An underground test facility (G-Tunnel) located in Rainier Mesa.
3. Topopah Spring Member outcrops at Busted Butte.

When the NNWSI Project began, no suitable site-specific samples were available for studying the effects of parameters like temperature and pressure on the mechanical properties of tuff. Both welded and nonwelded tuffs are exposed in G-Tunnel at Rainier Mesa and were used in early studies of parameter effects. Laboratory testing on samples from G-Tunnel also has been performed to support in situ testing in the tunnel. These data have been included in the existing geengineering properties data base because the tuffs at G-Tunnel are similar (Section 2.8.2) to those found at Yucca Mountain. Data on the properties of tuffs in G-Tunnel will be replaced by data specific to Yucca Mountain tuffs as such data become available.

Since the Topopah Spring Member was recommended as the repository horizon (Johnstone et al., 1984), testing has been performed on samples from outcrops of the Topopah Spring Member at Busted Butte. Large samples (about 0.5 m<sup>3</sup>) have been cored (up to 30 cm in diameter) for use primarily in measuring the effects of lithophysae on thermal and mechanical properties and for establishing the effect of sample size on the measured strength of the Topopah Spring Member. Examination of the properties of the lithophysae-rich material contributes to decisions regarding the volume of the Topopah Spring Member that is suitable for a repository, whereas the determination of sample-size effects enhances the ability to extrapolate laboratory test results to the rock mass in situ. Samples from Busted Butte also have been examined to determine whether surface weathering has changed the mineralogy, texture, or porosity from that found in underground samples to determine whether data from Busted Butte samples are representative of the upper lithophysal and immediately underlying lithophysal-poor zones of the Topopah Spring Member under Yucca Mountain (Price et al., 1985; Price et al., 1987).

An important aspect of the laboratory testing is confidence in the quality of the data on which design analyses and performance assessments are based. Test procedures, listed in Section 8.6.4, have been prepared for all the more routine (nondevelopmental) tests including thermal expansion, thermal conductivity, bulk and grain density, and uniaxial and triaxial compression testing. Where applicable, American Society of Testing and Materials (ASTM) Standard Test Procedures and International Society for Rock Mechanics (ISRM) procedures, as shown in Table 2-1, have been compared with the test procedures. In developmental tests, such as those for the measurement of either time-dependent thermal expansion coefficients or joint slip, detailed documentation of the test procedures is provided in the Technical Procedure relevant to each type of test.

A second part of the data base development has been the field testing program currently under way in welded and nonwelded tuff in G-Tunnel. The extent of the underground openings in the G-Tunnel rock mechanics facility

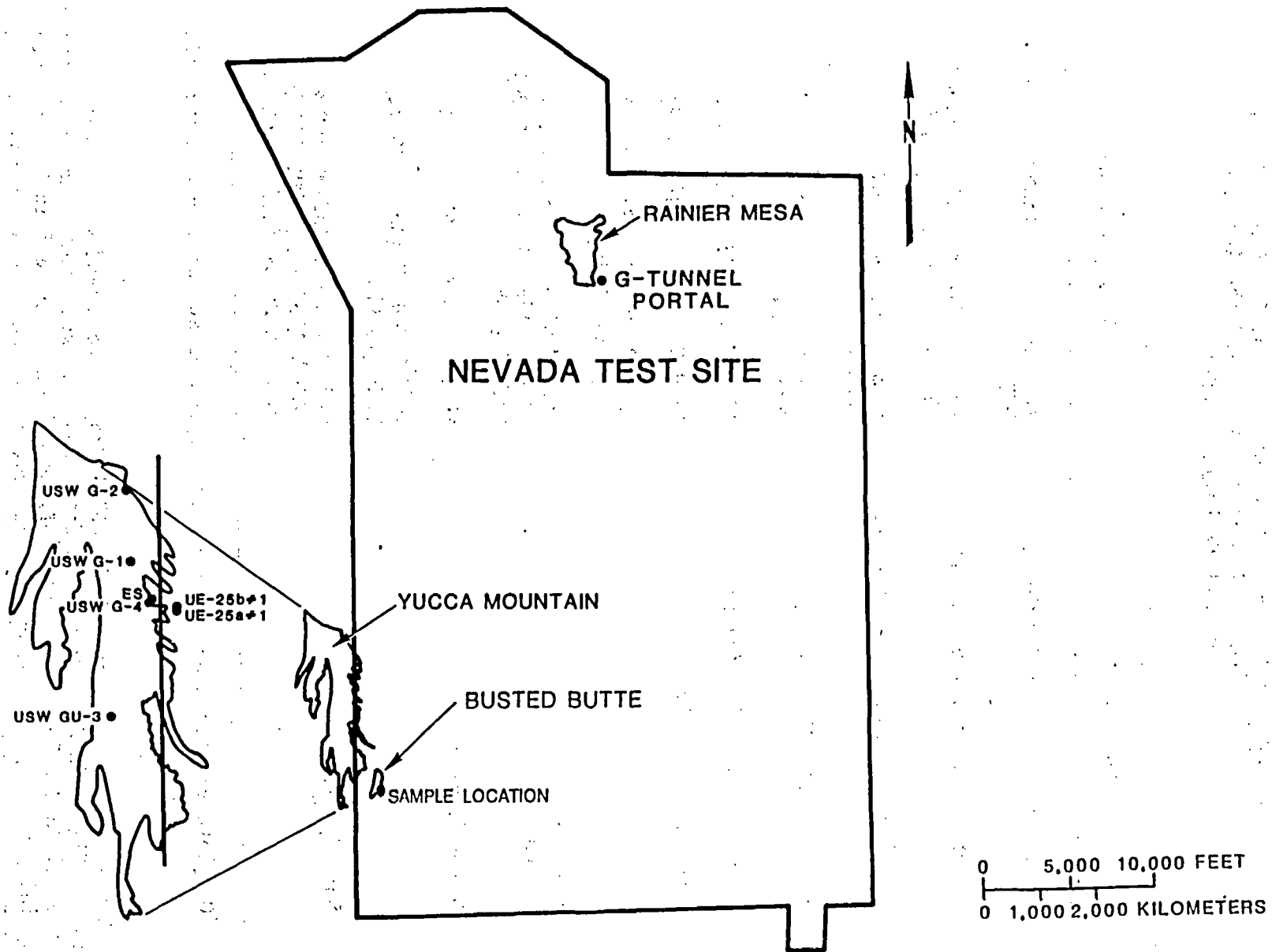


Figure 2-1. Locations of corehole samplings for the Nevada Nuclear Waste Storage Investigations Project.

CONSULTATION DRAFT

Table 2-1. Applicable test procedures from the American Society of Testing and Materials (ASTM) and the International Society for Rock Mechanics (ISRM)

Measurement	Test procedures <sup>a</sup>
Uniaxial compressive strength	ASTM D 2938-79 (ASTM, 1979b) ISRM (1979a)
Triaxial compressive strength	ASTM D 2664-80 (ASTM, 1980a) ISRM (Kovari et al., 1983)
Tensile strength (Brazilian test)	ASTM D 3967-81 (ASTM, 1981b) ISRM (1978)
Elastic properties (static)	ASTM D 3148-80 (ASTM, 1980b) ISRM (1979a)
Elastic properties (dynamic)	ASTM D 2845-83 (ASTM, 1983b)
Thermal conductivity	ASTM C 202-84 (ASTM, 1984)
Thermal expansion	ASTM E 228-71 (ASTM, 1971) (reapp. 1979)
Bulk density (paraffin coated)	ASTM C 97-83 (ASTM, 1983a) ASTM C 1188-83 (ASTM, 1983c) ISRM (1979b)
Grain density	ASTM C 135-66 (ASTM, 1966) (reapp. 1976) ASTM C 604-79 (ASTM, 1979a) ISRM (1979b)
Soil density	ASTM D 1556-82 (ASTM, 1982) ASTM D 1557-78 (ASTM, 1978) ASTM D 2922-81 (ASTM, 1981a)

<sup>a</sup>Complete citations are provided in references at the end of Chapter 2.

which was developed as part of the NNWSI Project rock mechanics program, is shown in Figures 2-2 and 2-3. The data from the experiments and observations in the welded Grouse Canyon Member of the Belted Range Tuff in G-Tunnel are especially valuable to the current design evaluation of the Topopah Spring Member emplacement horizon for the following reasons:

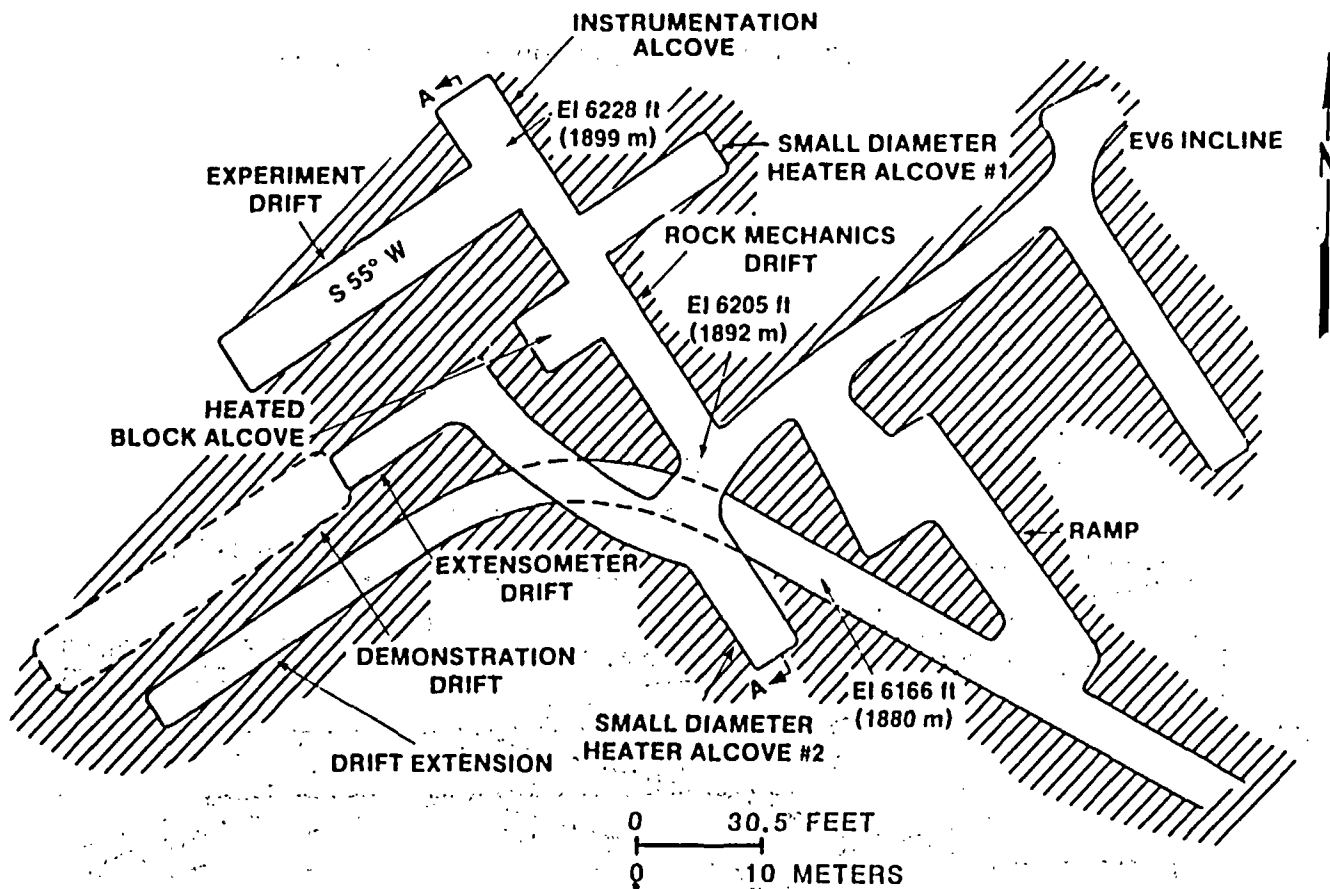


Figure 2-2. Plan view of G-Tunnel underground rock mechanics facility.

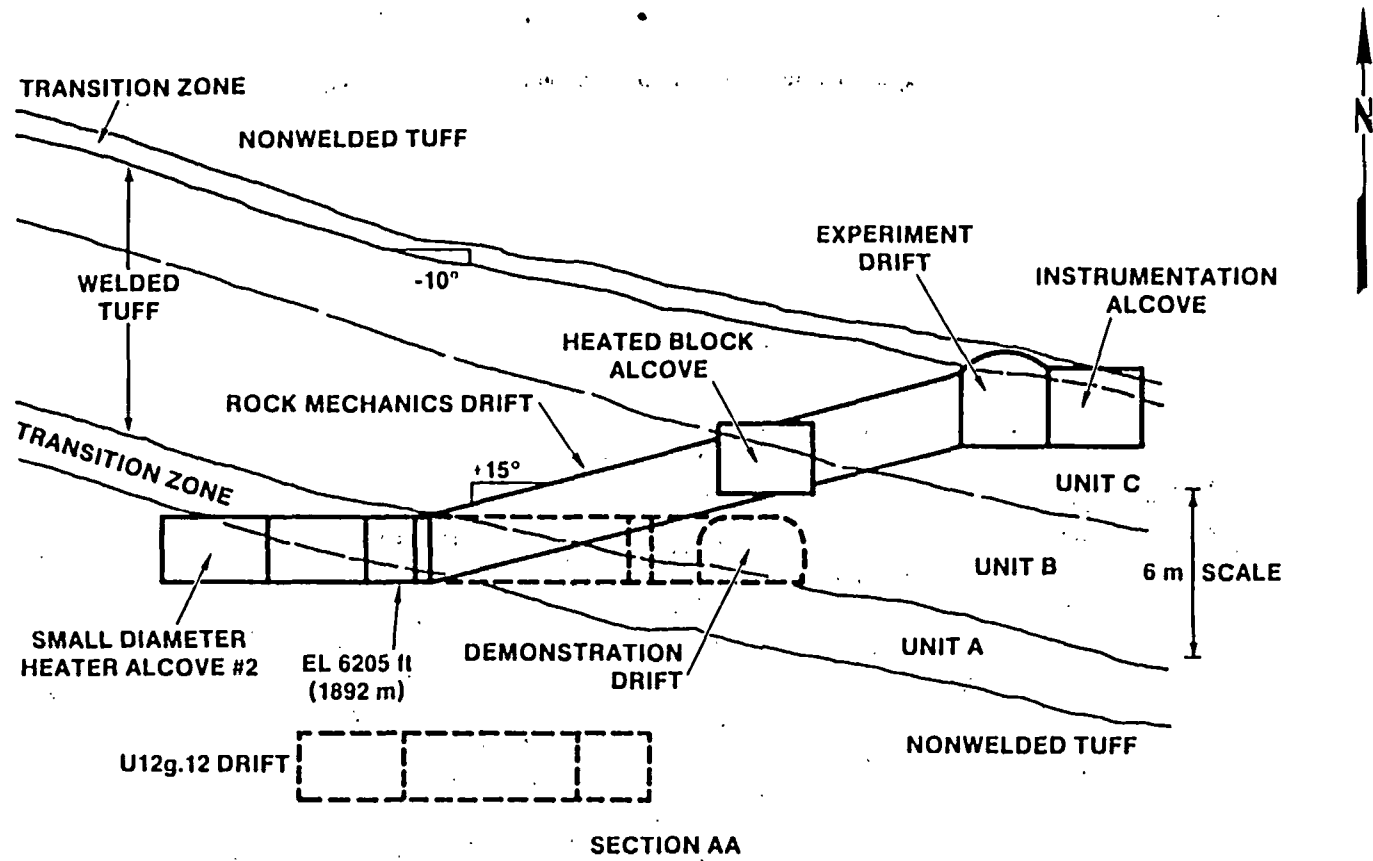


Figure 2-3. Elevation view of G-Tunnel underground facility.

## CONSULTATION DRAFT

1. The bulk, thermal, and mechanical properties of both formations are similar (Zimmerman et al., 1984b). (Lithophysae are, however, not present in the Grouse Canyon Member welded tuff in G-Tunnel. A detailed comparison of properties is presented in Section 2.8.)
2. The overburden loadings and opening dimensions (up to 5-m span) are similar (Tillerson and Nimick, 1984).
3. The degrees of saturation are similar for geoenineering purposes ( $0.65 \pm 0.19$  in the Topopah Spring Member (Montazer and Wilson, 1984) versus 0.6 to 0.9 in the Grouse Canyon Member (Zimmerman et al., 1984b)), however, for hydrologic purposes these differences may be significant.
4. The degree and nature of fracturing are similar (Langkopf and Gnirk, 1986).

Field data and observations (thermal conductivity, elastic moduli, strength, support requirements, room and borehole stability, motion on fractures, and water migration) obtained in G-Tunnel will be used as supporting data for site evaluations and repository conceptual design for Yucca Mountain.

The G-Tunnel tests also will allow development of measurement techniques and instrumentation evaluations before testing in the exploratory-shaft facility. As data are obtained from tests in the exploratory-shaft facility, these newer data will supplement, and will eventually replace, G-Tunnel data as input to the design and site evaluation processes.

The data gathered to date, as described in this chapter, have been used in preliminary performance assessment and design analyses. The testing in which the data originated may be classified as exploratory in the sense that an initial examination has been made of many of the geoenineering properties important to determination of compliance with regulatory criteria.

Future data gathering will be guided by issue resolution strategies and will focus on properties for which insufficient data are available or on properties that have been identified as potentially important by analysis but which have not yet been considered in the experimental program. Such interactions among the issue resolution strategies, experiments, and calculations will occur throughout the future of the repository program as the understanding of the system and the relevant physical processes becomes increasingly sophisticated.

Presently, the strategy for expansion of the data base, as designed to aid in resolution of issues discussed in Section 8.3, includes laboratory tests on material from, and field tests conducted in, the exploratory shaft facility as well as laboratory tests on material from new coreholes at Yucca Mountain. The resulting laboratory data will be used to confirm effects found to be important in previous tests as well as to aid in establishing the lateral variability of the properties of the Topopah Spring Member. The determination of lateral variability will allow design and performance

## CONSULTATION DRAFT

assessment analyses to be increasingly detailed and will permit the estimation of rock properties to be encountered in different portions of the repository area.

The field tests will increase confidence in the repository design by providing both direct measurements of rock mass properties as well as an opportunity to evaluate the coupled behavior resulting from excavation, mechanical, and thermal loadings predicted by thermal and structural computer models. In addition, field data will be used in the validation of computer models. A brief description of the geoenvironmental experiments planned for the exploratory-shaft facility is presented in Section 8.3.1.15.1.

Data gathering and interpretation activities, therefore, are planned to provide periodically updated values for material properties required for decisions that must be made throughout the design phase of the repository. These data will reflect steadily increasing quantities of site-specific and host-rock-specific information, and there will be an associated increase in confidence in the data. As exploratory shaft facility activities progress, an increasing amount of data will have been obtained directly from the rock mass rather than being inferred for the rock mass from laboratory measurements on cores, which should enhance confidence in the applicability of the data to the determination of compliance with regulatory criteria. In addition, the measured rock mass data will be specific to the Yucca Mountain site rather than having to infer such data based on field tests in G-Tunnel.

As an example of the implementation of the strategy, consider the timing and contribution of various laboratory and field tests to the development of recommended values for the geoenvironmental properties of the host rock, as shown in Figure 2-4. Currently, the data base consists of laboratory test results from samples from drillholes UE-25a#1, USW G-1, USW GU-3, USW G-4, and from Rainier Mesa. FY 1986 activities concentrated on adding the properties from laboratory tests of samples from drillhole USW G-2 and from outcrops of tuff at Busted Butte. Future input will include additional interpreted data from field tests conducted in G-Tunnel and from laboratory tests on cores obtained from additional coreholes and from the exploratory shafts. The interim products of this work will be values for the geoenvironmental properties of the rock mass based on data available at the time the design need is expressed (the scheduling of specific design milestones is discussed in Section 8.5). The final product of the work will be the recommended geoenvironmental properties (and their uncertainties) for the rock mass. The applicability of these laboratory-based rock mass properties to in situ material will have been examined by in situ tests and by observations made in the repository horizon during the exploratory shaft facility testing.

### SAMPLE SELECTION LOGIC

The procedures and philosophy used in sample selection for laboratory testing of cores from Yucca Mountain are important in assessing how representative the data base is of the in situ material. Within the NNWSI Project, this philosophy has evolved with time. Both the inherent sampling limitations (both procedural and lithological) and the progression of the philosophy are described in the following discussion.

YEAR	LABORATORY DATA	FIELD DATA	
1982	TUFF, RAINIER MESA DRILLHOLES UE-25a#1, USW G-1	BOREHOLE JACK TESTS IN SITU STRESS MEASURING SMALL DIAMETER HEATER TESTS	G-TUNNEL
	DRILLHOLE USW GU-3		
1983		HEATED BLOCK TEST	
1984	DRILLHOLE USW G-4	SMALL DIAMETER HEATER TEST PRESSURIZED SLOT TEST WELDED TUFF MINING EVALUATION	EXPLORATORY SHAFT FACILITY
	DRILLHOLE USW G-2		
	PARAMETRIC SENSITIVITY OF MECHANICAL PROPERTIES	SHAFT CONVERGENCE TESTING DEMONSTRATION BREAKOUT ROOM TESTING SEQUENTIAL DRIFT MONITORING PLATE LOADING MEASURING SLOT STRENGTH TEST CANISTER SCALE HEATER TEST SMALL SCALE HEATER TEST YUCCA MOUNTAIN BLOCK TEST	
	DATA FROM EXPLORATORY SHAFT FACILITY LATERAL BOREHOLES OR DRIFTS		

Figure 2-4. Data base development for host rock geoen지니어ing properties.

In general core from drillholes at Yucca Mountain is logged at the drill site, then transported to the core library at Mercury, Nevada, for storage. Some percentage of the core is wrapped and waxed at the drill site to preserve, as nearly as possible, the original moisture content of the rock as the core was removed from the ground. (The exact value of this original moisture content is not important in the determination of the properties discussed in Chapter 2 because the saturation state of the sample usually is changed before the measurement of thermal or mechanical properties.)

Several limitations to obtaining geoenvironmental property data have resulted from past coring procedures. Because the primary objective for every cored hole at Yucca Mountain has been the determination of the stratigraphic relationships in the cored interval, sections of core containing stratigraphic contacts had to be preserved in the NNWSI Project core library. Thus, these sections were unavailable for thermal and mechanical testing. This procedural limitation has little impact on the testing of relatively thick units, such as the lower devitrified portion of the Topopah Spring Member, but it could hinder representative sampling in thinner layers.

A more important limitation has been that of sample size. Compressive mechanical tests have required samples at least 2.5 cm in diameter and 5.1 cm in length, and samples for confined thermal tests have had to be approximately 5 cm in diameter and 10 cm long. The core obtained from drillholes at Yucca Mountain typically is 6 cm in diameter. In addition, core from welded tuffs such as the Topopah Spring Member is often fractured (Section 1.3.2.3), which limits the number and size of samples available for testing. Larger core samples have been obtained from outcrop material (Section 2.1.2.3.1.7); tests on these samples and in situ tests will provide additional information about the properties of the material.

Another problem related to sample size occurs when zones containing lithophysae are considered. Many lithophysae are larger than the typical core diameter of 5.7 cm and even in locations in which smaller lithophysae are present, the cavities are often too large in relation to core (and thus to test sample) diameter for meaningful test results to be obtained. This latter sampling problem has been addressed by the collection of samples of lithophysal tuff from Busted Butte (Price et al., 1985) and by plans to test large samples of lithophysal tuff collected from the exploratory shaft.

The laboratory testing program was initiated in 1979. At that time, the program focus was to investigate generally several tuff formations located below the water table. Rather than obtaining samples from evenly spaced vertical intervals, emphasis was placed on testing core samples from below the water table in drillhole UE-25a#1 (particularly from the Bullfrog Member) and on a limited number of samples from other units.

During the testing of samples from drillhole USW G-1 (mid-1981 through mid-1982) and the initial tests made using core from drillholes USW G-2, USW G-3, and USW GU-3 core, two important events took place:

1. The concept of a functional engineering-properties stratigraphy was implemented (see next section). A functional stratigraphy categorizes units according to some set of characteristic properties; in this instance, mechanical and thermal properties.

## CONSULTATION DRAFT

2. The tuffs in the zone above the water table began to receive serious consideration for waste disposal.

The sampling process at this stage was designed to provide regularly spaced bulk-property data and thermal and mechanical measurements. Such sampling allows the thermal and mechanical properties of layered-tuff stratigraphies to be estimated with an accuracy that is adequate for input data for the needed analyses and computer codes. As a result of the revised sampling process, the uniformity of the coverage, especially with respect to bulk properties, is much better in these later drillholes. In addition, more samples were obtained in the Topopah Spring Member than were collected from drillhole UE-25a#1. Sample depths and frequencies at which bulk-property samples were to be taken from the continuous core were requested in drilling criteria before the initiation of each drillhole. The emphasis has been toward maintaining an even spacing of samples rather than toward selecting the best material in each interval.

Two additional considerations are being incorporated in the planning of future sample selection. In instances in which properties have not been reliably determined because of sample-size limitations, larger samples have been obtained from outcrop material and also will be obtained from the exploratory shaft.

Increasing attention is being paid to the number of measurements necessary to provide statistical confidence that a true measure of a property has been obtained. To date, replicate tests have been made sporadically to explore what statistical variation in properties is present in the tuff units. Ideally, the first step in a statistical determination of the number of replicate tests that will be necessary is to conduct parametric sensitivity studies to determine how well a property must be known. Such sensitivity studies have not been made but are planned (Section 8.3.5). As results from these studies become available, existing plans for sample selection (e.g., those for the laboratory tests described throughout Section 8.3) will be modified to optimize the number of tests for each geoenvironmental property.

### STRATIGRAPHIC FRAMEWORK FOR TESTING

The increasing number of data on laboratory properties has provided increasing evidence that the formal stratigraphic units at Yucca Mountain, described in Section 1.2, could be subdivided into a different stratigraphy. In this functional stratigraphy, each unit has values of the bulk, thermal, and mechanical properties that are characteristic of that unit and at least one of which differs from the corresponding property for adjacent units. The functional division is better suited to the presentation of geoenvironmental properties than are the formal stratigraphic units, which may encompass large variations in mineralogic composition, porosity, and fracturing. Nevertheless, the formal stratigraphy provides a useful framework for defining functional stratigraphies. (Other functional stratigraphies are defined for hydrogeology and geochemistry.)

The first functional stratigraphy for Yucca Mountain, proposed by Lappin et al. (1982), was based on the bulk and thermal properties measured on tuff

## CONSULTATION DRAFT

samples from drillhole USW G-1. Refinement of this initial stratigraphy to a system applicable to all Yucca Mountain (Ortiz et al., 1985) has resulted in the set of thermal/mechanical units shown in Figure 2-5 which also lists the lithologic equivalents of these units. The majority of the thermal/mechanical units are identifiable in all the drillholes at Yucca Mountain and, therefore, serve as a useful framework for examining the spatial variation of geoengineering properties. The proposed horizon for repository development is a nonlithophysal portion of the Topopah Spring Member. The Topopah Spring Member is composed of a number of distinct ash flows, some of which contain more lithophysae than others. Further, the lithophysae content varies laterally within individual flows. Therefore, although the major flows can be correlated reliably, they can be categorized only as nonlithophysal, moderately lithophysal, or heavily lithophysal. The actual lithophysae content can be predicted reliably only in these broad classes. The thermal/mechanical stratigraphy is used as such a framework for summarizing data on geoengineering properties in the remainder of Chapter 2, as well as in Section 6.1.2.

The thermal/mechanical stratigraphy as presently defined is based on the properties of intact rock. As more information on rock mass properties is obtained, the thermal/mechanical stratigraphy may need to be revised to better reflect the large-scale property variation.

To increase efficiency in performance assessment and design analyses, the NNWSI Project is in the process of defining the parameters for which reference data are to be assigned for each of the thermal/mechanical units, and a reference data set is being collated. This data set will be updated periodically as new data become available. Thus, at any given time, all ongoing analyses should be consistent from the point of view of input data and initial conditions.

### CURRENT DATA BASE

The current data base consists primarily of measurements on relatively small-diameter cores. Thermal/mechanical properties have been defined for the thermal and mechanical functional units in and above the Tram Member. The data base consists of approximately 100 thermal conductivity tests, 300 thermal expansion tests, 75 mineralogic-petrologic analyses, 700 bulk-property (porosity, density) measurements, and 350 mechanical-property tests. Most of the data are from drillholes UE-25a#1, USW G-1, and USW GU-3; in some instances, samples from drillholes USW G-2 and USW G-4, as well as from Rainier Mesa have been included. Additional information from these latter sources will be added as it becomes available. Interpretations of the thermal and mechanical properties and their statistical variations have relied heavily upon the use of the bulk-property data and mineralogic analyses to establish correlation. The properties for the thermal/mechanical units (including statistical variations) are described in Sections 2.1.3, 2.3.3, and 2.4.3.

Data gathering efforts are now directed at evaluating the mechanical behavior of the densely welded portion of the Topopah Spring Member, with emphasis on lateral variability; lithophysal effects; temperature, pressure,

CONSULTATION DRAFT

m	DEPTH ft	THERMAL/ MECHANICAL UNIT	LITHOLOGIC EQUIVALENT
		UO	ALLUVIUM
		TCw	WELDED, DEVITRIFIED TIVA CANYON
		PTn	VITRIC, NONWELDED TIVA CANYON, YUCCA MOUNTAIN, PAH CANYON, TOPOPAH SPRING
	500	TSw1	LITHOPHYSAL TOPOPAH SPRING; ALTERNATING LAYERS OF LITHOPHYSAE-RICH AND LITHOPHYSAE-POOR WELDED, DEVITRIFIED TUFF
	200		
	1,000	TSw2	NONLITHOPHYSAL TOPOPAH SPRING <u>POTENTIAL REPOSITORY HORIZON</u> (CONTAINS SPARSE LITHOPHYSAE)
	400	TSw3	VITROPHYRE, TOPOPAH SPRING
	1,500	CHn1	ASH FLOWS AND BEDDED UNITS, TUFFACEOUS BEDS OF CALICO HILLS; MAY BE VITRIC (v) OR ZEOLITIZED (z)
		CHn2	BASAL BEDDED UNIT OF CALICO HILLS
		CHn3	UPPER PROW PASS
	800	PPw	WELDED, DEVITRIFIED PROW PASS
	2,000	CFUn	ZEOLITIZED LOWER PROW PASS AND UPPER BULLFROG
	2,500	BFW	WELDED, DEVITRIFIED BULLFROG
	800	CFMn1	ZEOLITIZED LOWER BULLFROG
		CFMn2	UPPER ZEOLITIZED TRAM
		CFMn3	ZEOLITIZED BASAL BEDDED UNIT OF BULLFROG
	3,000	TRw	WELDED, DEVITRIFIED TRAM

Figure 2-5. Thermal/mechanical stratigraphy at Yucca Mountain. (Depths and thicknesses plotted are averages from drillholes UE-25a#1, USW G-1, USW G-2, USW GU-3, and USW G-4.)

## CONSULTATION DRAFT

strain rate, and sample size effects on the mechanical properties of the matrix material; and the mechanical properties of the fractures.

### CONCEPTUAL ROCK MECHANICS MODELS

The analysis of the response of the rock at Yucca Mountain to applied loads requires the definition of initial conditions, boundary conditions, material properties, and a description of the rheologic behavior of the material. These four requirements together contribute to the definition of the conceptual rock mechanics models being applied in the design process to understand the material response of Yucca Mountain.

The initial conditions for such a model are the geometry of the unit (see previous section on stratigraphic framework for testing), the pre-existing state of stress (Sections 1.3.2.3 and 2.6), the in situ temperature (Section 1.3.2.5), and the saturation (Section 3.9.2.1). Boundary conditions are assigned on the basis of the scale, geometry, loading conditions, and the time frame of the analysis. More details on these two topics are provided in Chapter 6.

The portion of the conceptual models to which Chapter 2 contributes most is the rheologic behavior and the material properties of the tuff units. These two topics are intimately related in that the measurement of certain index material properties assists in estimating the rheologic behavior of the tuff units. Once the rheologic behavior has been established, additional determinations of material properties can be used to provide a statistical basis for the parameters called for in design analysis. Much of Chapter 2 is devoted to these parameters.

The empirical approaches used in analyses of the mechanical behavior of the welded Topopah Spring Member, by definition, are not founded in system or theory. In contrast, state-of-the-art numerical methods are founded on constitutive laws that mathematically describe or define the physical nature of deformation of fractured tuff. The constitutive laws that have been selected to describe mechanical deformation of tuff are elastic, elastic-plastic, and compliant-joint. A description of each of these constitutive laws and the justification for their applications to tuff follows.

Almost all engineering materials possess to a certain extent the property of elasticity. The term "elastic" describes a material for which, if the external forces producing deformation do not exceed a certain limit, the deformation disappears with the removal of the forces. Chapter 2 discusses mechanical properties of both the intact rock and the rock mass that indicate that for certain stress and strain states tuff behaves as an elastic solid (Section 2.1.2.2). For example, like many other crustal rocks, the stress-strain response for intact tuff is approximately linear through approximately two-thirds of the short-term breaking strength.

The tuff rock mass at Yucca Mountain contains fractures, as described in Chapter 1. For large stress changes, the normal and shear behavior of fractures has been observed to be inelastic and nonlinear (Goodman, 1980). For small stress changes, such as those predicted in the vicinity of underground

openings for the proposed tuff repository, linear elastic material behavior has been considered appropriate. This same material response has been considered appropriate in many mining applications. Field experiments in densely welded tuff performed over small (10 MPa) stress ranges intended to measure the rock-mass material response have thus far indicated that an elastic constitutive model can be used to adequately represent deformation of the rock mass (Zimmerman et al., 1986). However, these field studies also suggest that the elastic constants that serve as input parameters to this model should be different from those measured in the laboratory to account for the contribution of fractures to the rock mass mechanical response.

Elastic-plastic constitutive behavior is an extension of the material behavior just described where some limiting value of stress is reached. At stresses below the limiting value, elastic behavior is prescribed, and beyond the limit, plasticity theory applies. Plasticity theory models the phenomenon of irrecoverable strains, regardless of which energy dissipation (deformation) mechanism is operating. Material behavior can be simulated by the following: (1) an initial yield condition that defines the domains of elastic and plastic behavior; (2) a flow rule that defines plastic strain increments on the basis of current stresses and previous plastic strains; and (3) a hardening rule that describes how the size, shape, and orientation of the yield surface (the boundary separating elastic and elastic-plastic behavior) changes during the deformation.

Elastic-plastic analyses have been used in some instances to assess the state of stress resulting from excavation and thermally induced loads. This type of constitutive description is considered applicable to a fractured rock mass because both slip on fractures and intact rock failure are mechanisms through which irrecoverable strain must be accounted for, given sufficient deviatoric stress. Two general types of plasticity models have been used by the NNWSI Project. In the first model, a general yield condition may be satisfied by consideration of the deviatoric stress resulting from the general applied stress state. This type of analysis has been used extensively in assessments of stability of underground tunnels in other rock types (see summary and review by Goodman, 1980). In the second model, the yield condition may be satisfied by consideration of the deviatoric stress and a prescribed direction of fracturing. This second plasticity model has been called the ubiquitous joint model and carries with it the assumption that there is one predominant direction of fractures in the rock along which slip may be accommodated. Thus far, field studies at Yucca Mountain have indicated that the preponderance of fractures are near vertical (Spengler and Chornack, 1984), so that use of this type of model is considered to be justified.

Compliant-joint constitutive models (Thomas, 1982; Chen, 1987) are an extension and improvement upon the models just described. Extensive field and drillhole data at Yucca Mountain (Chapter 1) suggest that a constitutive model should incorporate the mechanical response of both the intact rock (matrix) and fractures. In general these models are composed of two parts: (1) a continuum-based technique to average the discontinuous displacements across fracture planes within a representative elementary volume and (2) a constitutive description based on the linear elastic behavior of the matrix material and the nonlinear behavior of the fractures. The constitutive model takes the continuum approach in the sense that every material point in the

## CONSULTATION DRAFT

model behaves as would a representative elementary volume composed of a matrix material and a suitably large number of fractures. The total strains are decomposed into contributions from the matrix and fractures so that load sharing takes place. Normal and shearing motions of fractures are related to the conjugate stresses through the stiffness matrix.

Material property constants are required for both the rock matrix and the fractures. The matrix is assumed to be isotropic and linearly elastic, requiring specifications of only Young's modulus and Poisson's ratio. The assumed shear behavior of the fractures was deduced from laboratory experiments on fractures (Teufel, 1981; Olsson, 1987) to be elastic-perfectly plastic. The elastic part is described by a joint shear stiffness, and the plastic part is described by a linear slip criterion with a friction coefficient and cohesion. The normal stiffness is nonlinear elastic in accord with observed laboratory results (Goodman, 1980; Olsson, 1987). It is described by a hyperbolic function that contains two material constants: the half-closure stress and the unstressed aperture.

The compliant-joint model as described then contains the primary components that can contribute to mechanical deformation in a rock mass. Models of this type have been used to analyze field experiments in densely welded tuff (Zimmerman et al., 1986). In this experiment the stress changes imposed were small, so that the experiment cannot be used as a means to discriminate between this modeling approach and an elastic analysis.

The conceptual rock mechanics models, and especially the detailed treatment of the rheologic behavior of tuff, will continue to evolve as more data are obtained and as the understanding of the system matures. Such changes will be made as either test data or observed in situ behavior indicate the need for changes in the mathematical representations of the mechanical behavior of tuff.

The data described in Chapter 2 are necessary, but are not yet sufficient, for the complete implementation of the available rheologic models. Where the measured data required by a model are not available, values have been assumed based either on experimental data from similar rock types or on theoretical calculations, and tests to obtain the data are either underway or planned. Section 8.3.1.15 describes tests planned to acquire additional data.

### DATA UNCERTAINTY FOR GEOENGINEERING PROPERTIES

Evaluation of uncertainty associated with measured parameters has been addressed, where possible, by testing and sampling programs that are structured so that experimental uncertainty and sampling uncertainty are independently or jointly characterized.

Experimental uncertainty is attributed to variations in sample handling and preparation, instrument response, and human factors, which affect experimental outcome. Standard practice typically calls for evaluation of experimental uncertainty by repeated testing, replicate testing, or testing of special materials with known properties. Investigations of this type were

performed during the testing reported in this chapter and generally yielded experimental uncertainties of 3 and 10 percent of measured values of mechanical and thermal (or thermomechanical) properties, respectively.

Sampling uncertainty occurs when a population containing variability is sampled a finite number of times. Natural spatial variability is a principal source of sampling uncertainty. Because natural variation is relatively unknown at the outset of sampling, a distribution function for the population is explicitly or implicitly assumed before the design of a sampling program. For geoenvironmental properties investigations reported in this chapter, this has meant assuming that (1) variability is random within functional stratigraphic units (parameters are uncorrelated with depth), (2) lateral variation between coreholes is insignificant compared with the combined experimental and sampling uncertainties for a functional unit within any one corehole, and (3) populations are normally distributed, so that the applicable statistics are relatively straightforward. The small number and distributed locations of coreholes drilled to date does not yet justify geostatistical analysis of lateral variability of parameters, however, such an approach is planned for site characterization as discussed in Section 8.3.1.4.

Throughout the functional stratigraphy there are strong associations between index properties, such as porosity, and parameters for which data coverage is relatively sparse, such as strength and deformability. The most common reason for scarcity of mechanical properties test data is limited availability of samples, especially core samples of a minimum size. Correlations have been developed using data originating from wherever samples were available in the tuff sequence at Yucca Mountain and also from lithologically similar tuffs at G-tunnel. Generally there is some conceptual basis for using correlation with index properties. These correlations were used in compiling Table 2-7 (2.1.3) and are discussed in later sections as follows:

Compressive strength vs. porosity	(2.1.2.3.1.8)
Tensile strength vs. porosity	(2.1.2.3.2)
Coulomb failure criteria vs. porosity	(2.1.2.3.1.2)
Young's modulus vs. porosity	(2.1.2.2)

It is important to note that the data uncertainty for parameter values that are based on correlation with index properties is compounded by the uncertainty of index property determination and the uncertainty implicit in correlation. Parameter values based on correlation are presented for comparison purposes only and will eventually be replaced, if possible, with values based directly on test results. Accordingly, the relatively large standard deviations for values based on correlation are not included in Tables 2-7 (Section 2.1.3) or 2-14 (Section 2.4.3).

The properties of tuffs from locations other than Yucca Mountain, which have not been investigated by the NNWSI Project, are presented in Chapter 2 for comparison purposes. Mechanical properties, large-scale mechanical properties, and thermal and thermomechanical properties for other rocks are tabulated in Tables 2-2 (Section 2.1.1), 2-8 (Section 2.3.1), and 2-10 (Section 2.4.1), respectively. These comparison data are typically from published studies for which uncertainty information is available in some form, but is not included in the tables because it is not applicable to site characterization. Another application of data from other rocks is the

analysis of excavation characteristics and rock mass classification in Sections 2.8.2.2 and 2.8.2.3. Rating systems for rock classification will be used in site characterization to evaluate conformity with design criteria. Uncertainty information is provided for these empirically derived ratings and support specifications in the form of a range of values that may apply to the site.

## 2.1 MECHANICAL PROPERTIES OF ROCK UNITS--INTACT ROCK

Predicting the mechanical response of the rock surrounding the repository requires knowledge of the properties of the intact (matrix) rock and the discontinuities that are present (joints, faults, fractures, and bedding planes). This section summarizes current information and data on the intact rock properties of tuff, including elastic constants and strength parameters. These and subsequent data will be used as input to the calculational models of the underground structures to evaluate the design and compliance with performance objectives. An extensive data base is required to understand the spatial distribution and variability of these properties, so that conservatism in the calculations is ensured.

The properties of intact rock samples represent upper limit values of the strength and deformability of the in situ rock mass, which includes discontinuities and other defects not reflected in the intact rock alone. The reduction of strength and stiffness typically observed in the field is a function of the frequency and nature of existing discontinuities (Section 2.2).

Detailed results of laboratory mechanical tests on samples from drill-holes in Yucca Mountain are contained in numerous reports (Olsson and Jones, 1980; Blacic et al., 1982; Olsson, 1982; Price and Jones, 1982; Price and Nimick, 1982; Price et al., 1982a,b; Price, 1983; Price et al., 1984; Nimick et al., 1985). Data from these reports are discussed in Section 2.1.2.

These reports also include detailed discussions of sample treatment, equipment, experimental procedures, and calibrations. Most of the samples tested in compression have been right-circular cylinders with a diameter of 2.54 cm and a length-to-diameter ratio of approximately 2:1, which is in accord with the recommended American Society for Testing and Materials (ASTM) procedures (ASTM D 2664-80 (ASTM, 1980a), ASTM D 2938-79 (ASTM, 1979b)), but is less than the minimum ratio of 2.5:1 suggested by the International Society for Rock Mechanics (ISRM) (1979a). Because of this disagreement between the specifications, comparative tests on samples with a ratio of 2.5:1 or greater will be undertaken as discussed in Section 8.3.1.5.2. For the present purposes, however, the 2:1 ratio is advantageous because it allows more test samples to be obtained. Because the amount of core material is limited, the smaller sample size maximizes the statistical data base of individual measurements.

The effect of sample size on the mechanical properties of intact tuff is addressed further in Section 2.1.2.3.1.7. For most of the samples tested, the grain and flaw (pore) sizes were less than one-tenth of the specimen

diameter. Thus, the effects of such individual features on the bulk mechanical properties are minimal.

Calibrations of force and displacement gages using materials with well-established properties before each experimental series have shown that the accuracy and the precision of these measurements are better than  $\pm 3$  percent in all instances. The inference is that these accuracies and precisions are representative of those to be expected on tuff samples. Any major differences in mechanical properties for adjacent tuff samples, therefore, result from sample variability (mineralogic composition, porosity, grain density, crack frequency, etc.) or test conditions.

Tensile tests were performed on right-circular cylinders with nominal dimensions of 2.54 cm (diameter) and 1.25 cm (thickness) (Blacic et al., 1982). The Brazilian indirect strength test was the technique used because of the relative ease with which the test can be performed and because more samples could be tested than in other methods that require larger samples. The limitations of the Brazilian test are recognized (McWilliams, 1966); future testing will examine the applicability of existing data. No estimates of measurement errors have been made.

#### 2.1.1 MECHANICAL PROPERTIES OF OTHER ROCKS

To provide a basis for understanding the mechanical behavior of the tuff at Yucca Mountain, it is appropriate to present a brief summary of mechanical properties of other tuffaceous rocks. A survey of the mechanical properties of tuff is provided by Guzowski et al. (1983). The data collected by these investigators on the mechanical properties of tuffs other than those discussed later in this section are summarized in Table 2-2. The table is intended to provide perspective on the ranges of the mechanical properties of tuff. Data for the welded, devitrified portion of the Topopah Spring Member (Section 2.1.2, especially Table 2-7, Section 2.1.3) indicates that the potential repository horizon (TSw2) has a high unconfined compressive strength and Young's modulus compared with other tuffs.

#### 2.1.2 MECHANICAL PROPERTIES OF ROCKS AT THE SITE

##### 2.1.2.1 Existing mechanical properties data

Detailed results of laboratory mechanical property tests on samples from drillholes at Yucca Mountain and from G-Tunnel at Rainier Mesa are contained in numerous reports (Olsson and Jones, 1980; Blacic et al., 1982; Price and Jones, 1982; Price and Nimick, 1982; Price et al., 1982a,b; Price et al., 1984; Nimick et al., 1985). These references cover approximately 280 unconfined compression tests, 100 indirect tensile tests, and 30 triaxial compression tests; the extent of the compressive tests is shown in Table 2-3. In addition, the results of all compression experiments performed on samples from drillholes UE-25a#1 and USW G-1 have been compiled (Price, 1983). Where

Table 2-2. Summary of mechanical properties of tuffs not studied by the Nevada Nuclear Waste Storage Investigations Project<sup>a</sup>

Location or tuff unit	Unconfined compressive strength (psi) <sup>b</sup>	Young's modulus (10 <sup>6</sup> psi) <sup>b</sup>	Poisson's ratio	Lithology <sup>c</sup>
Ohya tuff, Japan	0.804	-- <sup>d</sup>	--	Nonwelded
Rainier Mesa tuff units	1,350-5,125	0.45-2.26	0.09-0.38	Nonwelded
Tuff, E-Tunnel, NTS <sup>e</sup>	3,500	--	--	Nonwelded
Tuff, NTS	5,282-9,512	--	--	--
Oak Springs Formation, NTS	3,400-8,700	0.40-1.60	0.02-0.04	Bedded
Oak Springs Formation, NTS	6,800-29,100	0.86-1.75	0.05-0.15	Welded
Tuff, Oregon	3,141-4,999	0.85	--	--
Tuff, Red Hot Deep Well Experiment, NTS	1,560-4,910	0.33-0.95	0.13-0.49	--
Tuff and tuff breccia, USSR	--	3.23	0.13	--
Tuff, Japan	--	1.32-3.47	--	--
Tuff breccia, India	--	0.20-3.62	--	--
Tuff, locality unknown	--	0.99-2.92	--	--

<sup>a</sup>Source: Guzowski et al. (1983).

<sup>b</sup>To convert from psi to Pa, multiply the entries by 6,895.

<sup>c</sup>Lithologies have been assessed on the basis of original references when available.

<sup>d</sup>-- = data not available..

<sup>e</sup>NTS = Nevada Test Site.

CONSULTATION DRAFT

Table 2-3. Summary of compressive mechanical testing for the Nevada Nuclear Waste Storage Investigations Project. Numbers of compressive mechanical tests performed at baseline test conditions<sup>a</sup> and with variations in one or more test parameters.

Reference	Drillhole or location	Thermal/mechanical unit or formation <sup>b</sup>	Number of tests						Total <sup>c</sup>
			Confining pressure	Saturation	Temperature	Sample size	Strain rate	Standard tests	
Olsson and Jones (1980)	UE-25a#1	TCw	3	-- <sup>d</sup>	1	--	--	1	4
		PTn	3	--	--	--	--	1	1
		TSw1	1	--	1	--	--	1	2
		TSw2	2	--	--	--	--	1	3
		CHn1x	3	--	--	--	--	2	5
		FPw	3	--	--	--	--	0	3
		CFUn	--	--	--	--	--	2	2
		BFw	3	--	--	--	--	1	4
	G-Tunnel	Grouse Canyon	--	9	--	--	20	0	20
Blacic et al. (1982)	UE-25a#1	TSw1	--	--	--	7 <sup>e</sup>	--	0	7 <sup>e</sup>
		TSw2	--	--	--	20 <sup>e</sup>	--	0	20 <sup>e</sup>
		TSw3	--	--	--	4 <sup>e</sup>	--	0	4 <sup>e</sup>
		CHn1x	--	--	--	25 <sup>e</sup>	--	0	25 <sup>e</sup>
	USW G-1	BFw	--	--	--	14 <sup>e</sup>	--	0	14 <sup>e</sup>
		TRw	--	--	--	14 <sup>e</sup>	--	0	14 <sup>e</sup>
Price and Jones (1982)	USW G-1	CHn1x	16	4	--	--	4	18	40
		CHn2x	--	--	--	--	--	4	4
Price, et al. (1982a)	USW G-1	CFUn	--	--	--	--	--	6	6
		BFw	--	--	--	--	--	6	6
		CFMn1	--	--	--	--	--	4	4
		CFMn2	--	--	--	--	--	2	2
		CFMn3	--	--	--	--	--	1	1
Price and Nimick (1982)	USW G-1	CFMn3	--	--	--	--	--	2	2
		TRw	--	--	--	--	--	6	6
Price, et al. (1982b)	USW G-1	TSw2	4	--	--	--	7	4	15
Price, et al. (1984)	USW GU-3	TSw1	--	7	--	8	--	3	11
		TSw2	--	7	--	7	--	17	24
Nimick, et al. (1985)	USW G-4	TSw2	6	--	--	--	7	24	37
		CHn1x	4	--	--	--	5	5	14

<sup>a</sup>Baseline conditions here are assumed to be ambient pressure and temperature, a strain rate of  $10^{-5} s^{-1}$ , saturated, and with a nominal sample diameter of 2.5 cm.

<sup>b</sup>See Figure 2-5 for definition of the thermal/mechanical units.

<sup>c</sup>Number given as total is the number of individual tests; numbers of tests in corresponding rows are for variations in individual test parameters without accounting for variations in more than one parameter in a single test. Therefore, "total" is not necessarily the sum of the numbers in the corresponding row.

-- = No variation.

<sup>e</sup>Some of these tests were performed on samples that had been soaked at elevated temperature and pressure for different periods of time. See Blacic et al. (1982) for details.

## CONSULTATION DRAFT

possible, statistical evaluations of the data have been made. These evaluations have culminated in the data presented in Section 2.1.3 as the mechanical properties stratigraphy for the Yucca Mountain tuffs.

Test results for the elastic properties and the compressive and tensile strengths of Yucca Mountain tuffs are summarized in the next two sections. The discussion includes the current status of evaluations of the effects of water saturation, confining and fluid pressure, elevated temperature, time-dependent behavior, lithophysae, mechanical anisotropy, and sample size.

### 2.1.2.2 Elastic properties

Data on Young's modulus and Poisson's ratio have been collected for Yucca Mountain tuffs for use in modeling the elastic response of repository rooms, waste emplacement holes, and shafts. All the data are from compression experiments run on nominally fully saturated samples at atmospheric pressure (unconfined), a nominal strain rate of  $10^{-5} \text{ s}^{-1}$ , and room temperature ( $23^{\circ}\text{C}$ ). The test conditions were chosen as baseline conditions because the majority of compressive tests on Yucca Mountain tuff samples to date have been performed under these conditions. The applicability of the data to other temperatures, pressures, or strain rates is being evaluated in an ongoing test program, as discussed in Section 8.3.1.15.

Figure 2-6 is a representative plot of axial stress versus axial strain measured on a sample of welded, devitrified tuff from the Topopah Spring Member. The figure demonstrates the strong linearity of the deformation response to a stress on the order of 95 percent of the failure stress. This behavior is typical for intact samples of this material, suggesting that the rock matrix of the Topopah Spring Member is an elastic material, at least for the baseline test conditions.

A preliminary study of the effects of differences in confining pressure and strain rate on the mechanical properties of the Topopah Spring Member from drillhole USW G-4 has been completed (Nimick et al., 1985). No definitive trend in Young's modulus was found as a function of either effective confining pressure or strain rate for the ranges tested ( $0$  to  $10 \text{ MPa}$ ;  $10^{-3}$  to  $10^{-1} \text{ s}^{-1}$ ). Additional studies of the effect of differences in test parameters on the mechanical properties of the Topopah Spring Member are ongoing using outcrop material, and a test series will be conducted on material from the exploratory shaft facility (Section 8.3.1.15.1). Both of these test series include variations in temperature and saturation as well as in confining pressure and strain rate.

An early study (Olsson and Jones, 1980) suggested that the elastic moduli of the Grouse Canyon Member are anisotropic. The results of this study indicated a correlation between the degree of welding (i.e., the amount of porosity) and the degree of anisotropy. Whereas welded tuff is stiffest perpendicular to bedding (i.e., approximately vertical), the nonwelded tuff is stiffest parallel to bedding (i.e., approximately horizontal). The dynamic elastic moduli for samples of the densely welded Topopah Spring Member from drillhole USW GU-3 showed that anisotropy of elastic properties for orientations parallel and perpendicular to the rock fabric is insignificant

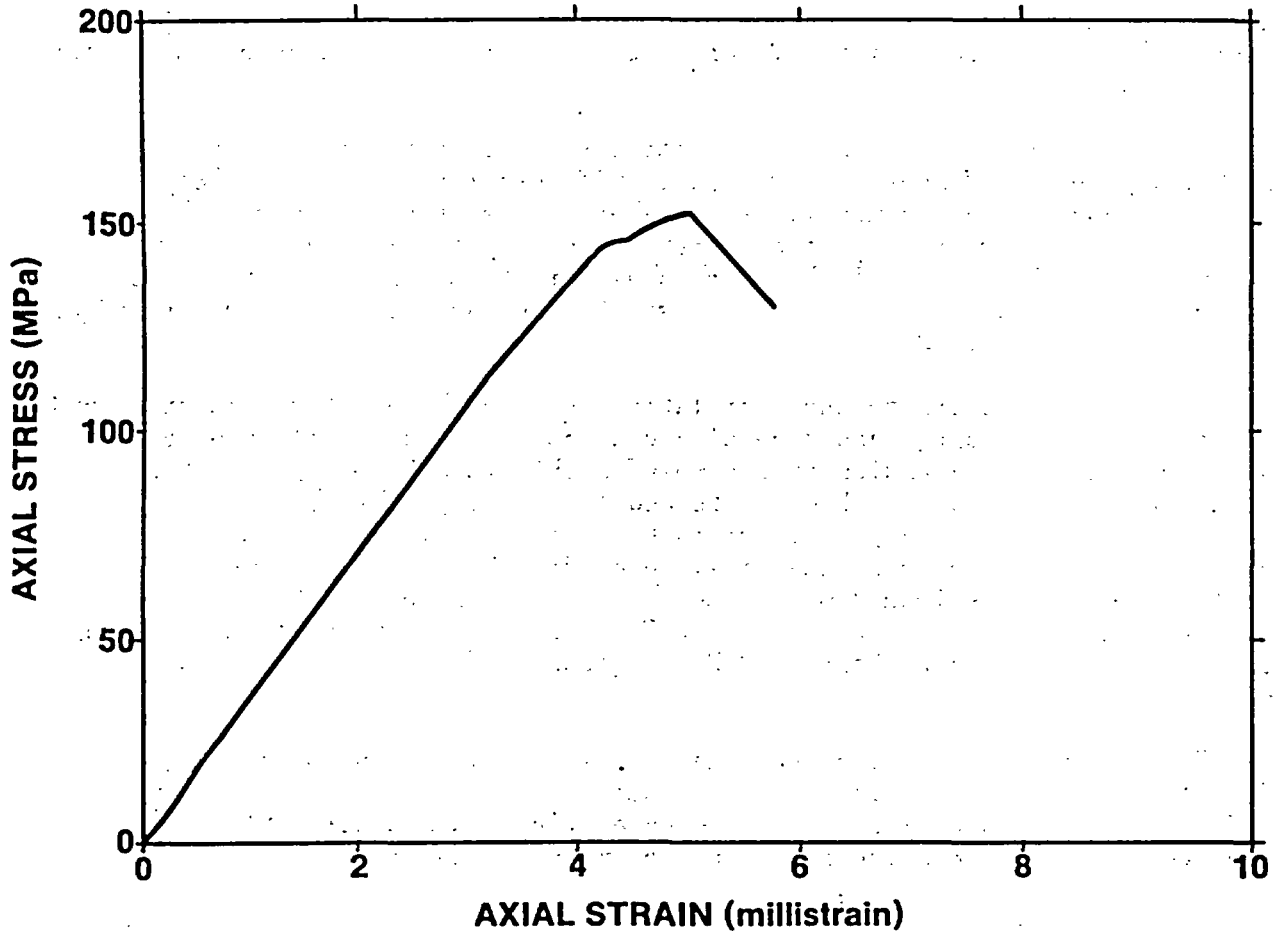


Figure 2-6. Representative axial stress-axial strain plot for the welded, devitrified Topopah Spring Member (test sample GU-3 1050.4/3; test conditions ambient temperature and pressure, saturated,  $10^{-5}/s$ ). Modified from Price et al. (1984).

## CONSULTATION DRAFT

(Price et al., 1984). On the basis of these results, the matrix of the Topopah Spring Member is assumed to be isotropic. The tests planned to investigate the possibility of anisotropic elastic response and strength anisotropy in samples from the Topopah Spring Member are discussed in Section 2.1.2.3.1.6.

Values have been obtained for dynamic elastic moduli for 10 samples of the Topopah Spring Member from drillhole USW GU-3 (Price et al., 1984). In general, dynamic Young's moduli were higher than static values measured on the same samples, whereas Poisson's ratios were approximately the same for both methods. The ratio of the average dynamic to the average static Young's modulus for the samples is 1.30, well within the range of ratios described by Lama and Vutukuri (1978).

Analyses to determine the correlation between the elastic properties and porosity, grain density, and mineralogic composition were performed to assess the possibility of extending such a relationship to other tuffs on which mechanical testing has not been performed (Price, 1983; Price and Bauer, 1985). Data for the analyses reported by Price (1983) were taken from compressive tests conducted at the baseline conditions on samples from the Bullfrog Member, the Tram Member, and the tuffaceous beds of Calico Hills. The analysis of the data set, which includes results from the Topopah Spring Member, is summarized by Price and Bauer (1985) and in the paragraphs that follow:

Price (1983) determined that there is a correlation between the porosity of tuff and the Young's modulus. Test data for 111 samples of Yucca Mountain tuffs have been fit by linear least squares (Price and Bauer, 1985) to provide the following equation relating the two parameters:

$$E = 85.5e^{-6.96n} \quad (2-1)$$

where  $E$  is Young's modulus (GPa) and  $n$  is the functional porosity (volume fraction), defined as the sum of the volume fraction of void space and the volume fraction of clay in the sample.

The correlation coefficient ( $r$ ) for this fit is 0.93. The range in  $n$  for which the equation is thought to be valid is approximately 0.10 to 0.65. However, the equation does not apply to welded vitric tuff (vitrophyre). The grain structure and bonding in a vitrophyre are sufficiently different from those in all other types of tuff at Yucca Mountain so that the physical processes leading to successful application of the correlation in equation 2-1 do not occur in the vitrophyre.

For the analysis of data on Poisson's ratio, Price (1983) reports using a multivariate fit. This fit has not been revised to include the data from the Topopah Spring Member. The equation relating Poisson's ratio to porosity and grain density as given by Price (1983) has an  $r$  value of 0.48. The correlation is not considered useful for estimating Poisson's ratio from these other measured properties.

Additional analyses will be performed as more data become available. The results should increase the confidence in estimates of the Young's modulus of tuff with a given porosity and grain density.

### 2.1.2.3 Matrix compressive and tensile strengths

#### 2.1.2.3.1 Compressive strength

Compressive strength values have been documented (Olsson and Jones, 1980; Olsson, 1982; Price and Jones, 1982; Price and Nimick, 1982; Price et al., 1982a,b; Price, 1983; Price et al., 1984; Nimick et al., 1985) for a wide range of tuff samples from Yucca Mountain. Additional data are being gathered and will be available before the start of exploratory shaft activities.

##### 2.1.2.3.1.1 Effect of water saturation on compressive strength

A series of drained uniaxial compression tests were run to quantify the effect of water saturation on the compressive strength of tuff (Olsson and Jones, 1980). Closely spaced samples were obtained from the Grouse Canyon Member of the Belted Range Tuff from G-Tunnel. A total of 18 samples were either oven-dried or water-saturated after machining and then were deformed at atmospheric pressure, room temperature, and nominal strain rates of  $10^{-2}$ ,  $10^{-4}$ , and  $10^{-6}$   $s^{-1}$ . The results are given in Figure 2-7 and Table 2-4. At each strain rate, the average strengths of nominally saturated specimens are approximately 30 percent lower than the average strengths of the corresponding dry samples. Data from another seven samples of the Grouse Canyon Member (Board et al., 1987) showed that the mean strengths of vacuum-saturated samples were approximately 15 percent lower than the mean strengths for corresponding dry samples. Similar results were obtained in four experiments on samples of the tuffaceous beds of Calico Hills (Price and Jones, 1982). These tests were conducted at approximately the same conditions (unconfined pressure, a constant strain rate of  $10^{-5}$   $s^{-1}$ , room temperature) with two fully saturated specimens and two room-dry specimens (unknown degree of saturation). The average strength of the saturated specimens was approximately 23 percent lower than the average strength of the air-dried samples.

The data just summarized indicate that water-saturated tuff is expected to have a lower compressive strength than tuff in which the saturation is less than 100 percent. Use of the strengths measured on saturated samples as input to calculations in support of the design process thus will add a degree of conservatism to the process. A quantitative estimate of this conservatism is not possible because the saturation state will vary during the history of a repository. Tests of samples from the exploratory shaft facility and surface outcrops will be conducted to investigate the effects of variations in temperature, saturation, confining pressure, and strain rate on the mechanical properties (including deformation modulus and compressive strength of the Topopah Spring Member).

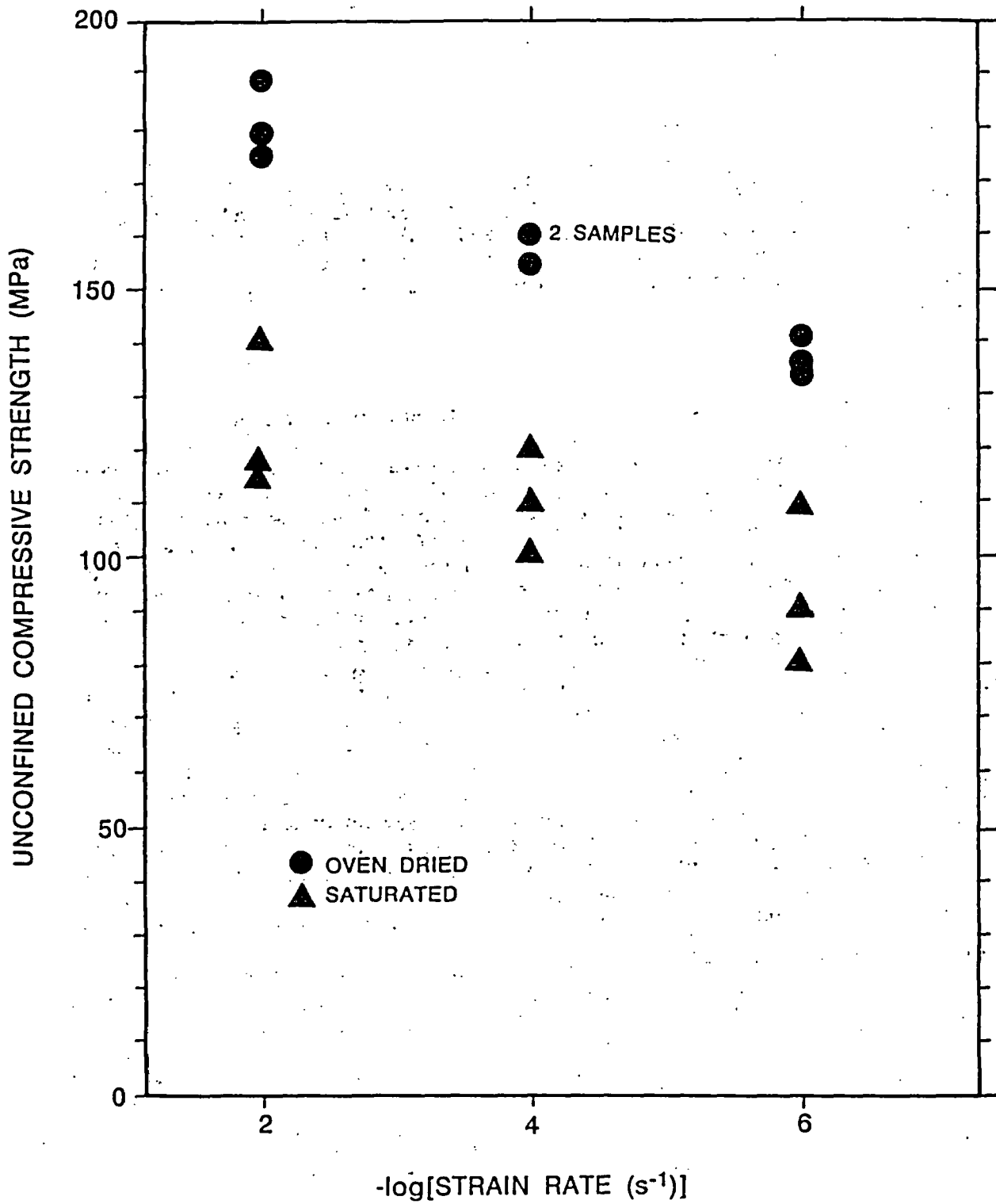


Figure 2-7. Compressive strength as a function of strain rate for dry and saturated samples of Grouse Canyon Member. Modified from Olsson and Jones (1980).

CONSULTATION DRAFT

Table 2-4. Effects of saturation and strain rate on the compressive strength of tuff samples from the Grouse Canyon Member<sup>a</sup>

Strain rate (s <sup>-1</sup> )	Compressive strength (MPa)	Young's modulus (GPa)
UNSATURATED SAMPLES		
10 <sup>-2</sup>	175	25.9
10 <sup>-2</sup>	189	28.7
10 <sup>-2</sup>	177	28.4
10 <sup>-4</sup>	160	26.2
10 <sup>-4</sup>	155	28.5
10 <sup>-4</sup>	160	27.4
10 <sup>-6</sup>	135	27.4
10 <sup>-6</sup>	141	28.3
10 <sup>-6</sup>	134	29.5
FULLY SATURATED SAMPLES		
10 <sup>-2</sup>	142	26.1
10 <sup>-2</sup>	114	22.8
10 <sup>-2</sup>	118	23.8
10 <sup>-4</sup>	112	24.8
10 <sup>-4</sup>	122	25.3
10 <sup>-4</sup>	102	24.0
10 <sup>-6</sup>	81.1	25.9
10 <sup>-6</sup>	110	25.4
10 <sup>-6</sup>	91.8	26.8

<sup>a</sup>Source: Olsson and Jones (1980). These data were obtained on tuff samples from the Grouse Canyon Member in unconfined, ambient temperature, uniaxial compression tests allowed to drain during testing. The porosity of all samples was estimated to be 13 to 18 percent.

## 2.1.2.3.1.2 Effects of confining and fluid pressure on compressive strength

Numerical analyses of the structural stability of mined openings, boreholes, and shafts require the use of a strength criterion for the rock. The commonly used criterion is the coulomb criterion, which defines the limiting state of stress for static equilibrium within the material at which inelastic deformation begins (Jaeger and Cook, 1979). The criterion itself is expressed as follows:

$$\tau = \tau_0 + \sigma \tan \phi \quad (2-2)$$

where

- $\tau$  = shear stress on the failure plane at the onset of failure
- $\sigma$  = normal stress on the failure plane at the onset of failure
- $\tau_0$  = cohesion
- $\phi$  = angle of internal friction.

Uniaxial and triaxial compression tests are used to determine these parameters.

Twenty sets of triaxial compression tests on 90 tuff samples have been run (Olsson and Jones, 1980; Olsson, 1982; Price and Jones, 1982; Price et al., 1982b; Morrow and Byerlee, 1984; Nimick et al., 1985). The experimental results for the test series in which all samples were obtained from a single location or depth were fit by using linear least squares to obtain the Coulomb parameters (cohesion and angle of internal friction) as listed in Table 2-5. The correlation coefficients for the fits also are given in Table 2-5. For nine of the test series, the coefficients are less than 0.8, suggesting that the correlation between compressive strength and confining pressure is not significant. The discussion that follows is limited to the test series for which correlation coefficients greater than 0.8 were obtained.

Four of the test series were conducted on room-dry samples. Three of these four series were at ambient temperature, two were on welded tuffs and one was on nonwelded tuff (tuffaceous beds of Calico Hills). The friction angles in the two welded tuffs are similar (68.0 and 66.7 degrees), whereas the cohesion of tuff from the Topopah Spring Member is lower than that of the Tiva Canyon Member. Both the cohesion and the friction angle are lower for the nonwelded tuff than for the welded tuffs. The one test series conducted on room-dry samples at 200°C used moderately welded tuff from the Bullfrog Member; the test results cannot be directly compared with those for ambient-temperature tests because of differences in both porosity and temperature.

Two test series were run on outcrop samples from the Bullfrog Member at two different strain rates. The results suggest that the friction angle is not sensitive to the strain rate. Cohesion, on the other hand, decreases with the strain rate. This behavior follows that of unconfined compressive strength (Section 2.1.2.3.1.4).

Table 2-5. Summary of coulomb failure criteria parameters<sup>a</sup>

Thermal/ mechanical unit <sup>b</sup>	Depth (m)			Effective pressure (MPa)	Temp- erature (°C)	Strain rate (s <sup>-1</sup> )	Satur- ation (S,R) <sup>c</sup>	Drained conditign (Y,N) <sup>d</sup>	Cohes- ion (MPa)	Angle of internal friction (°)	Correlation coefficient
	USW G-4	USW G-1	UE-25a#1								
TCw	---	---	26.7	0,10,20	23	10 <sup>-4</sup>	R	N	28.1	68.0	0.89
TSw2	---	---	381.0	0,10,20	23	10 <sup>-4</sup>	R	N	17.5	66.7	0.999
TS <sup>c</sup>	---	---	---	10,20,30,50	23	10 <sup>-4</sup>	S	N	92.0	29.1	0.47
TS <sup>c</sup>	---	---	---	10,20,30,40	23	10 <sup>-6</sup>	S	N	48.9	45.6	0.70
TSw2	209.3	---	---	0,5,10	23	10 <sup>-5</sup>	S	Y	37.1	51.8	0.31
TSw2	294.2	---	---	0,10	23	10 <sup>-5</sup>	S	Y	47.4	27.2	0.16
CHnlz	426.9	---	---	0,5,10	23	10 <sup>-5</sup>	S	Y	6.6	15.9	0.45
CHnlz	---	453.4	---	0,10,20	23	10 <sup>-5</sup>	S	Y	10.2	11.1	0.04
CHnlz	---	453.4	---	0,10,20	23	10 <sup>-5</sup>	S	N	10.6	7.8	0.62
CHnlz	---	507.6	---	0,10	23	10 <sup>-5</sup>	R	N	10.2	32.2	0.96
CHnlz	---	507.6	---	0,10,20	23	10 <sup>-5</sup>	S	N	13.2	6.8	0.55
CHnlz	---	508.4	---	0,10	23	10 <sup>-5</sup>	S	N	9.7	4.8	0.21
BFw	---	759	---	5,12,5,20,7	200	10 <sup>-4</sup>	S	Y	23.6	19.6	0.93
BFw	---	759	---	5,10,20,7	200	10 <sup>-4</sup>	R	Y	16.5	37.7	0.89
BF <sup>f</sup>	---	---	---	10,30,40,50	23	10 <sup>-4</sup>	S	N	22.7	42.1	0.93
BF <sup>f</sup>	---	---	---	10,20,30,40,50	23	10 <sup>-6</sup>	S	N	15.2	44.3	0.98

<sup>a</sup>Olsson and Jones (1980); Olsson (1982); Price and Jones (1982); Price (1983); Morrow and Byerlee (1984); Nimick et al. (1985).

<sup>b</sup>Unit identifications, thicknesses, and relation to the formal stratigraphy are shown in Figure 2-5.

<sup>c</sup>Saturation: R = room dried (unknown degree of saturation) and S = fully saturated.

<sup>d</sup>Drained Condition: N = Undrained and Y = drained.

<sup>e</sup>Data not available.

## CONSULTATION DRAFT

The seventh test series for which a relatively high correlation coefficient was obtained was conducted at 200°C. Comparison with the results from ambient temperature tests on similar material (Bullfrog Member) suggests that the friction angle decreases with increasing temperature but that cohesion is unaffected.

The observations in the preceding paragraphs are inconclusive because they are based on limited data. Mechanical tests on tuff samples have shown large variability at any single set of test conditions, especially for compressive strength. Thus, the trends inferred from the limited available data may be either spurious or real. More definitive conclusions cannot be made until more data become available. Additional scoping tests on the welded portion of the Topopah Spring Member are being conducted, and a test program with a better statistical basis has been designed for the Topopah Spring Member (Section 8.3.1.15).

In general both the cohesion and the friction angle are inversely related to sample porosity (Price, 1983). Relationships between the Mohr Coulomb parameters angle of internal friction ( $\phi$ ) and cohesion ( $C_o$ ), and functional porosity ( $n$ ) have been derived (Nimick and Schwartz, 1987):

$$\phi = \sin^{-1} \left[ \frac{(0.079n^{-1.856})}{(2 + 0.079n^{-1.856})} \right] \quad (2-3)$$

$$\text{and } C_o = 51.139 \tan \phi$$

where  $n$  is a volume fraction,  $\phi$  is in degrees, and  $C_o$  is in MPa. These two relationships are not in themselves least-squares fits, therefore, they do not have associated correlation coefficients. Data from approximately 122 tests have been used in the derivations. Therefore, in the absence of measured mechanical data, the porosity of tuff samples could be used to estimate cohesion and friction angle expected for samples of the tuffs from Yucca Mountain.

To date, only one series of tests has investigated the effects of pore-fluid pressure on the strength of tuffs from Yucca Mountain. Olsson (1982) reports results for samples from the Bullfrog Member deformed at 200°C and a nominal strain rate of  $10^{-4} \text{ s}^{-1}$ . Four samples were tested in a dry state at confining pressures of 5, 10, and 20 MPa. Three samples were saturated and tested at effective pressures (confining pressure minus pore-fluid pressure) of 5, 12.5, and 20 MPa. The test results are provided in Figure 2-8. Although data are limited to these seven tests, the results indicate that the concept of effective stress developed for other porous rocks (Handin et al., 1963; Hubbert and Willis, 1957) may hold for tuff as well. Additional testing to examine pore pressure and confining pressure effects on the mechanical properties of the Topopah Spring Member is discussed in Section 8.3.1.15.

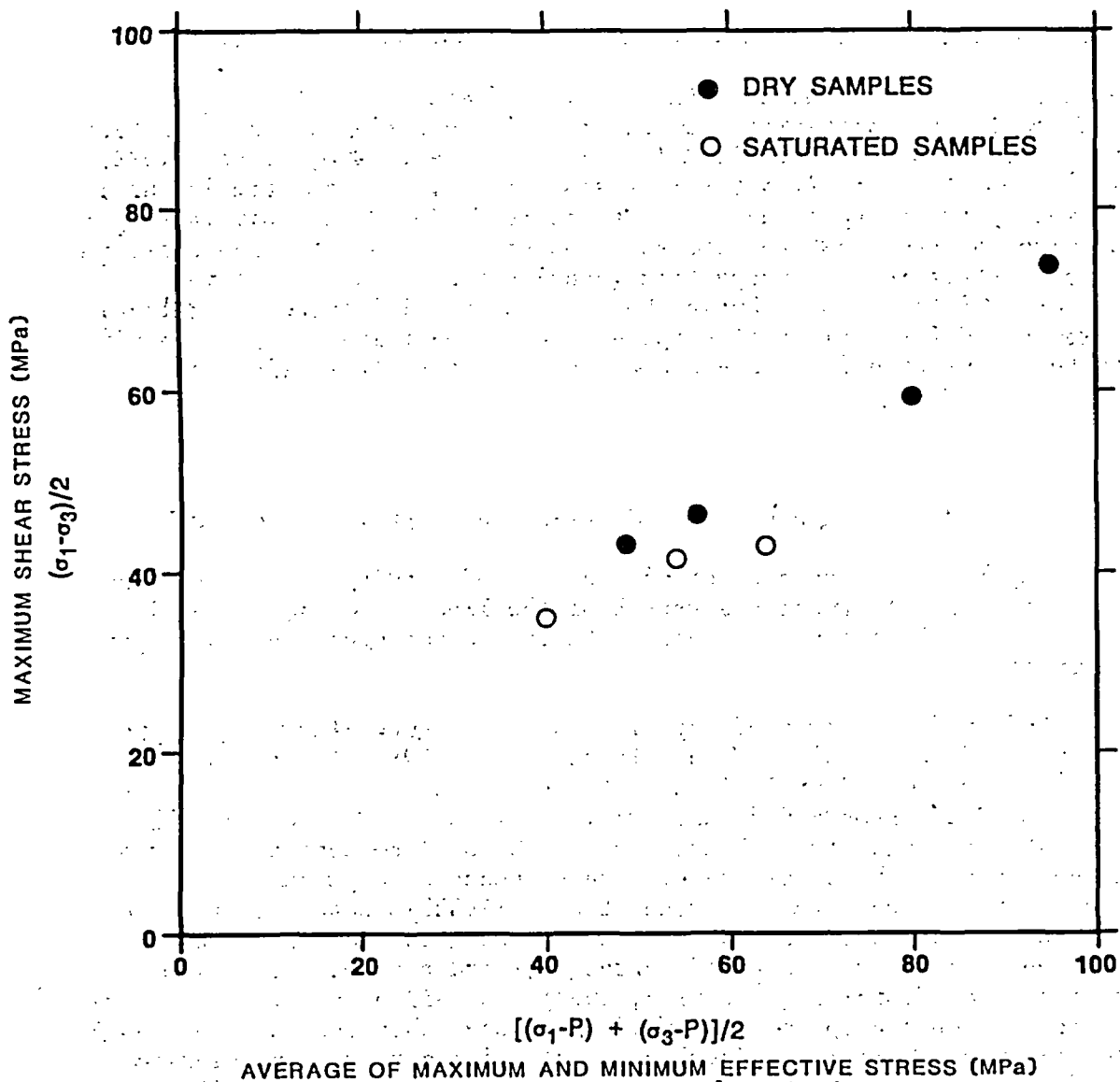


Figure 2-8. Maximum shear stress at failure for the Bullfrog Member, as a function of the average of maximum and minimum effective stresses (Mohr diagram for triaxial tests). Key:  $\sigma_1$  = maximum normal stress,  $\sigma_3$  = minimum normal stress, and P = pore pressure.

### 2.1.2.3.1.3 Effects of elevated temperature on compressive strength

The strength of most engineering materials (metals, plastics, concretes, rocks) decreases with increasing temperature. The experimental data on tuff at elevated temperatures are limited (Olsson and Jones, 1980; Olsson, 1982; Price, 1983), and the data from the 15 tests completed to date are inconclusive in quantifying strength changes. The tests differed not only in temperature but also in other test conditions (pressure, strain rate, and confining pressure) and intrinsic rock properties (density and porosity). A test series on cores of the Topopah Spring Member has been initiated to evaluate the strength and deformability of samples at elevated temperatures, and additional tests are planned for the exploratory shaft activities (Section 8.3.1.15.).

### 2.1.2.3.1.4 Rate-dependent behavior and effect on compressive strength

The strength of rock depends on of the rate of loading or strain. The possibility that the compressive strength of the Topopah Spring Member is rate-dependent must be assessed to help establish a conservative lower bound on this parameter.

The data from five series of experiments on site-specific tuffs (Price and Jones, 1982; Price et al., 1982b; Nimick et al., 1985; Nimick and Schwartz, 1987) are listed in Table 2-6, while the results from two series on Rainier Mesa tuffs (Olsson and Jones, 1980) are listed in Table 2-4. The test series show average strength decreases of 3 to 14 percent per order-of-magnitude decrease in the strain rate. The sequence of experiments on the Topopah Spring Member reported by Price et al., (1982b) showed virtually no strain rate effect on strength, but the three other test series on this material showed decreases of 5 to 14 percent per order-of-magnitude decrease in the strain rate (Nimick and Schwartz, 1987). No effect of strain rate was observed for the Topopah Spring and Bullfrog members when tested at elevated confining pressures (Morrow and Byerlee, 1984). These results showing no rate dependence may reflect the physical and mineralogical variability of the samples tested. Because of a lack of adjacent samples, the core used by Price et al., (1982b) was from an interval ranging from 371.3 to 390.0 m in depth (drillhole USW G-1) and, therefore, probably had a range of physical and mineralogical characteristics. The effects of variations in strain rate on the compressive strength of the Topopah Spring Member are being examined, and additional tests are planned as part of the exploratory shaft program (Section 8.3.1.15).

To predict rock behavior that is nonlinearly rate-dependent, Costin (1983) has developed a preliminary model that uses the assumption that rate- and stress-dependent microcrack growth is responsible for the deformation observed in mechanical tests on low-porosity (<15 percent) materials. The evolution of microcrack density is specified by extrapolating the experimentally determined behavior of single cracks to that of a random ensemble of microcracks. In the Costin (1983) model, stress corrosion is assumed to be the dominant mechanism of rate-dependent crack growth. Therefore, the model assumes an initial population of microcracks that is modified by the stress history.

Table 2-6. Effects of changes in strain rate on rock strength for Yucca Mountain tuffs<sup>a</sup>

Unit <sup>b</sup>	USW G-1 depth (m)	USW G-4 depth (m)	Strain rate <sup>f</sup> (s <sup>-1</sup> )	Strength (MPa)	Axial strain to failure (%)	Young's modulus (GPa)	Poisson's ratio	Reference <sup>c</sup>
TSw2	372.5	---	10 <sup>-2</sup>	157.2	0.48	29.2	0.31	P
TSw2	384.8	---	10 <sup>-2</sup>	149.7	0.49	36.6	---	P
TSw2	372.5	---	10 <sup>-4</sup>	133.8	0.57	27.7	---	P
TSw2	373.0	---	10 <sup>-4</sup>	157.2	0.46	37.5	0.25	P
TSw2	371.3	---	10 <sup>-6</sup>	176.6	0.51	40.8	0.25	P
TSw2	373.0	---	10 <sup>-6</sup>	156.6	0.47	35.3	0.21	P
TSw2	390.0	---	10 <sup>-6</sup>	44.9	0.41	22.9	0.27	P
TSw2	---	226.4	10 <sup>-3</sup>	319	0.95	37.4	0.29	N1
TSw2	---	226.4	10 <sup>-3</sup>	283	0.94	34.0	0.28	N1
TSw2	---	226.4	10 <sup>-3</sup>	280	0.89	38.4	0.25	N1
TSw2	---	226.4	10 <sup>-5</sup>	235	0.72	35.6	0.21	N1
TSw2	---	226.4	10 <sup>-5</sup>	256	0.83	36.8	0.21	N1
TSw2	---	226.4	10 <sup>-5</sup>	279	0.93	34.6	0.21	N1
TSw2	---	226.4	10 <sup>-7</sup>	243	0.69	37.5	0.20	N1
TSw2	---	226.4	10 <sup>-7</sup>	230	0.75	33.6	0.11	N1
TSw2	---	305.5	10 <sup>-5</sup>	179	0.56	33.6	0.32	N1
TSw2	---	305.5	10 <sup>-5</sup>	137	0.45	31.1	---	N1
TSw2	---	305.5	10 <sup>-7</sup>	123	0.44	22.0	0.11	N1
TSw2	---	305.5	10 <sup>-7</sup>	138	0.45	32.8	0.20	N1
TSw2 <sup>f</sup>	---	---	10 <sup>-5</sup>	167	0.46	42.0	0.30	N2
TSw2 <sup>f</sup>	---	---	10 <sup>-5</sup>	157	0.33	49.0	0.26	N2
TSw2 <sup>f</sup>	---	---	10 <sup>-7</sup>	115	0.30	41.9	0.26	N2
TSw2 <sup>f</sup>	---	---	10 <sup>-7</sup>	117	0.32	42.1	0.26	N2
CHn1z	508.4	---	10 <sup>-3</sup>	24.7	0.61	5.41	0.33	PJ
CHn1z	508.4	---	10 <sup>-3</sup>	23.4	0.58	5.45	---	PJ
CHn1z	508.4	---	10 <sup>-5</sup>	25.4	0.57	6.15	0.36	PJ
CHn1z	508.4	---	10 <sup>-5</sup>	16.7	0.43	4.92	0.18	PJ
CHn1z	508.4	---	10 <sup>-7</sup>	21.5	0.55	7.86	0.21	PJ
CHn1z	508.4	---	10 <sup>-7</sup>	19.9	0.51	7.03	0.22	PJ

<sup>a</sup>Data from unconfined, ambient temperature, constant-strain-rate tests on saturated samples allowed to drain during testing.

<sup>b</sup>Unit identifications, thicknesses, and relation to formal stratigraphy are shown in Figure 2-5.

<sup>c</sup>References: P = Price et al. (1982b); PJ = Price and Jones (1982); N1 = Nimick et al. (1985); N2 = Nimick and Schwartz (1987).

<sup>d</sup>The symbol "—" in this column indicates that the column is not relevant to the row in which the dashes appear.

<sup>e</sup>Data not available.

<sup>f</sup>Samples from drillhole USW G-2, 289.1 m depth.

## CONSULTATION DRAFT

As a test of the model's capability, simulations of uniaxial compression tests were performed at various strain rates over the range  $10^{-1}$  to  $10^{-10}$   $s^{-1}$ . The material parameters of the model were chosen to match those of the previously tested Grouse Canyon Member (Olsson and Jones, 1980). The results of the simulation are compared with the mechanical data in Figure 2-9 (data are the same as those shown in Figure 2-7 for saturated samples).

For strain rates between  $10^{-2}$  and  $10^{-6}$   $s^{-1}$ , the model predictions show a reasonable agreement with the limited experimental data that are available. The model predicts that at lower strain rates, the strength decrease with strain rate is less than that indicated by a linear extrapolation from the experimental data. Because in situ strain rates are expected to be lower than the limit of  $10^{-10}$   $s^{-1}$  for which the model has been applied (on the order of  $10^{-12}$  to  $10^{-13}$   $s^{-1}$  before the permanent closure of the repository), determination of the most realistic trend in strength decrease is important in order to perform realistic calculations during the design process. Testing on intact samples from the Topopah Spring Member is planned to determine whether the linear or the nonlinear model (Costin, 1983) is a better representation of the actual conditions expected at Yucca Mountain. This testing is described in Section 8.3.1.15.

The expected strain rates around the repository and in the far field are low enough that deformation mechanisms may be different from those occurring at higher strain rates. The possibility of creep closure of openings in the Topopah Spring Member can be examined using information obtained for other rock types at the pressures and temperatures expected to occur in situ. Exploratory tests to examine the possibility of creep deformation in Grouse Canyon and Bullfrog Member tuffs are summarized by Blacic and Andersen (1983). Experimental problems with this test program, involving loading and data acquisition, introduce some question as to the direct applicability of the test results. Tests are ongoing to determine whether creep deformations are likely in the matrix of the Topopah Spring Member, as discussed in Section 8.3.1.15.

### 2.1.2.3.1.5 Effects of lithophysae on compressive strength

The effects of lithophysae are important in determining the thickness of the Topopah Spring Member that is acceptable for waste emplacement. Should lithophysae-rich portions of the member prove acceptable, more flexibility would exist in the placement, geometry, and spatial extent of a repository within the repository horizon. Of the tuffs studied as part of the NNWSI Project, only portions of the Topopah Spring Member have been observed to contain abundant lithophysal cavities. Ten samples of lithophysae-rich Topopah Spring Member collected from an outcrop at Busted Butte (Figure 2-1) have been deformed in mechanical tests (Price et al., 1985). Samples were right-circular cylinders with diameters of 26.7 cm and lengths of 53.3 cm and contained lithophysal cavities up to several centimeters in diameter. The tests were conducted at room temperature, atmospheric pressure, and a strain rate of  $10^{-5}$   $s^{-1}$ . In addition, to obtain a lower bounding value for strength, the samples were water saturated. The resulting unconfined compressive strengths ranged from 10.3 to 27.8 MPa, somewhat lower than those

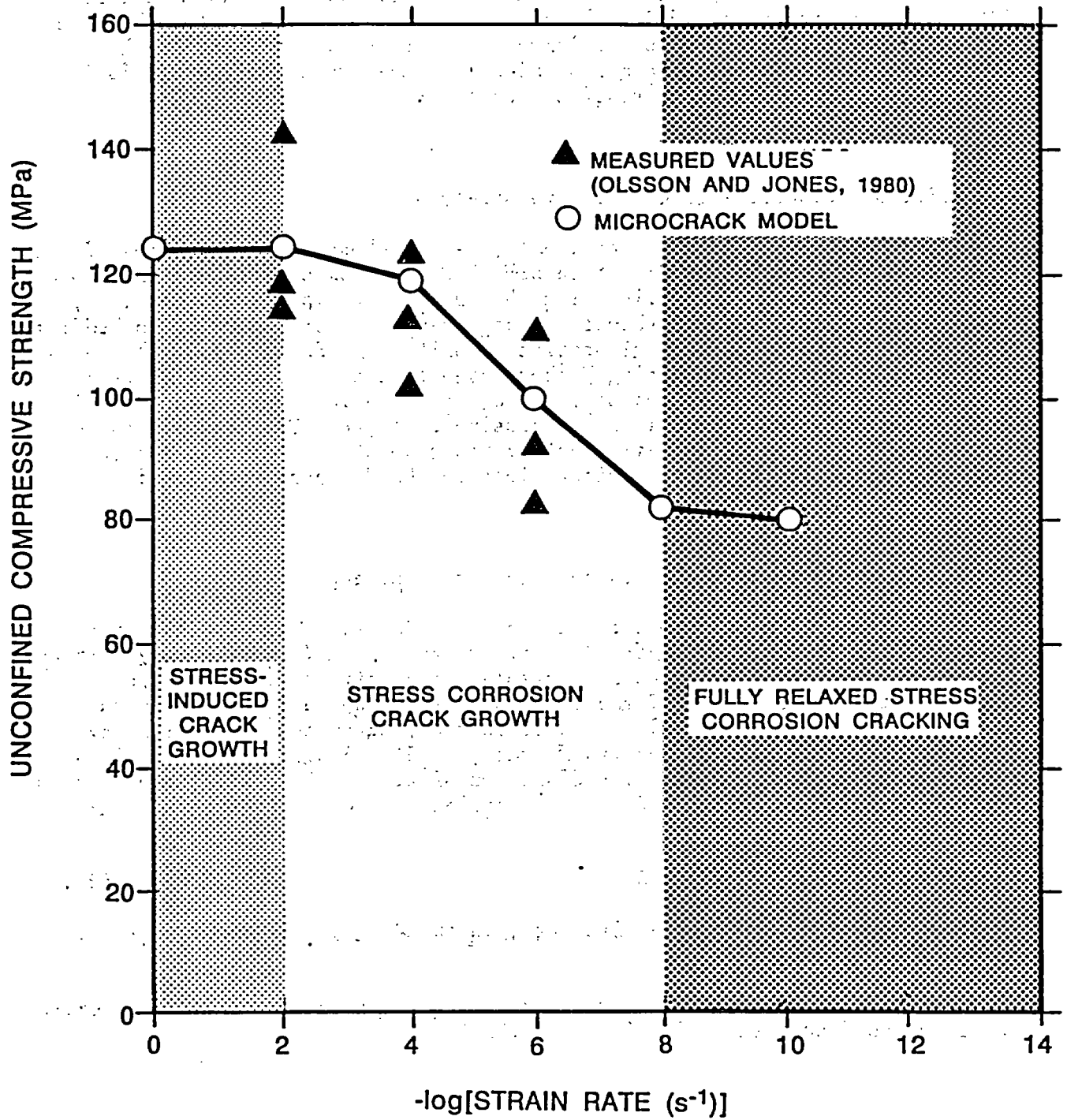


Figure 2-9. Unconfined compressive strength as a function of strain rate for microcrack model, and tuff samples from the saturated Grouse Canyon Member. Modified from Olsson and Jones (1980).

predicted by the model presented in Section 2.1.2.3.1.8 for the porosities (31 to 40 percent) measured for the samples (Price et al., 1985). The lower strengths probably are due to the large cavity sizes in relation to the sample diameter. Tests on larger samples from the exploratory-shaft facility are planned to confirm these results (Section 8.3.1.15).

#### 2.1.2.3.1.6 Anisotropy of compressive strength

To date, all mechanical experiments, except those on five samples of the Topopah Spring Member from drillhole USW GU-3, have been performed on samples with their loading axes parallel with the original coring direction; i.e., approximately vertical and, therefore, approximately perpendicular to bedding (Price et al., 1984). (For orientation of units, see Section 1.2.2.) Tests on samples of the Topopah Spring Member taken from the outcrop at Busted Butte will be conducted to quantify the degree of anisotropy in the elastic properties and in the unconfined compressive strength. The test series, discussed in Section 8.3.1.15, will include measurements on adjacent samples with at least three different orientations to the dominant rock fabric.

#### 2.1.2.3.1.7 Sample size effects on compressive strength

Most tests completed to date have been performed on samples that have a diameter of 2.5 cm and a length of 5 cm. Because of defects (inhomogeneities and fractures) inherent in the rock samples, size effects are expected in both the strength and the deformation behavior of the tuff. Sample size effects are expected to result in lower rock strengths and moduli for the larger samples (Bieniawski and Van Heerden, 1975). A series of unconfined compression tests on samples with diameters of 2.5, 5, 8.3, 12.7, and 22.8 cm has been completed (Price, 1986). A power-law fit to the test results gives the following equation:

$$\sigma_c = 1944D^{-0.846} + 69.5 \quad (2-4)$$

where  $\sigma_c$  is unconfined compressive strength in MPa and D is sample diameter in mm.

Additional tests will be performed on samples from the exploratory shaft facility, as discussed in Section 8.3.1.15.1.

#### 2.1.2.3.1.8 Statistical correlation of compressive strength and functional porosity

Approximately the same sets of tests (unconfined compression, constant strain rate, room temperature on saturated samples) analyzed for elastic properties were also studied to determine whether the uniaxial strength could be related to functional porosity or grain density (Price, 1983; Price and Bauer, 1985). The results showed that changes in compressive strength

between samples can be correlated with changes in functional porosity (except for the vitrophyre of the Topopah Spring Member, as discussed in Section 2.1.2.2).

With the availability of data from the Topopah Spring Member, the analysis of data from 113 samples has provided the following empirical relationship (Price and Bauer, 1985):

$$\sigma_c = 4.04n^{-1.85} \quad (2-5)$$

where  $\sigma_c$  is the unconfined compressive strength (MPa) and  $n$  is expressed as a volume fraction.

The correlation coefficient  $r$  for this fit is 0.93. The approximate range of  $n$  for which this correlation is valid is 0.10 to 0.60.

Analysis of existing data by Nimick and Schwartz (1987) suggests that the equation given above will provide a reliable estimate of the unconfined compressive strength of unit TSw2 (see Figure 2-5 for definitions of units). The equation estimates strengths that are lower than experimental values for the nonlithophysal portion of unit TSw1. Additional analysis is under way to refine the equation.

#### 2.1.2.3.2 Tensile strength

Data on the tensile strength of Yucca Mountain tuffs can be used in the interpretation of in situ stress data obtained by hydraulic fracturing or in the definition of a failure criterion for intact rock. Tensile strengths of Yucca Mountain tuff were calculated from Brazilian (indirect tensile) tests on 20 samples from 4 lithologic units (Blacic et al., 1982). The relationship between these calculated tensile strengths and the corresponding porosities is approximately linear, as determined by Price (1983) and shown in Figure 2-10. This linear relationship may be used for a first-order approximation of the tensile strength of any tuff from Yucca Mountain for which physical properties have been determined; however, a linear extrapolation to lower porosities than those already tested may not be reasonable. As described in Section 8.3.1.15, additional tests on outcrop material are planned to measure the tensile strength of the Topopah Spring Member. The measurements will include both direct tensile tests and Brazilian tests on adjacent material in order to assess the applicability of existing data obtained by the latter test method. In addition, some tensile strength data will be obtained from samples of the Topopah Spring Member from the exploratory shaft facility.

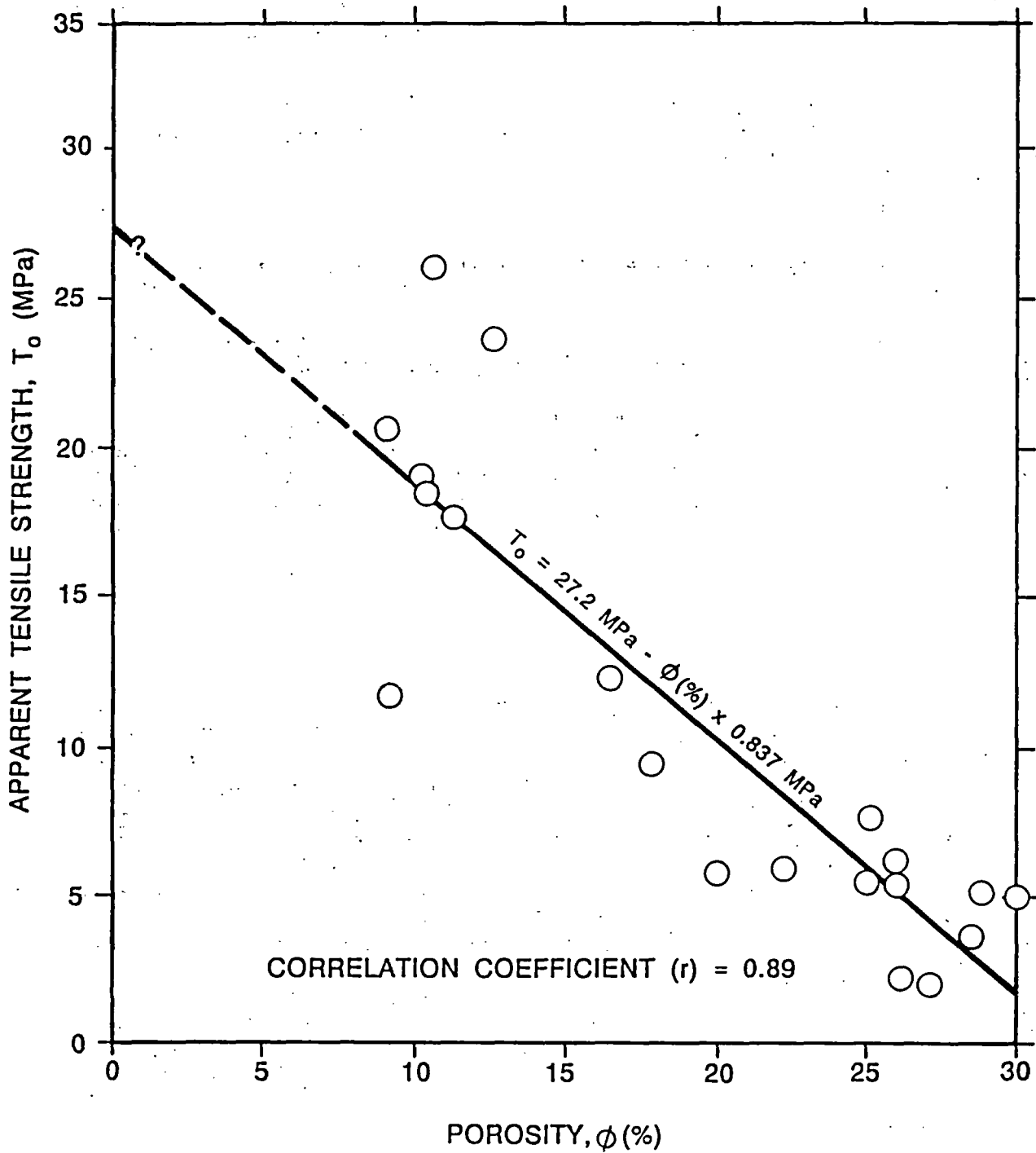


Figure 2-10. Apparent tensile strength of saturated Yucca Mountain tuff as a function of porosity. Modified from Price (1983)

### 2.1.3 STRATIGRAPHIC VARIATIONS OF THE MECHANICAL PROPERTIES OF TUFF

To reduce the large volume of data referenced in the preceding sections to a comprehensible basis for analyses of the repository conceptual design, a mechanical-property stratigraphy has been defined (Figure 2-5 and Table 2-7). Each zone in the thermal/mechanical stratigraphy represents an interval for which mean matrix mechanical properties (and, in some instances, standard deviations) have been determined. Zone boundaries were defined to reflect changes in mineralogical and bulk properties (hence, significant changes in the mechanical properties) and are not always the same as the formal (geologic) stratigraphic divisions described in Section 1.2. The properties presented in Table 2-7 for each zone are the results of experiments where data are available. For other zones, the values of properties have been calculated from the empirical equations presented in Sections 2.1.2.2 and 2.1.2.3 relating mechanical properties to functional porosity, using mean porosity values given in Section 2.4.3. As discussed in Sections 2.1.2.2 and 2.1.2.3, the correlations cannot be used for the vitrophyre of the Topopah Spring Member (Unit TSw3).

The bulk properties used to calculate mechanical properties are discussed in Section 2.4.2.4. The properties predicted with the correlation equations in Section 2.1 inevitably will differ somewhat from experimental data, primarily because of the natural variability of the various tuff units.

### 2.2 MECHANICAL PROPERTIES OF ROCK UNITS--DISCONTINUITIES

Discontinuities (e.g., joints, faults, bedding planes) and inhomogeneities (e.g., lithophysae and inclusions of pumice or lithic fragments) cause the mechanical response of the rock mass to be different from that of the unfractured intact rock. In general, the strength and deformation modulus of the rock mass will be lower than that of the matrix material. The approach taken in the NNWSI Project has been to include the effects of lithophysae and inclusions in studies of intact rock properties (Section 2.1). Thus, this section addresses only the mechanical properties of joints, faults, and bedding planes. Data concerning the geologic and mineralogic characteristics of these features at Yucca Mountain are provided in Chapter 1.

In conventional mine design approaches, the effects of fractures are approximated by assuming that the effective rock mass strength is some percentage of the strength measured for intact material, as shown by experience in similar rocks. More detailed stress analyses use the frictional properties (cohesion and coefficient of friction), orientation, and spacing of joints to determine whether slip can occur along the discontinuities and to evaluate the impact of the slip on support requirements or the usability of the opening. The unique aspect of repository analyses and testing is that the changes in the joint properties with temperature need to be bounded to evaluate opening stability at the temperature expected in the rock before permanent closure. Analyses to bound the effects of possible underground conditions in the tuff will be made to determine whether there are likely to be regions where significant support is required to maintain a stable opening. The data from laboratory tests on jointed tuff that form the basis of current detailed stress analyses are discussed below.

Table 2-7. Mechanical properties for intact rock in the Yucca Mountain tuff zones

Zone <sup>a</sup>	Young's modulus (GPa)	Poisson's ratio	Unconfined compressive strength (MPa)	Tensile strength (MPa)	Angle of internal friction (°)	Cohesion (MPa)
TCw	40.0	0.24(TSw2) <sup>b</sup>	240	17.9	44.7	51
PTn	3.8	0.16(CHn1z) <sup>b</sup>	19	1.0	8.5	8
TSw1	31.7±17.9 <sup>c,d</sup>	0.25±0.07 <sup>c,d</sup>	127±16 <sup>c,d</sup>	21.1±4.6 <sup>c</sup>	34.9 <sup>c</sup>	36 <sup>c</sup>
	15.5±3.2 <sup>d,e</sup>	0.16±0.03 <sup>d,e</sup>	16±5 <sup>d,e</sup>	1.0 <sup>e</sup>	12.5 <sup>e</sup>	11 <sup>e</sup>
TSw2	30.4±6.3 <sup>d</sup>	0.24±0.06 <sup>d</sup>	166±65 <sup>d</sup>	15.2	23.5 <sup>d</sup>	34.5 <sup>d</sup>
TSw3	NA <sup>g</sup>	NA	NA	NA	NA	NA
CHn1v	7.1	0.16(CHn1z) <sup>b</sup>	27	1.0	12.0	11
CHn1z <sup>f</sup>	7.1±2.1 <sup>d</sup>	0.16±0.08 <sup>d</sup>	27±9 <sup>d</sup>	1.0	7.6±2.6 <sup>d</sup>	10.9±1.6 <sup>d</sup>
CHn2	11.5	0.16(CHn1z) <sup>b</sup>	40	2.6	16.4	15
CHn3	7.1	0.16(CHn1z) <sup>b</sup>	27	1.0	12.0	11
PPw	16.3	0.13(BFw) <sup>b</sup>	57	6.9	21.0	20
CFUn	7.6±3.8 <sup>d</sup>	0.16(CHn1z) <sup>b</sup>	31±11 <sup>d</sup>	1.8	15.6	14
BFw <sup>f</sup>	10.8±4.7 <sup>d</sup>	0.13±0.02 <sup>d</sup>	42±14 <sup>d</sup>	6.9	21.0	20
CFMn1	15.2	0.16(CHn1z) <sup>b</sup>	52	6.0	19.9	19
CFMn2	16.3	0.16(CHn1z) <sup>b</sup>	57	6.9	21.0	20
CFMn3	13.2	0.16(CHn1z) <sup>b</sup>	45	4.3	18.0	17
TRw <sup>f</sup>	17.6±3.8 <sup>d</sup>	0.13(BFw) <sup>b</sup>	72±23 <sup>d</sup>	11.1	27.6	27

<sup>a</sup>Zone identifications, thicknesses, and relation to formal stratigraphy are shown in Figure 2-5.

<sup>b</sup>Value assumed to be the same as mean value of thermal/mechanical unit listed in parentheses.

<sup>c</sup>Representative of nonlithophysal zones within unit TSw1.

<sup>d</sup>Experimental results for mechanical properties at baseline test conditions (see text); standard deviations are 1σ. All other mechanical data entries are calculated using porosity with empirical equations; no standard deviations are available for these entries.

<sup>e</sup>Representative of lithophysal zones within unit TSw1.

<sup>f</sup>Zones previously considered for waste emplacement horizon.

<sup>g</sup>NA = not available.

Laboratory-derived mechanical properties of joints are believed to provide data applicable to the mechanical properties of faults and bedding planes (Barton, 1973; Byerlee, 1978). Therefore, current investigations have concentrated on the laboratory properties of joints. Initial tests used simulated joints (precut) in about 60 samples of both welded and nonwelded tuffs to determine the coefficient of friction for the joints and to compare the results with those for other rock types. The use of relatively smooth simulated joints is a reasonable means of estimating lower-bound properties for natural fractures, especially for exploratory tests; however, inferences about the behavior of natural fractures that can be drawn from test results may be limited. Additional tests are being conducted on samples of the Topopah Spring Member with both simulated and natural joints, as discussed in Section 8.3.1.15. The applicability of these data ultimately will be determined by comparison with larger-scale in situ tests.

The data discussed below constitute an initial data base for conceptual design and performance assessment modeling studies. Such studies are required to ensure compliance of a repository with regulatory criteria. Specifically, to estimate stability of openings, the retrievability of the emplaced waste, and the effect of potential changes in joint apertures on ground-water movement and radionuclide releases, the response of joints to the presence of a repository must be understood.

In the laboratory tests performed on joints, specimens in the form of right-circular cylinders with sawcuts at 35 degrees to the cylinder axis were deformed in triaxial compression at room temperature, confining pressures to 40 MPa, and axial displacement rates from  $10^{-2}$  to  $10^{-6}$  cm/s with various saturation states (Olsson and Jones, 1980; Teufel, 1981). Because neither the American Society for Testing and Materials nor the International Society for Rock Mechanics has published standard procedures for jointed-rock testing, these reports include detailed discussions of the test apparatus, instrumentation, sample preparation techniques, and test procedures.

### 2.2.1 MECHANICAL PROPERTIES OF DISCONTINUITIES IN OTHER ROCKS

The magnitude of shear stress that can be transmitted across a joint depends on the cohesion and the frictional properties of the joint, or joint infilling, or both. Shear-strength parameters for discontinuities in similar rock types have been reviewed and are summarized here to allow comparison with the tuff properties presented in the remainder of Section 2.2.

The coefficient of friction is generally independent of rock type and increases only with increasing surface roughness (Paterson, 1978). The effect of surface roughness, found to be important only at low normal stresses, is a result of the interlocking of asperities along the sliding surface. Quasi-static experiments on a variety of jointed-rock types with extreme variations in surface roughness have shown that the coefficient of friction can vary from 0.4 to 5.7 at low normal stresses (Barton, 1973). The higher value is probably not a true friction angle at low normal stresses, because multiple surfaces are involved in sliding (Patton, 1966). At higher normal stresses, surface roughness becomes less significant because asperities are sheared off and incorporated into gouge along the sliding surface.

Quasi-static measurements of coefficients of friction for joints of differing surface roughness in a wide variety of rock types have been compiled (Byerlee, 1978). They show that the coefficient of friction ranges from 0.4 to 1.0 at normal stresses greater than 10 MPa. The results of an experimental study (Teufel, 1981) on simulated joints in welded tuff are consistent with Byerlee's compilation. Normal stresses across the joints in the experimental study were 5 to 40 MPa (Byerlee's compilation considered 8 to 70 MPa), and all measured values of the coefficient of friction in both studies were less than 1.0.

The cohesion of jointed rock also shows no strong dependence on rock type and generally is less than 0.4 MPa (Jaeger and Cook, 1979). For jointed, welded tuff with smooth joint surfaces, cohesion was found to be less than 1 MPa (Teufel, 1981).

The deformation that occurs normal to a fracture will depend on the magnitude of the effective stress, the aperture and roughness of the fracture when the stress is applied, and on the elastic and strength properties of the material bounding the fracture. In general, a fracture will be less compliant (more stiff) as the stress increases, as the aperture decreases, or as the bounding material is less compliant (e.g., has a higher Young's modulus). Sun et al. (1985) summarize data on various types of rocks that indicate monotonic but nonlinear decreases in normal compliance with increasing normal stress. Zimmerman et al. (1986) summarize theoretical and experimental studies of normal response of joints in the Grouse Canyon Member to stress. Results for the Grouse Canyon Member suggested that the normal compliance is sensitive to stress history (i.e., stress cycling results in hysteretic response).

## 2.2.2 MECHANICAL PROPERTIES OF DISCONTINUITIES IN ROCKS AT THE SITE

Existing data on the mechanical properties of discontinuities in tuff are limited to simulated joints (Olsson and Jones, 1980; Teufel, 1981; Morrow and Byerlee, 1984). In these studies, sawcuts were made in samples from the Grouse Canyon Member from Rainier Mesa and from the Prow Pass, Bullfrog, and Topopah Spring members from Yucca Mountain. A summary of mechanical-test results on discontinuities in tuff is presented below under several topics: mechanical properties of simulated joints, mechanical properties of natural joints, effects of water saturation, effects of displacement rate, and time-dependent behavior. At present, no data have been measured to quantify the normal stiffness of joints in tuff (used to estimate the deformation modulus of the rock mass). Tests are in progress to obtain these data (Section 8.3.1.15).

### 2.2.2.1 Simulated fractures

Teufel (1981) determined the shear strength in triaxial compression of a simulated joint in the welded Grouse Canyon Member as a function of normal stress, time of stationary contact, displacement rate, and saturation. Joints were simulated by using a right-circular cylinder with a precut

inclined at 35 degrees to the cylinder (load) axis. Room temperature tests were conducted at confining pressures from 5 to 40 MPa, at axial displacement rates from  $10^{-2}$  to  $10^{-6}$  cm/s, and with both dry and fully saturated samples.

The shear strength of a simulated joint in welded tuff fits the linear relation

$$\tau = \tau_0 + \sigma \tan \phi \quad (2-6)$$

where

$\tau$  = shear strength  
 $\tau_0$  = cohesion  
 $\sigma$  = applied normal stress  
 $\phi$  = friction angle  
 $\tan \phi$  = coefficient of friction:

The coefficient of friction at the initiation of slip was found to be independent of the normal stress for air-dried samples, with a value of 0.64 at a displacement rate of  $1.2 \times 10^{-4}$  cm/s (Figure 2-11). Similar results ( $\tan \phi = 0.59$ ) were obtained for air-dried samples of partially welded tuff (Prow Pass Member) at a displacement rate of  $10^{-3}$  cm/s (Olsson and Jones, 1980) (Figure 2-12). Data provided by Morrow and Byerlee (1984, Figure 2) can be used to derive a coefficient of friction of 0.59 for the initiation of slip in saturated samples of the Topopah Spring Member at a strain rate of  $10^{-4}$  s<sup>-1</sup> (equal to a displacement rate on the fracture surface of approximately  $7 \times 10^{-4}$  cm/s). The independence of the coefficient of friction with respect to the confining pressure and the corresponding normal stress across the sliding surface is consistent with rock-friction literature as reviewed by Byerlee (1978). However, at low normal stresses the coefficient for friction of rough natural joints may have some dependence on normal stress. This possibility will be examined in future testing (Section 8.3.1.15).

Data presented by Morrow and Byerlee (1984, Figures 2 and 6) suggest that the coefficient of friction increases with progressive-shear displacement across a joint. For saturated samples of the Topopah Spring Member at a strain rate of  $10^{-4}$  s<sup>-1</sup>, the increase would be from 0.59 to 0.76.

#### 2.2.2.2 Natural joints

The mechanical properties of natural and artificial joints in the Topopah Spring Member are being investigated. The natural joints present at Yucca Mountain can be categorized into three groups: (1) healed joints with mineralized surfaces, (2) unhealed joints with no infilling, and (3) unhealed joints with infilling. Frictional behavior will depend on the composition of the infilling. From a mechanical effects standpoint, the behavior of the unhealed joints is expected to be more significant to rock mass response. The condition of core from Yucca Mountain with unhealed joints has been inadequate for representative laboratory mechanical tests. It is expected that joints or faults containing gouge or other infilling may have a lower coefficient of friction than clean, unfilled joints (Byerlee, 1978). The coefficient of friction for typical saturated gouges generally ranges from

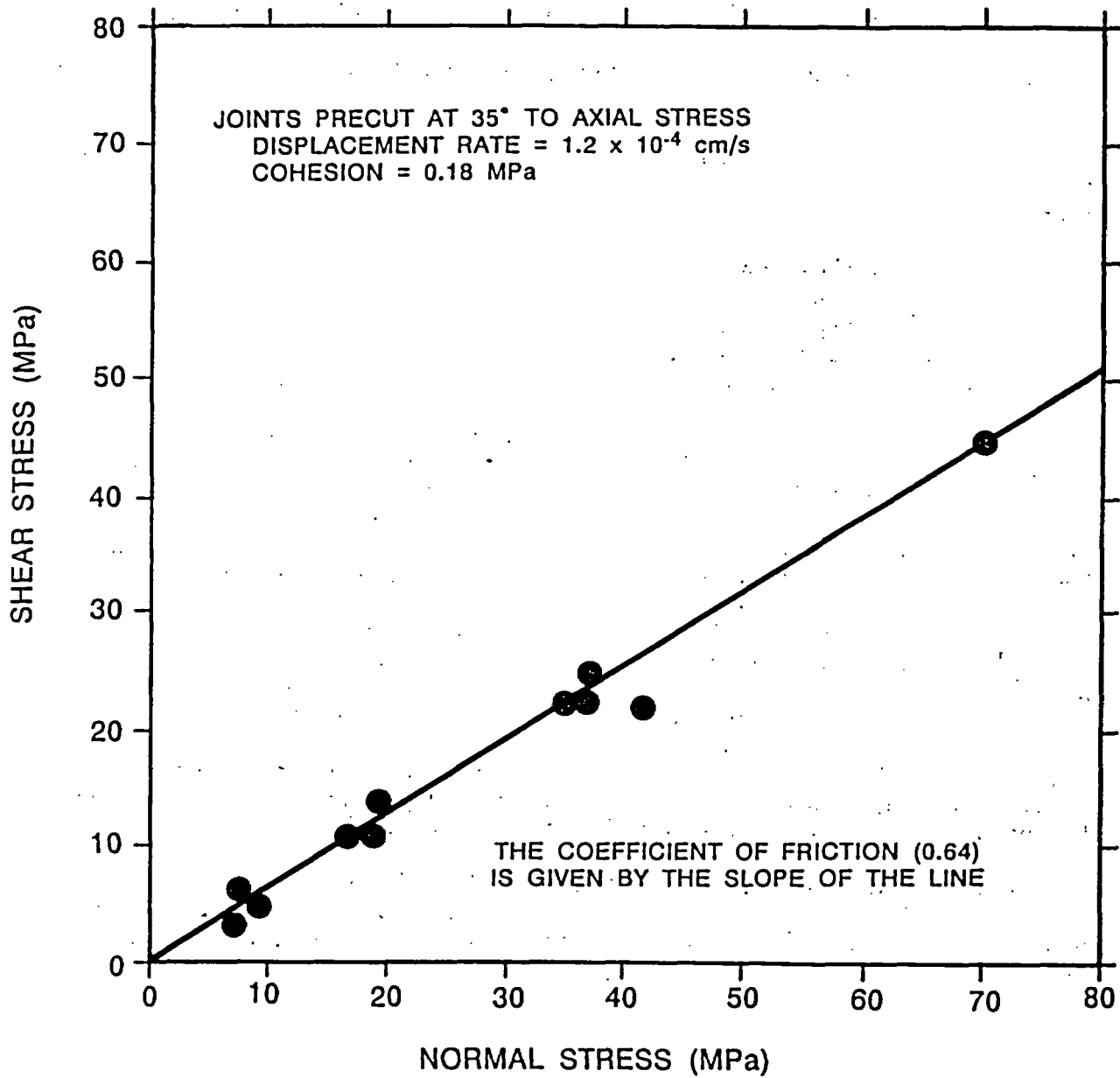


Figure 2-11. Shear stress-to-normal stress relation at slip initiation for air-dried, precut joints in Grouse Canyon Member welded tuff. Modified from Teufel (1981).

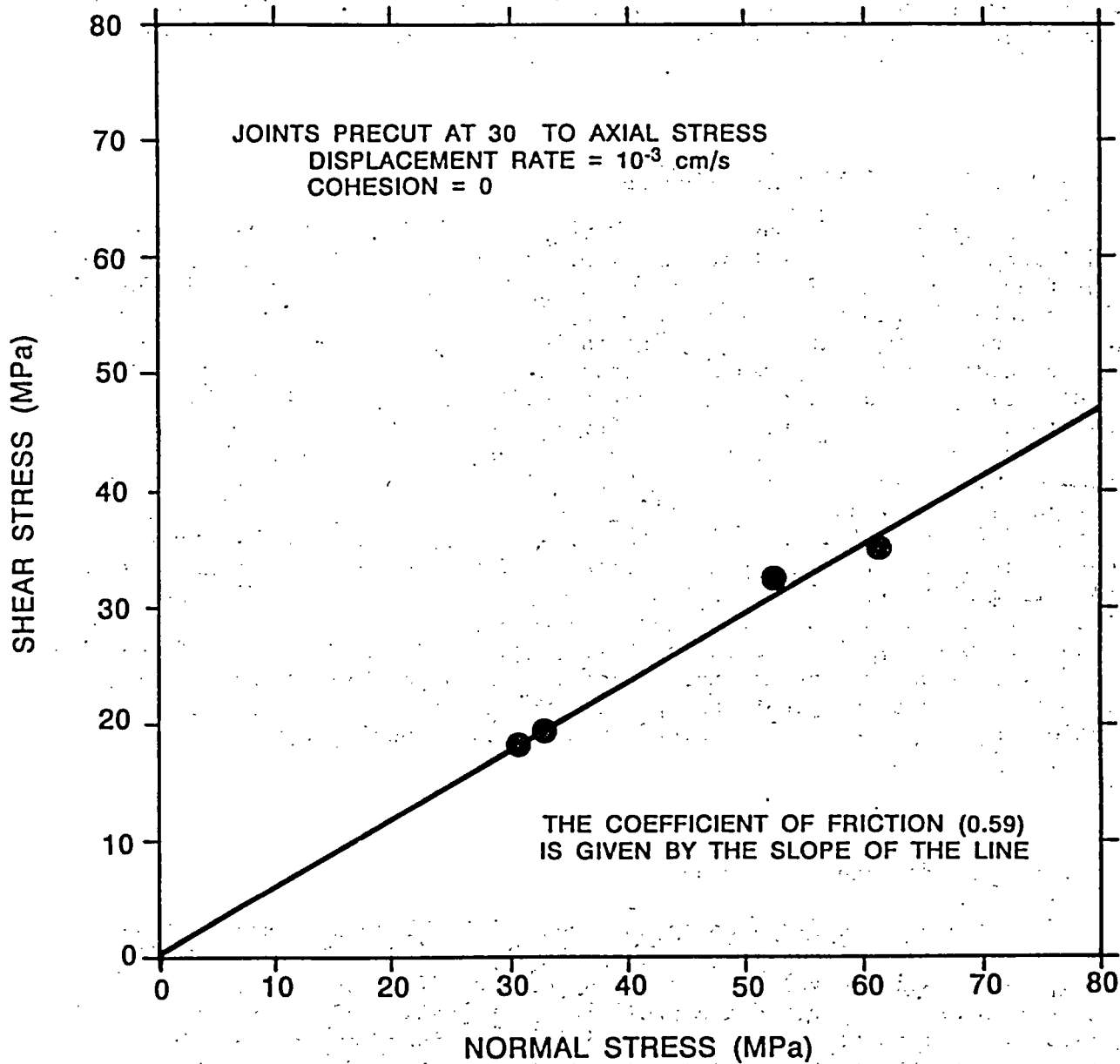


Figure 2-12. Shear stress-to-normal stress relation at slip initiation for air-dried, precut joints on Prow Pass Member partially welded tuff. Modified from Olsson and Jones (1980).

0.2 to 0.6 (Morrow et al., 1982), whereas the coefficient of friction for dry clay gouges has a range of 0.2 to 0.7 (Shimamoto and Logan, 1981). Lower values for the coefficient of friction will result in lower shear strengths for the joints, at constant values of cohesion  $\tau_0$  and applied normal stress  $\sigma$  (Section 2.2.2.1).

#### 2.2.2.3 Effects of water saturation

Even though the Topopah Spring Member is above the water table, Montazer and Wilson (1984) suggest that very limited amounts of water may flow through some fractures. The effects of water saturation on the mechanical properties of simulated joints were investigated by Teufel (1981). The coefficient of friction of a saturated precut joint is independent of normal stress (and thus of moderate fluid pressures within the fracture, by virtue of the effective stress principle), and the shear strength fits the linear relation described earlier. However, the coefficient of friction for the water-saturated precut is 9 percent greater than that for dry precuts, having a value of 0.70 (Figure 2-13). This behavior is attributed by Teufel (1981) to a larger effective contact area along the joint resulting from increased localized failure of the matrix material when saturated. Whereas this has been observed previously, no clear pattern of change in joint strength with saturation state is evident in tests reported for other rocks (Paterson, 1978). From the tuff data obtained to date and observations made in tunnels in Rainier Mesa, variations in joint strength resulting from local changes in the degree of saturation are not expected to lead to major changes in local support requirements. Tests are planned to investigate the effects of saturation on the properties of joints in the Topopah Spring Member (Section 8.3.1.15).

#### 2.2.2.4 Time-dependent behavior

Time-dependent effects on joint strength have been addressed in two ways. Constant displacement-rate tests have provided insight into the effect of changes in sliding velocity on the sliding coefficient of friction. Hold times in these tests provided a preliminary evaluation of the increase in the static coefficient of friction of the joint as a function of time. The data were taken to attempt to quantify the joint strength increases that occur with time for use in evaluating the maximum in situ joint strength.

To determine the effect of sliding velocity on the coefficient of friction of a precut joint, a series of room-temperature tests was conducted at a confining pressure of 10 MPa and axial displacement rates from  $10^{-2}$  to  $10^{-6}$  cm/s (Teufel, 1981). As shown in Figure 2-14, the coefficient of friction for oven-dry samples increased from 0.62 at  $10^{-2}$  cm/s to 0.66 at  $10^{-6}$  cm/s, a 6 percent increase in the coefficient of friction over four orders of magnitude decrease in displacement rate. These results are consistent with the work of Dieterich (1978) and Teufel and Logan (1978) for granites and sandstones, respectively. For water-saturated joints, the displacement rate effects are slightly greater, but again, the effect is small; only a 9 percent increase in the coefficient of friction over 4 orders of magnitude

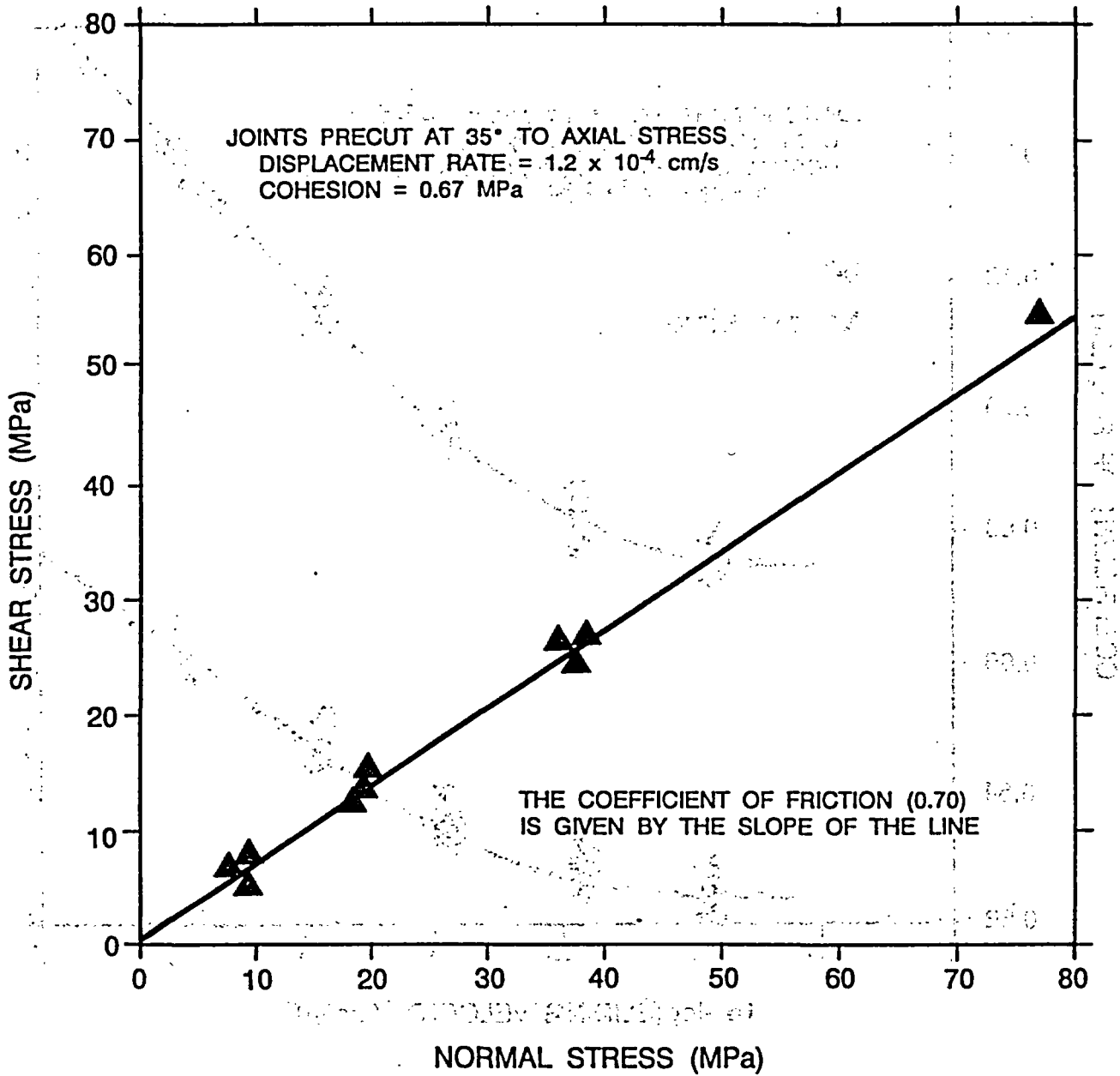


Figure 2-13. Shear stress-to-normal stress relation at slip initiation for water-saturated precut joints in Grouse Canyon Member welded tuff. Modified from Teufel (1981).

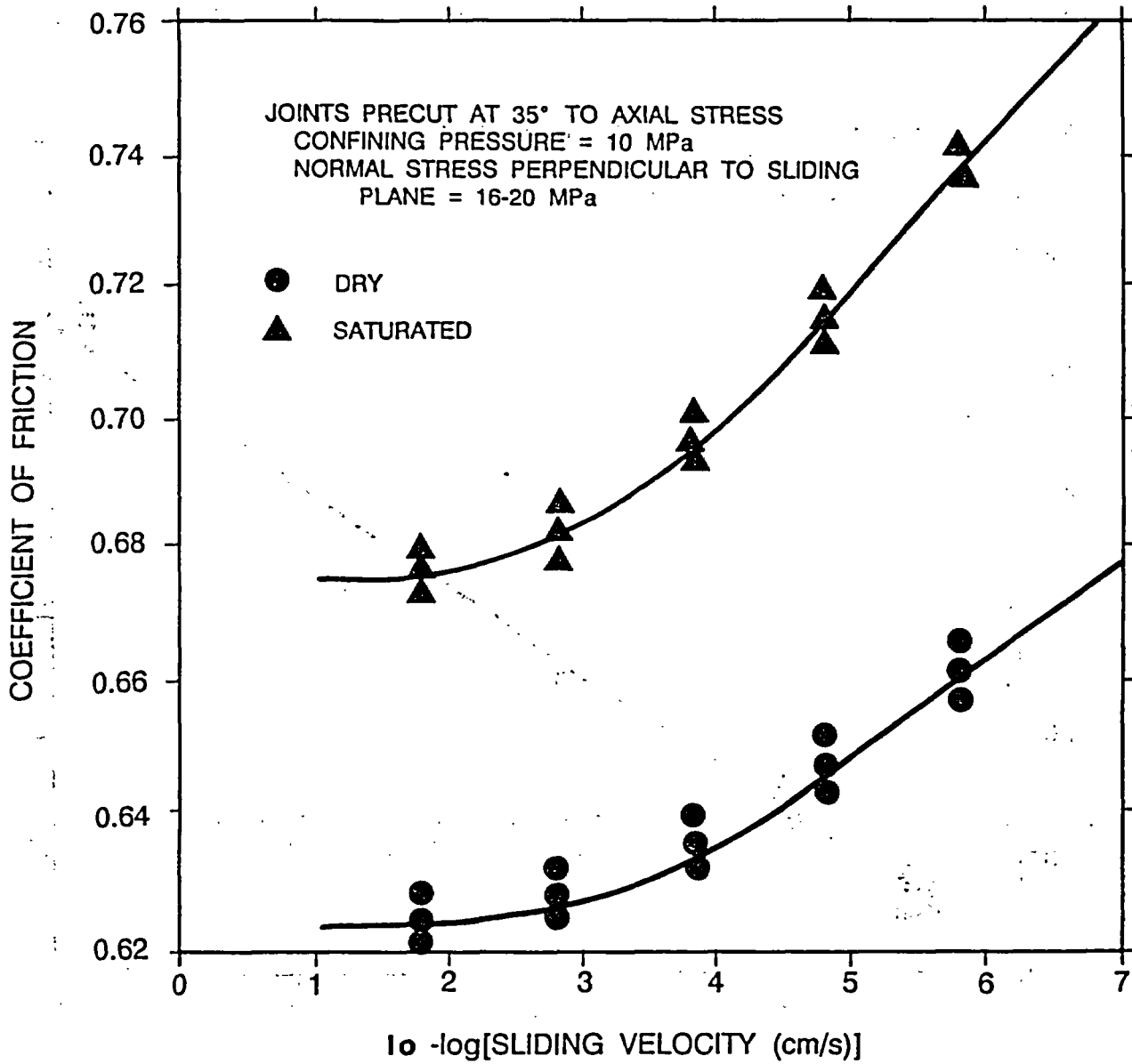


Figure 2-14. Plot of the coefficient of friction against log sliding velocity for oven-dried and water-saturated joints for Grouse Canyon Member welded tuff. Modified from Teufel (1981).

decrease in displacement rate (Figure 2-14). As noted in the previous section, over the observed range of displacement rates the coefficient of friction for water-saturated precuts is slightly greater than for dry precuts.

To evaluate time-dependent joint strength increases, the time dependence of the frictional shear strength of oven-dried and water-saturated Grouse Canyon Member welded tuff was investigated in triaxial compression by examining the response of 35 degree precuts (Teufel, 1981). A confining pressure of 10 MPa was used. The test procedure was slightly different from that used in the previous quasi-static tests. In the tests of time-dependent behavior, axial load was increased until slip occurred along the precut at a constant sliding velocity of  $1.2 \times 10^{-3}$  cm/s. The test was stopped for a given time under load, and then was started again at the same sliding velocity. This procedure was repeated for several different durations of contact.

The results of the test resembled stick-slip phenomenon observed in many other rock types (Paterson, 1978). A plot of the change in shear stress as a function of displacement (Figure 2-15) shows that when a test was stopped for 60 s and then started again, there was an abrupt increase of approximately 0.4 MPa in the shear stress necessary for slip; then there was a drop back to the former stress level as slip continued at the previous sliding velocity of  $1.2 \times 10^{-3}$  cm/s. With an increase in the time of stationary contact (2,400s), both the stress rise required to initiate slip and the corresponding stress drop were larger. However, the stress required for stable sliding did not change significantly. A plot of the static coefficient of friction at peak stress versus the logarithm of the time of contact for oven-dried samples (Figure 2-16) shows that as the time of contact increased, there was a consistent increase in the friction resisting the initiation of sliding. During these tests, the displacement rate was  $1.2 \times 10^{-3}$  cm/s. The data in Figure 2-16 are considered a lower bound on the static coefficient of friction. Extrapolation of these data to much longer times is not warranted, if only because of the variability of fracture surfaces in situ.

As also shown in Figure 2-16, the time-dependent increase in the coefficient of friction is enhanced with water saturation. The increased time dependence of the frictional resistance of the water-saturated tuff is attributed (Teufel, 1981) to hydrolytic weakening and time-dependent stress corrosion of asperity contacts on the sliding surface.

Because the Topopah Spring Member is heavily fractured (up to 42 fractures per cubic meter in drillhole USW GU-3 (Scott and Castellanos, 1984), the mechanical response to excavation and thermal loading may well be dominated by joint behavior. As such, the time dependence of joint properties would be considered in the evaluation of opening stability, especially with the elevated temperatures expected in the vicinity of a repository. Tests will be conducted to investigate the time dependence of joint properties as a function of temperature (Section 8.3.1.15).

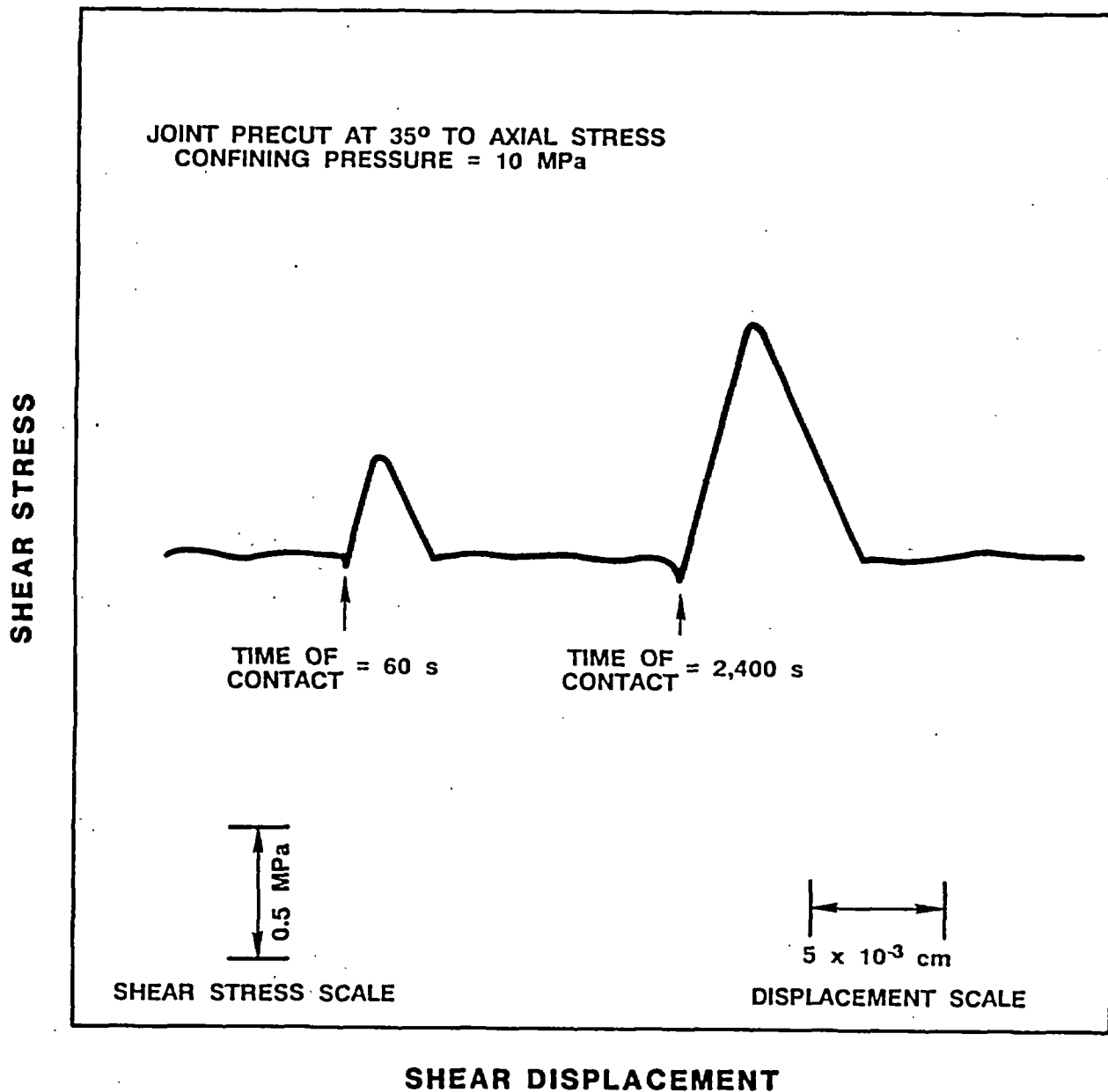


Figure 2-15. Shear stress versus shear displacement for oven-dried Grouse Canyon Member welded tuff sample for 60 and 2,400 s. periods of static contact. Modified from Teufel (1981).

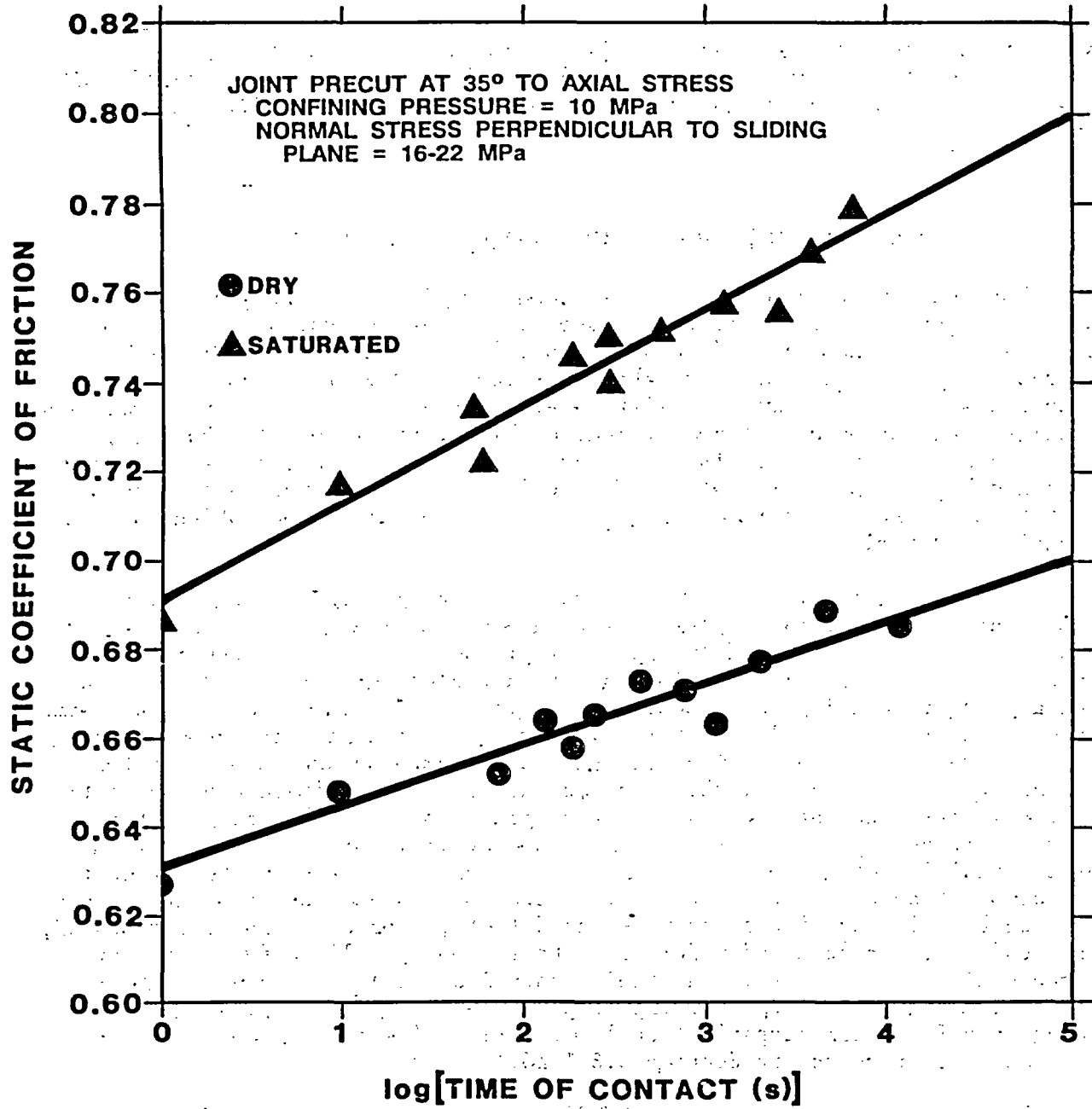


Figure 2-16. Plot of static coefficient of friction against the log time of contact for oven-dried and water-saturated joints in Grouse Canyon Member welded tuff. Modified from Teufel (1981).

### 2.2.2.5 Scale effects

Experimental and theoretical examinations of joints in other rock types suggest that the shear behavior of joints is scale-dependent (see, for example, Bandis et al., 1981). Scaling relationships between the properties of small- and large-scale joints will be evaluated for their applicability to tuff.

## 2.3 MECHANICAL PROPERTIES OF ROCK UNITS--LARGE SCALE

Rock mass mechanical properties (deformability and strength) from in situ tests are desirable for use in repository design analyses and performance assessment and for confirming or establishing scaling techniques for extrapolating data measured in laboratory tests. When rock mass mechanical properties and their variation with time, temperature, and pressure have been obtained, either by direct measurement or by extrapolation of laboratory data, then the response of the rock mass to applied loads (induced by excavation and heat) can be estimated. The definition of this response is important to the task of demonstrating compliance with performance objectives and technical criteria.

Laboratory measurements of strength and elastic modulus, performed on intact unfractured rock samples, are upper-bound values for the in situ rock mass. Where joints are widely spaced, field moduli and strengths may approach moduli and strengths for intact laboratory specimens. However, as the degree of jointing increases, as in welded tuffs, laboratory measurements become less representative of field values. Handbook methods for estimating the degraded properties of the rock mass are known and used widely in the mining industry. However, these methods are only approximate and have not been developed and used to evaluate the effects of thermal stress. Therefore, it is necessary to verify their applicability for a repository because of the addition of thermal stresses to the rock mass. Because the strength and deformation characteristics of the repository-scale rock mass may be controlled by existing discontinuities and defects, representative estimates of, or bounds on, strength and moduli for the rock mass will be determined by large-scale in situ tests. The field tests also will provide an opportunity for evaluating the validity of the coupled thermal and mechanical models being used for thermomechanical analyses. Plans for these field tests and analyses are presented in Section 8.3.1.15.1.

Rock-mass properties for the NNWSI Project have been measured in field tests in the Grouse Canyon Member in G-Tunnel (heated-block and pressurized-slot tests) and will be measured during in situ tests in the Topopah Spring Member in the exploratory shaft (Yucca Mountain heated-block test, shaft convergence, and plate loading measurements). Currently available data and plans for large-scale testing are summarized below.

An important design consideration for subsurface openings is the change in the stress state of the rock resulting from excavation of the openings. A field parameter that is useful in describing this process is the ratio of stress change to the total strain change (elastic and inelastic). This parameter is termed the "modulus of deformation." In contrast, the modulus of

elasticity is based only on the ratio of the stress change to the elastic strain change (the linear portion of the stress-strain curve, as shown in Figure 2-17). If no inelastic behavior occurs, the moduli will be identical. Both the modulus of deformation and the modulus of elasticity are used to predict how the rock surrounding the repository opening deforms after excavation.

The amount of eventual stress change that occurs in the rock around an underground opening in response to excavation is a strong function of the distance from the opening. As discussed in the preceding paragraph, the modulus may change with a change in stress, but other properties (e.g., fracture permeability, thermal conductivity, and strength) may also be affected. Thus, to perform relevant analyses of the repository and the surrounding rock, it is important to incorporate the effects of the zone around a repository wherein property changes have occurred. Tests to provide the required data are described in Section 8.3.1.15.1.

Before 1984, field measurements on G-Tunnel tuffs were limited to borehole jacking tests (Zimmerman and Vollendorf, 1982) to determine rock deformability. The parameter derived from such testing is the modulus of deformation. The original data have been updated by Nimick (1987) to reflect recent changes in the theoretical basis for reduction of the test data (Hustrulid, 1976; Heuze and Salem, 1977; Heuze and Amadei, 1985).

Large-scale studies performed or underway in G-Tunnel include a heated-block test and three pressurized-slot experiments. Standardized test procedures for these tests are unavailable, although a suggested American Society for Testing and Materials procedure for heated-block tests has been published (Hardin et al., 1985). A thorough evaluation of the limitations of the instrumentation and data will be made to define in detail the procedures for testing in the exploratory-shaft facility.

### 2.3.1 MECHANICAL PROPERTIES OF OTHER ROCKS

Available data on large-scale mechanical properties of other rocks have been reviewed to assess the relative magnitude of typical in situ and laboratory-scale moduli values and to compare tuff properties. These data are presented in Table 2-8. Seventy percent of the ratios of field-to-laboratory moduli fall between 0.2 and 0.62 with an average ratio for this group of 0.43. If all the ratios in the table are included, the average ratio is 0.53. Comparison with the data for the Grouse Canyon Member (Section 2.3.3) shows the ratio to be slightly higher than for the average of other rocks.

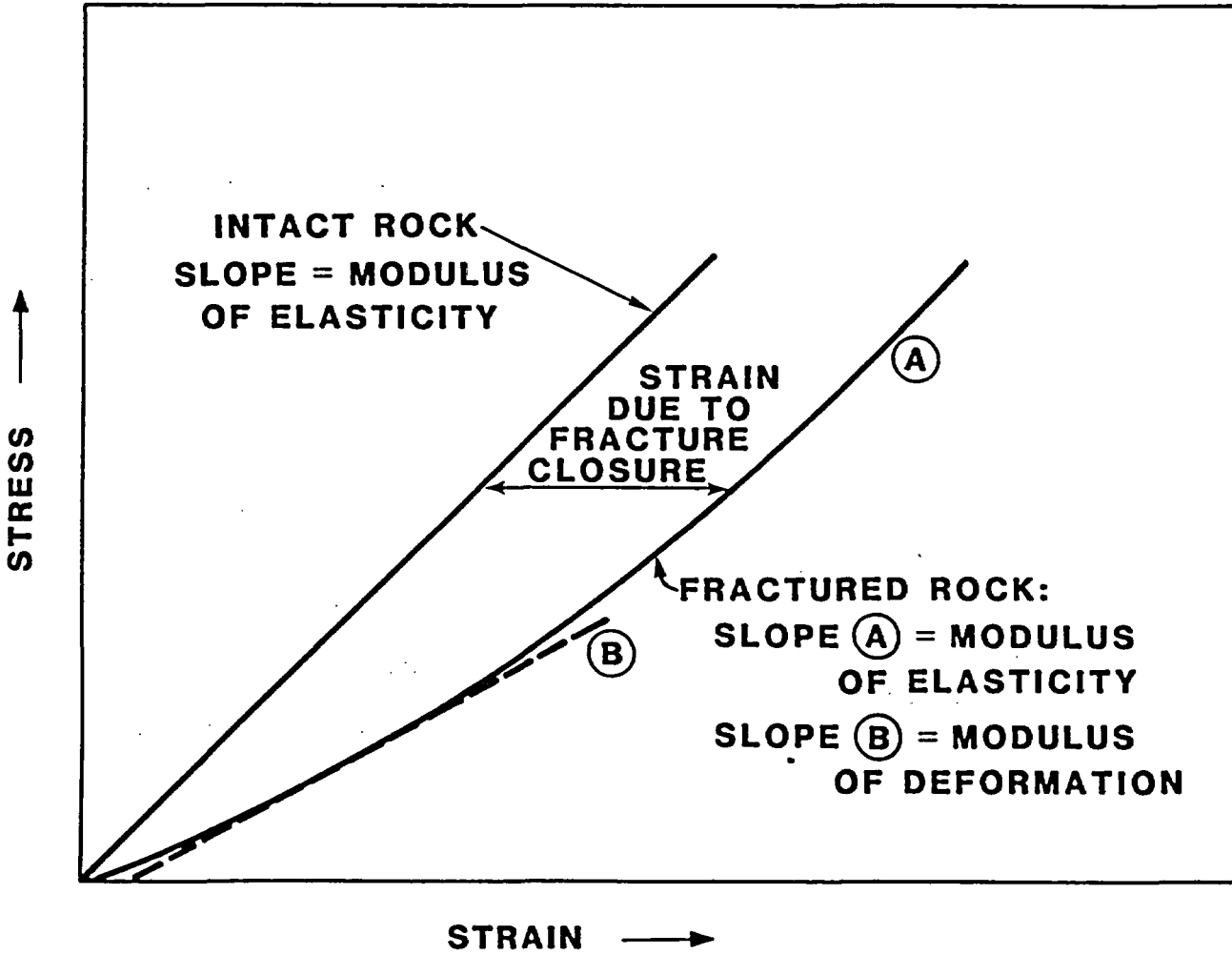


Figure 2-17. Schematic comparison of stress-strain relationship for intact rock and fractured rock mass. Modified from Tillerson and Nimick (1984).

CONSULTATION DRAFT

Table 2-8. Large-scale mechanical properties of other rock<sup>a</sup>

Rock type	Field test method	Average field modulus of deformation (GPa)	Corresponding laboratory modulus of elasticity (GPa)	Ratio of field to laboratory value
Massive amphibolite	Flatjacks	51.8	89.0	0.58
Gneiss/granite	Flatjacks	57.5	59.1	0.97
Mudstone	Flatjacks	20.6	34.5	0.60
Massive granite gneiss	Goodman jack	23.6	51.7	0.45
Fractured diorite gneiss	Goodman jack	5.8	77.9	0.07
Blocky marble	Flatjacks	12.4	47.5	0.26
	Goodman jack	14.0	47.5	0.30
Granite	Large flatjacks	29.2	15.0	1.95
Quartzite	Flatjacks	58.0	67.0	0.87
Quartzite gneiss	Flatjacks	28.8	27.0	1.07
	Goodman jack	16.6	27.0	0.61
Greywacke	Small flatjacks	45.5	73.4	0.62
	Large flatjacks	42.2	73.4	0.57
	Goodman jack	28.4	73.4	0.39
Phyllite	Small flatjacks	33.7	56.0	0.60
	Goodman jack	12.0	56.0	0.21
Copper Ore	Flatjacks	13.3	94.5	0.14
		19.0	94.5	0.20
Quartzite	Borehole jack	27.9	56.5	0.49
Granite <sup>b</sup>	Borehole jack	26	70	0.37
Basalt <sup>c</sup>	Flatjacks	40	87	0.46
	Borehole jack	20	87	0.23
Quartz diorite <sup>d</sup>	Block test	3.0	3.7-4.5	0.67-0.81
Granodiorite <sup>d</sup>	Block test	22.8	37.2-57.9	0.39-0.60
Basalt <sup>e</sup>	Block test	35.1-42.7	89	0.39-0.48
Gneiss <sup>f</sup>	Block test	10.7-13.0	63.0	0.17-0.21
Basalt <sup>g</sup>	Modified borehole deformation gage	28.4	75-85	0.33-0.38

<sup>a</sup>Data from Heuze (1980) except as noted.

<sup>b</sup>Hueze et al. (1981).

<sup>c</sup>Lanigan et al. (1983).

<sup>d</sup>Pratt et al. (1972).

<sup>e</sup>Hart et al. (1985).

<sup>f</sup>Richardson et al. (1985).

<sup>g</sup>Dischler and Kim (1985).

### 2.3.2 MECHANICAL PROPERTIES OF ROCKS AT THE SITE

Using a borehole jack the modulus of deformation has been measured in two boreholes in G-Tunnel. The uncorrected average modulus of deformation obtained from the 20 measurements is 12.1 GPa with a standard deviation of 5.0 GPa (Zimmerman and Vollendorf, 1982). Nimick (1987) reports a corrected mean value between 14.7 and 17.6 GPa. This modulus of deformation represents a relatively small volume of material around a borehole; heated-block and pressurized-slot tests should provide modulus values for larger volumes. Ambient temperature testing of the G-Tunnel heated block has been conducted, and field values for the modulus of deformation are available (Zimmerman et al., 1984a). Figure 2-18 shows a schematic diagram of the test. Flatjacks grouted in slots around the block are used to create uniaxial or biaxial stress fields in the block. The heaters (located outside the block) have been positioned so that relatively uniform temperatures can be obtained in the block (Blanford, 1982). Hence, independent thermal and mechanical loads can be applied to a 2-m block of jointed tuff. Ambient temperature testing is used to determine the mechanical properties, and thermal cycle testing is used to measure the coefficient of thermal expansion and changes in the modulus of deformation at elevated temperatures.

A range in deformation moduli of 9.7 to 17.0 GPa was determined during the ambient temperature testing, with stresses ranging from 3.1 to 10.6 MPa (Zimmerman et al., 1984a). Figure 2-19 is a typical load-deformation curve. The lower end of the stress range from Figure 2-19 is considered representative of the in situ pre-excavation stress conditions at the test facility. No anisotropy was observed, which is not surprising because of the orientation of the joints (45 degrees to block edges) and the equal spacing (approximately 0.4 m) for the two orthogonal joint sets. In addition, no change in the modulus with temperature was observed (Zimmerman et al., 1986). The modulus of deformation would be expected to be lower near excavated surfaces because of the joint relaxation and fracturing related to excavation.

Values for the elastic moduli of the G-Tunnel welded tuff were obtained during unconfined compressive strength tests in the laboratory. An average value of 24.7 GPa was obtained at a strain rate of  $10^{-4} \text{ s}^{-1}$  and a value of 26.0 GPa at  $10^{-6} \text{ s}^{-1}$  (Olsson and Jones, 1980). Comparison of the laboratory moduli with the field value suggests a preliminary value for the average field modulus of deformation of between 51 and 56 percent of the intact rock modulus.

Ellis and Swolfs (1983) have published data on the in situ dynamic elastic moduli of tuff units in drillhole USW G-1 that were below the fluid level in the drillhole at the time geophysical logging was performed. The dynamic Young's moduli for units like the tuffaceous beds of Calico Hills and the Bullfrog and Tram members are much higher than values estimated for the in situ static Young's modulus from laboratory data. As discussed in Section 2.1.2.2, dynamic moduli typically are higher than correlative static values (Lama and Vutukuri, 1978).

A pressurized slot (modified Rocha slot) technique (Rocha, 1970) is being developed to measure the modulus of deformation and to evaluate the effect of joint proximity and orientation on the modulus. In this test (Figure 2-20), a flatjack is inserted in a relatively narrow slot and

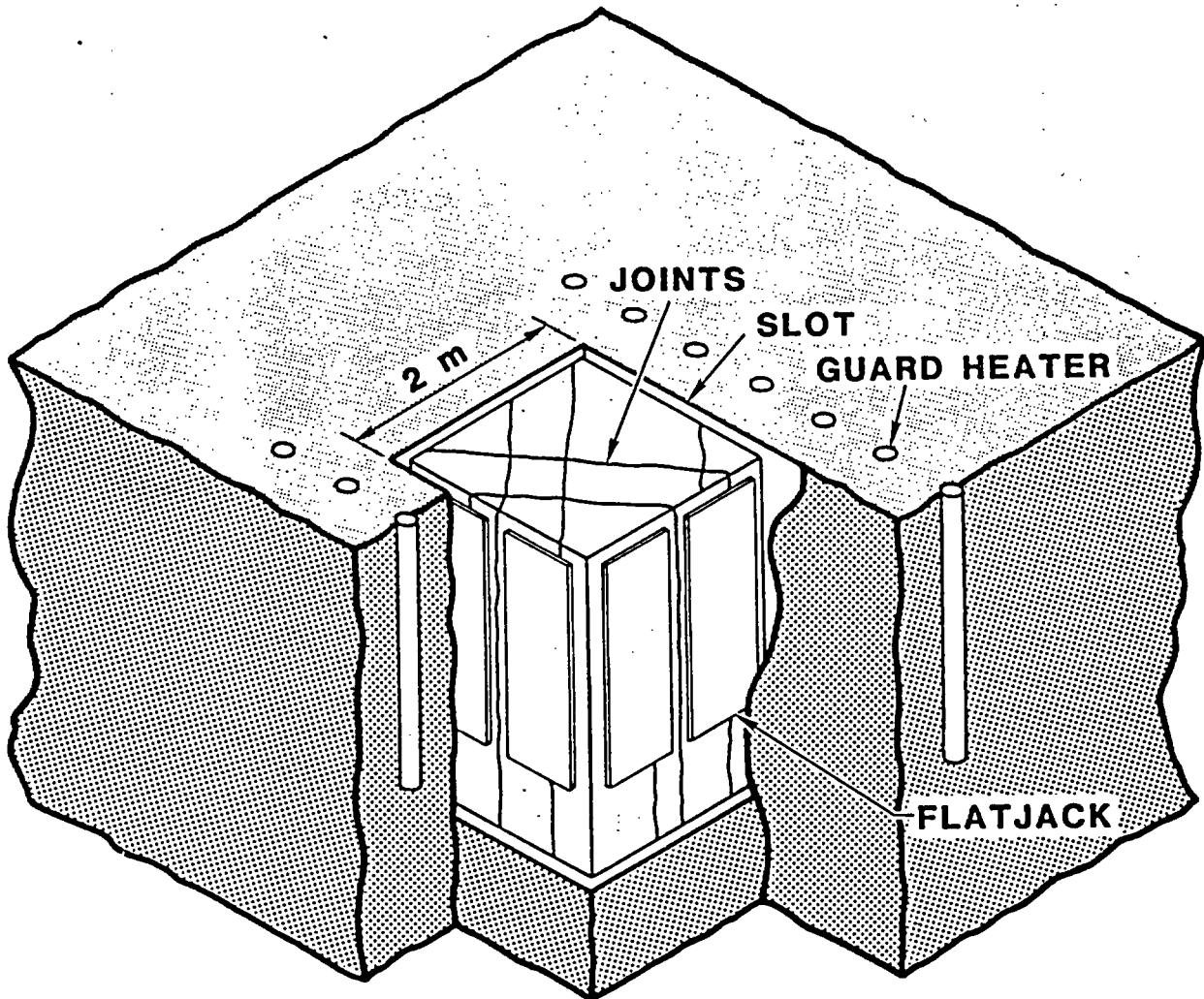


Figure 2-18. Schematic diagram of the heated-block experiment in G-Tunnel underground facility.

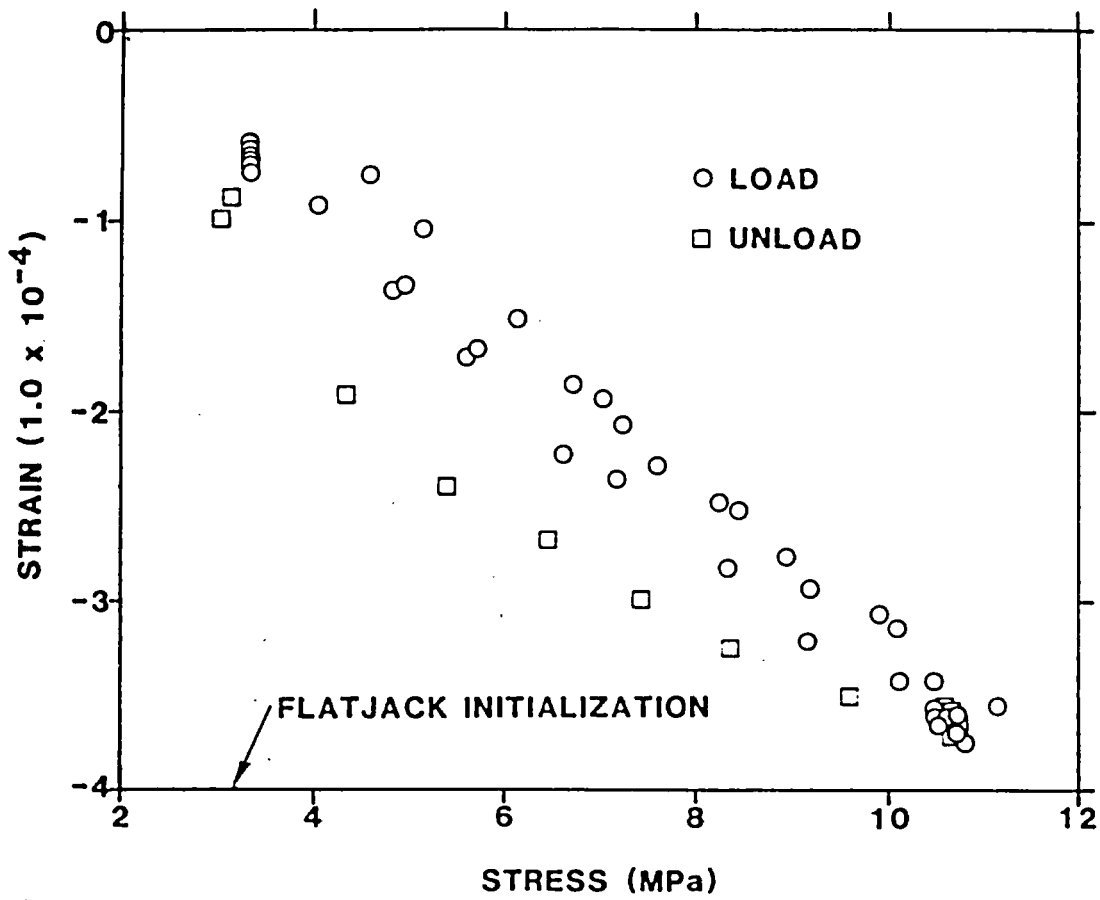
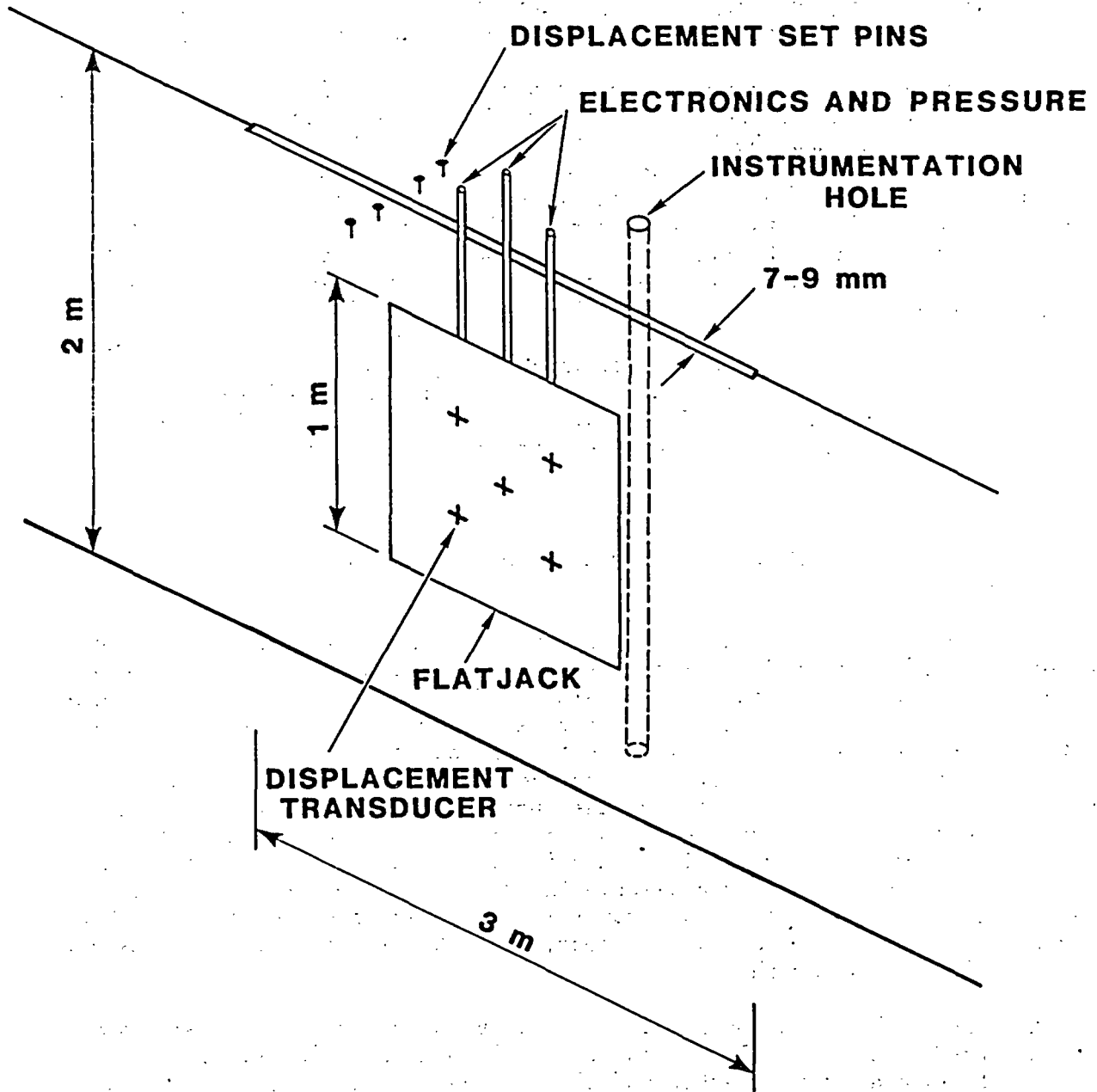


Figure 2-19. Representative plot of horizontal strain versus flatjack pressure (stress) for G-Tunnel heated-block test. Modified from Zimmerman et al. (1984a).



RLN-08/85a

Figure 2-20. Schematic diagram of the pressurized slot test in G-Tunnel underground facility.

## CONSULTATION DRAFT

pressurized. As in the borehole-jacking test, the displacement of the flat-jack is monitored during loading and unloading for use in determining the deformation modulus of the rock mass. In this test, the modulus measured is representative of a larger volume of rock than in the borehole measurements. Slot-cutting techniques being developed for these tests were evaluated in field trials in 1984, and the slot tests were fielded in 1985 and 1986.

Measurements of large-scale rock-mass properties will be made in several of the tests planned for the exploratory shaft facility (Section 8.3.1.15). Plate-loading tests and the Yucca Mountain heated-block test are planned to provide direct measurements of the modulus of deformation. If the rock-mass properties are known, then planned shaft-convergence measurements, excavation-monitoring data (stress, permeability, roof-bolt loads, displacements), and the motion observed in the canister-scale heater test will evaluate the degree to which complicated rock mass response can be modeled with the aid of numerical analysis codes. The use of data from field tests for the validation of these codes is discussed in Chapter 8. The feasibility of in situ evaluation of rock-mass strength is being examined in terms of geometry, loading techniques, fracture spacing, and mining requirements. An in situ strength test will be performed in the exploratory shaft facility, and evaluation is ongoing to determine the appropriate test method.

### 2.3.3 RELATIONSHIP BETWEEN INTACT ROCK, DISCONTINUITIES, AND LARGE-SCALE ROCK PROPERTIES

The preceding section describes efforts to measure the in situ mechanical properties of the tuff, which generally involves a rock volume greater than can be accommodated in the laboratory. However, calculations for design and performance assessment may require rock mass properties before such properties have been measured in field tests. In addition, the number of in situ tests that can reasonably be performed is probably not sufficient to provide direct measurements of rock-mass properties under every unique set of geologic conditions that may be encountered in the rock mass. Therefore, as discussed in Section 8.3.1.15.1, predictive models are necessary to estimate these properties from widely available information. Various methods can be used to estimate these rock mass properties from laboratory data; Table 2-9 provides data pertinent to these methods, and a brief discussion is provided in the following paragraphs.

As discussed in Section 2.3.2, the modulus of deformation in situ has been measured to be 51 to 56 percent of the laboratory value for the block test in the Grouse Canyon Member and 57 to 71 percent for data from Goodman jack tests. The data summarized in Table 2-8 for other rock types suggest corresponding ratios of 0.6 and 0.35, respectively, whereas data for flatjack tests indicate a ratio of 0.58 for field-to-laboratory values. In the absence of field tests in tuffs at Yucca Mountain, a ratio of 0.5 was assumed for field-to-laboratory moduli in order to obtain the moduli in Table 2-9.

Other mechanical properties of the rock mass (unconfined compressive strength, tensile strength, Poisson's ratio, angle of internal friction, and cohesion) can be related to corresponding values for laboratory samples, by various methods. In the absence of a single preferred method, entries for

Table 2-9. Reference values for intact rock and rock-mass mechanical properties and fracture properties for use in analysis of rock-mass mechanical behavior

Unit <sup>b</sup>	Intact rock properties <sup>a</sup>					Cohesion (MPa)	Rock-mass deformation modulus (GPa) <sup>c</sup>	Fracture properties	
	Unconfined compressive strength (MPa)	Young's modulus (GPa)	Poisson's ratio	Tensile strength (MPa)	Angle of internal friction (°)			Cohesion (MPa)	Coefficient of friction
TCw	240	40.0	0.24	17.9	44.7	51	20.0	0.2	0.54
PTn	19	3.8	0.16	1.0	8.5	8	1.9	0.2	0.59
TSw1	127±16	31.7±17.9	0.25±0.07 <sup>d</sup>	12±4.6 <sup>d</sup>	34.9 <sup>d</sup>	36 <sup>d</sup>	15.9 <sup>d</sup>	0.2 <sup>d</sup>	0.54 <sup>d</sup>
	16±5 <sup>e</sup>	15.5±3.2 <sup>e</sup>	0.16±0.03 <sup>e</sup>	1.0 <sup>e</sup>	12.5 <sup>e</sup>	11 <sup>e</sup>	7.8 <sup>e</sup>	0.2 <sup>e</sup>	0.54 <sup>e</sup>
TSw2	166±65	30.4±6.3	0.24±0.06	15.2	23.5	34.5	15.2	0.2	0.54
TSw3	NA	NA	NA	NA	NA	NA	NA	0.2	0.54
CHnlv	27	7.1	0.16	1.0	12.0	11	3.6	0.2	0.59
CHnlz	27±9	7.1±2.1	0.16±0.08	1.0	7.6±2.6	10.9±1.6	3.6	0.2	0.59
CHn2	40	11.5	0.16	2.6	16.4	15	5.8	0.2	0.59
CHn3	27	7.1	0.16	1.0	12.0	11	3.6	0.2	0.59
PPw	57	16.3	0.13	6.9	21.0	20	8.2	0.7	0.59
CFUn	31±11	7.6±3.8	0.16	1.8	15.6	14	3.8	0.7	0.64
BFw	42±14	10.8±4.7	0.13±0.02	6.9	21.0	20	5.4	0.7	0.59
CFMn1	52	15.2	0.16	6.0	19.9	19	7.6	0.7	0.64
CFMn2	57	16.3	0.16	6.9	21.0	20	8.2	0.7	0.64
CFMn3	45	13.2	0.16	4.3	18.0	17	6.6	0.7	0.64
TRw	72±23	17.6±3.8	0.13	11.1	27.6	27	8.8	0.7	0.59

<sup>a</sup>Data from Table 2-7.

<sup>b</sup>See Figure 2-5 for definition of thermal/mechanical units.

<sup>c</sup>Taken as 50 percent of values in Table 2-7, as discussed in text.

<sup>d</sup>Nonlithophysal layers within unit TSw1.

<sup>e</sup>Lithophysal layers within unit TSw1.

<sup>f</sup>NA = not available.

## CONSULTATION DRAFT

these parameters in Table 2-9 are identical to the intact rock values in Table 2-7. The use of these parameters in estimating corresponding rock mass values for use in design analysis is discussed in detail in Section 6.1.2.

The fracture properties given in Table 2-9 are preliminary because of the scarcity of experimental data on the frictional properties of joints in tuff. Fracture cohesion values are assumed to be independent of the degree of welding of the rock in which the fracture occurs, so that values for air-dry joints and saturated joints are about 0.2 and 0.7 MPa, respectively (Figures 2-11 and 2-13). The first value is assigned to all units above the water table (assumed to be unit CHn3 and above), and the second value is assigned to all saturated units.

Two experimental results indicate that saturated welded tuff and air-dry nonwelded tuff both have coefficients of friction of 0.59 at the initiation of slip. On the basis of the observations of Teufel (1981), values for saturated joints are assumed to be 9 percent greater than those for dry joints. Thus, the coefficient of friction for dry joints in welded tuff is assumed to be 0.54, whereas that of saturated joints in nonwelded tuff is assumed to be 0.64. The appropriate values are given in Table 2-9, with the assumption about the location of the water table as previously stated.

Additional discussion of environmental effects on joint frictional parameters is provided in Section 6.1.2, which also provides estimates of values appropriate to design analyses.

### 2.4 THERMAL AND THERMOMECHANICAL PROPERTIES--INTACT ROCK

An understanding of the temperatures and stresses resulting from heating is important in (1) predicting thermal effects on ground-water movement and radionuclide releases and (2) establishing underground design criteria (e.g., tunnel size and spacing, emplacement hole geometry, and waste container thermal output) for the repository at Yucca Mountain. Thermal and thermomechanical data ordinarily have been obtained from small-scale laboratory tests on intact rock. This section summarizes available information from such tests, whereas Section 2.5 deals with data from large-scale measurements in the field.

The thermal properties of the rock necessary to calculate transient heat flow are the thermal conductivity, the density, and the heat capacity. The calculation of thermal strain requires a knowledge of the thermal expansion behavior of the rock, hence thermal-expansion coefficients must be determined. Thermally induced stresses (in an elastic material) can be calculated from the thermal strains, the modulus of deformation, and Poisson's ratio. The data for the last two properties are provided in Sections 2.1.2.2, 2.1.3, and 2.3.3.

Thermal conductivity is a measure of the ability of a material to transmit heat. With regard to a repository, thermal conductivity relates to the ability of the geologic host rock to conduct heat away from waste containers. Thermal conductivity is thus one of the critical input parameters for computer modeling of the temperature field generated by the emplaced waste. For

## CONSULTATION DRAFT

a given thermal loading, repository geometry, and rock mass thermal capacitance, higher thermal conductivity means more rapid heat diffusion and lower temperatures in the rock surrounding the waste container. Lower thermal conductivity results in slower heat dispersal and higher temperatures in the waste container and in the rock surrounding the container.

Heat capacity is a measure of the amount of energy required to raise the temperature of a substance by a fixed amount. In a repository setting, heat capacity affects the amount of heat stored in the rock. Higher values of heat capacity result in more energy use for a given increase in temperature, which results in lower temperatures for a given heat source, assuming constant values of other parameters.

Thermal expansion is a result of the tendency of a material to undergo a volume or length change as a result of a change in temperature. Thermal expansion is used here in a broader sense than by most physical scientists because it is taken to include all phenomena that affect material volume changes, including the simple expansion of constituent grains as well as dehydration-induced contraction or pore collapse.

A thermal expansion coefficient is generally used to describe a volume or length change resulting from a temperature change for a temperature range in which the volume or length change per degree change in temperature is relatively constant. The coefficient, usually recorded as a change in linear dimension per unit original length, can be either positive or negative.

The heat generated by stored radioactive waste will significantly raise the temperature of the host rock in the vicinity of the waste containers. If the rock mass expands or contracts excessively as a result of this temperature change, then thermally induced stress fields may result in rock fracture or displacement that could affect the stability of waste emplacement holes and rooms during the periods of repository operation and waste retrievability.

Most thermal conductivity measurements reported here, for both saturated and dry conditions, were made with the transient-line-source technique under controlled confining and fluid pressures (Lappin et al., 1982). Except at temperatures near the boiling point of water (which is variable under the experimental conditions used), these measurements appear to be accurate and precise to  $\pm 4$  percent or less for fused silica samples (Lappin et al., 1982). Accuracy appears to be on the order of 10 percent for actual samples of tuff (Lappin et al., 1982), with a precision similar to that for fused silica (i.e., 4 percent).

Measurements examining the possibility of thermal-conductivity anisotropy in tuff and those aimed at evaluating the effects of lithophysae were made with a thermal comparator (Moss et al., 1982a). This technique is based on steady-state thermal gradients. It has the advantage of allowing measurements in anisotropic materials and in those containing irregular voids like lithophysae. However, it is not easily amenable to the use of both confining and fluid pressures. Precision for the thermal comparator appears to be about 5 percent, with accuracies of 5 to 10 percent (Moss et al., 1982a). Comparative calibrations with fused silica indicate that, at ambient temperature, the thermal conductivities measured with the thermal comparator are

## CONSULTATION DRAFT

about 8 percent lower than those measured with the transient line source (Lappin et al., 1982; Moss et al., 1982a).

Experimental equipment and analytical procedures for unconfined thermal expansion measurements have been described (Lappin, 1980a). Sample sizes are 6 by 6 by 25 mm for these measurements, whereas representative sizes of components are 0.1 to 2.0 mm (phenocrysts), <0.05 mm (matrix), and <3 mm (lithic fragments) (Broxton et al., 1982). Some pumice fragments may be 10 mm in diameter (Broxton et al., 1982); these constituents have been avoided or accounted for during expansion measurements. The uncertainty in the measured expansion coefficients is  $1 \times 10^{-6} \text{K}^{-1}$  for welded, devitrified samples analyzed to date, the same as that for a fused silica standard (Lappin, 1980a). This uncertainty corresponds to an accuracy of 3 to 9 percent for welded tuff.

The thermal expansion of welded, devitrified tuffs is independent of heating rate between 0.5 and  $10^\circ\text{C}/\text{min}$  (Lappin, 1980a). Unconfined thermal expansion measurements on zeolitized tuffs are sensitive to additional variables (Lappin, 1980a). These tuffs, like tuffs containing appreciable amounts of hydrated glass, expandable clays, or both contract when dewatered. Thus, their behavior is sensitive to the locally effective fluid pressure, which in laboratory tests depends on sample size, heating rate, and permeability. Unconfined measurements on this type of tuff indicate only minimum contractions at a given temperature. Even this interpretation must be based on tests run at a slow rate. Such tuffs may continue to contract slowly for more than 24 h when held at constant temperature. The times required to reach stable length in situ at a given temperature might be much longer if the fracture spacing is large.

Because of concern about the possible effects of both microcracking and variable fluid pressures, a method has been developed to measure thermal expansion under controlled confining and fluid pressures. Test and calibration procedures suggested by the American Society for Testing and Materials are detailed by Van Buskirk et al. (1985). Multiple measurements on fused silica indicate that the precision and accuracy of the confined testing apparatus at a confining pressure of 10 MPa and a pore pressure of 0.1 to 1.5 MPa are on the order of  $\pm 1.5 \times 10^{-6} \text{K}^{-1}$  (Lappin and Nimick, 1985b).

Bulk properties--including grain density, dry bulk density, natural-state bulk density, saturated bulk density, and porosity--are also required for thermal and thermomechanical analyses. These properties can be measured on small samples taken either from core or from outcrop material. The minimum sample size should be 20 g, although data have been obtained directly from mechanical test samples with diameters of up to 26.7 cm (Price et al., 1985). Smaller samples are the usual starting material. In general, the dry bulk density and the grain density of a sample are measured, and the other bulk properties are calculated as follows:

$$\rho_b = (1 - \phi)\rho_g + s \quad (2-7)$$

## CONSULTATION DRAFT

where

$\rho_b$  = dry, natural-state, or saturated bulk density  
 $\phi$  = porosity (volume fraction)  
 $\rho_g$  = grain density  
 $s_g$  = saturation (volume fraction)

(The density of water was assumed to be 1.0 g/cm<sup>3</sup>).

On the basis of replicate measurements on tuff samples, dry bulk density values have a precision of  $\pm 0.1$  g/cm<sup>3</sup>, whereas grain-density measurements on welded tuff are precise to  $\pm 0.04$  g/cm<sup>3</sup> and grain densities of zeolitic tuffs have a precision of  $\pm 0.06$  g/cm<sup>3</sup> (Lappin et al., 1982). The accuracies for these measurements are assumed to be similar to the precisions (Lappin et al., 1982).

The existing information consists almost exclusively of data from laboratory measurements on core samples. The laboratory studies reported here have been conducted for two purposes:

1. To develop a data base that defines the spatial variations in the thermal properties of the tuffs encountered at Yucca Mountain.
2. To correlate the measured thermal properties with measured physical properties like porosity, grain density, and bulk density to develop a functional thermal-conductivity and thermal-expansion stratigraphy for use in heat-transfer and thermomechanical stress analyses. These correlations allow the extrapolation of the measured thermal properties to regions of the boreholes for which only geophysical logs and bulk-property data are available.

### 2.4.1 THERMAL AND THERMOMECHANICAL PROPERTIES OF OTHER ROCKS

Ranges of the published values of the thermal conductivity, heat capacity, coefficient of thermal expansion, and bulk properties of tuffs other than those studied in the NNWSI Project are presented in Table 2-10. As indicated in the table, there is a relatively small amount of data published on the thermal properties of tuffs; data on bulk properties are more extensive. Some of the data were measured at pressures and temperatures above ambient, and hence the upper limits of the ranges are probably slightly higher than those that would be obtained at ambient conditions. Comparison of these data on tuffs with those for the tuffs at Yucca Mountain (Section 2.4.3) indicates that the ranges for each parameter are generally similar.

Table 2-10. Thermal and thermomechanical properties of tuffs not studied by the Nevada Nuclear Waste Storage Investigations Project<sup>a</sup>

Lithology or tuff unit	Thermal conductivity (W/mK)	Heat capacity (J/gK)	Coefficient of thermal expansion ( $10^{-6} \text{ K}^{-1}$ )	Grain density (g/cm <sup>3</sup> )	Porosity (%)
Mt. Helen tuff	-- <sup>b</sup>	--	--	2.45	37
Diamond Dust tuff	--	--	--	2.43	35
Schooner tuff	--	--	--	2.64	40.5
Schooner tuff	--	--	--	2.60	--
Zeolitized tuff, Survey Butte	--	--	--	2.44-2.47	--
Diamond Mine tuff	--	--	--	2.38	--
Mt. St. Helens tuff	--	--	--	2.32	35-39
Oak Springs Formation, Bedded tuff	--	--	--	2.44 ± 0.11	38.8 ± 7.0
Friable tuff	--	--	--	2.33 ± 0.24	35.5 ± 13.8
Welded tuff	--	--	--	2.55 ± 0.09	14.1 ± 8.9
Tuff	--	--	--	2.38-2.57	31-42
Oak Springs Formation	--	--	--	2.6 ± 0.16	30.6 ± 3.2
Ohya tuff	--	--	--	2.38	34.8
Tuff, Ontario	--	--	--	2.78	--
Tuff	--	--	--	--	34.7-43.1
Tuff, Yucca Flat	1.12-1.36	--	--	--	16
Tuff, Red Hot Deep Well Experiment	--	--	--	--	15.9-23.3
Ash-fall tuff	--	--	--	--	30-40
Tuff and tuff breccia, USSR	--	--	--	--	8.3
Ignimbrite, Italy	--	--	--	--	≈20
Tuff, Japan	--	--	--	--	10.2-21.6
Obsidian	--	--	--	--	1.2-11.5
Tuff, Oregon	--	--	--	--	44.4
Tuff, Rhine Valley	--	--	--	--	24.7-45.1
Tuff, southern Italy	--	--	--	--	6-58.4
Ignimbrite, New Zealand	--	--	--	--	9.0-28.7
Andestic to dacitic tuff	0.60-1.03	0.38-1.24	--	--	--
Oak Springs Formation	0.44-1.05	--	--	--	--
Tuff, drillhole U12b07	0.64-2.14	--	--	--	--
Welded tuff, locality unknown	--	--	4.2-12.9	--	--
Tuff, locality unknown	--	--	-22.2-6.0	--	--
Bandelier tuff, New Mexico	--	--	13.1-17.1	--	--

<sup>a</sup>Source: Guzowski et al. (1983).

<sup>b</sup>-- = data not available.

## 2.4.2 THERMAL AND THERMOMECHANICAL PROPERTIES OF ROCK AT THE SITE

### 2.4.2.1 Thermal conductivity

The thermal conductivities of saturated and dry samples of tuffs from Yucca Mountain are summarized in Table 2-11. Each of these values applies for a range of temperatures because the temperature dependence of the thermal conductivity of tuffs from Yucca Mountain is small (Nimick and Lappin, 1985). Values for the zero-porosity (matrix) conductivity for each sample, calculated by the geometric means approach (Lappin, 1980b), are also given. The matrix thermal conductivities can be used, together with values for porosity and saturation, to calculate thermal conductivity for any saturation state.

#### 2.4.2.1.1 Measured thermal conductivities

The thermal conductivities of saturated and dehydrated tuff are variable, depending on variations in porosity and grain density (mineralogic composition). The average saturated conductivities of nonzeolitized, welded, devitrified material from the Bullfrog and Tram members of the Crater Flat Tuff and from the Topopah Spring Member of the Paintbrush Tuff are essentially the same within the limits of experimental error (10 percent).

The conductivities of dehydrated samples of these same tuffs appear to be different, with the Topopah Spring and Tram members losing relatively little conductivity when dried. The matrix porosities and grain densities of the Bullfrog and Tram members are nominally the same, whereas both the porosity and the grain density of the nonlithophysal Topopah Spring Member are significantly lower. The lower grain density in the Topopah Spring Member results from the presence of cristobalite (the Topopah Spring Member has been found to contain 0 to 30 volume percent cristobalite, as discussed in Section 4.1.1.3).

The conductivities of saturated and dehydrated samples, porosities, and grain densities of all nonwelded to partially welded zeolitized ash flows examined to date appear to be consistent and independent of stratigraphic unit, depth, and drillhole location (Nimick and Lappin, 1985). The conductivities and grain densities are lower than those for corresponding nonzeolitized material, while porosities are generally higher. Zeolitized bedded intervals have higher grain densities and conductivities than do the zeolitized ash flows (Nimick and Lappin, 1985).

#### 2.4.2.1.2 Calculated zero-porosity conductivities

The zero-porosity or matrix conductivities given in Table 2-11 are the calculated conductivity of the matrix in the absence of porosity and contained pore water. The matrix conductivities were calculated from experimental data by the geometric means approach outlined by Lappin (1980b); alternatives to the geometric means approach are being examined. The matrix conductivities are different below and above the dehydration temperature

CONSULTATION DRAFT

Table 2-11. Average values and standard deviations for measured thermal conductivities ( $K^{avg}$ ) and calculated zero-porosity conductivities ( $K_o$ ) for various tuff units and rock types<sup>a</sup>

Rock type	Unit	$K^{avg}$ sat (W/mK) <sup>d</sup>	$K^{avg}$ dry (W/mK) <sup>d</sup>	$K_o^{sat}$ <sup>b</sup> (W/mK)	$K_o^{dry}$ <sup>c</sup> (W/mK)
Nonzeolitized/ welded	Topopah Spring	2.16 ± 0.19	1.93 ± 0.17	2.43	3.45
	Bullfrog	2.00 ± 0.27	1.35 ± 0.30	2.71	NA <sup>e</sup>
	Tram	2.09 ± 0.18	1.78 ± 0.36	2.77	NA
Vitric	Topopah Spring	1.35 ± 0.08	1.37 ± 0.12	1.31	1.98
Zeolitized/non- welded to partially welded	Topopah Spring	1.33 ± 0.05	1.04 ± 0.12	1.88	4.77
	Calico Hills	1.51 ± 0.16	1.03 ± 0.15	2.36	4.24
	Prow Pass	1.40 ± 0.03	1.04 ± 0.08	1.79	NA
	Bullfrog	1.44 ± 0.01	1.07 ± 0.06	1.94	NA
	Tram	1.46	1.11	NA	NA

<sup>a</sup>Source: Nimick and Lappin (1985).

<sup>b</sup> $K_o^{sat}$  calculated at 25°C.

<sup>c</sup> $K_o^{dry}$  calculated at 200°C.

<sup>d</sup>Estimated accuracy in thermal conductivity measurements is 10 percent of reported value (Lappin et al., 1982).

<sup>e</sup>NA = not available.

because any hydrous phases present lose some of the water within their structures during dehydration. The extent of the discontinuity in matrix conductivity at the dehydration temperature depends on the type of hydrous phases in a given sample.

The matrix conductivity of tuffs depends weakly on temperature except for the behavior at the dehydration temperature discussed earlier. The matrix conductivities given in Table 2-11 for saturated and dry samples were calculated at 25 and 200°C, respectively, and are representative of the temperature interval over which the relevant saturation state applies.

The matrix conductivity, which depends primarily on mineralogic composition is generally related to the measured grain density (i.e., the density at zero porosity) for tuff samples from Yucca Mountain. The calculated zero-porosity conductivity for a mineralogically homogeneous tuff layer can be

used to estimate the in situ conductivity of that tuff for any given porosity and saturation (Lappin, 1980b; Lappin et al., 1982).

#### 2.4.2.1.3 Influence of textural anisotropy and lithophysae on conductivity

##### 2.4.2.1.3.1 Textural anisotropy

Thermal-comparator measurements on welded tuff from the Grouse Canyon Member of the Belted Range Tuff were collected to examine potential effects of layering anisotropy in welded tuffs (Moss et al., 1982b). The results indicate that there is no statistically significant anisotropic effect of layering on the matrix thermal conductivity of welded tuffs, even in the fully dehydrated state. The difference in thermal conductivities for different orientations relative to bedding is less than 5 percent as compared with variations of more than 20 percent between samples (Moss et al., 1982b; Nimick and Lappin, 1985). Because welded ash-flow tuffs have the strongest fabric anisotropy, it is concluded that the matrix thermal anisotropy is also negligible for nonwelded ash flows.

##### 2.4.2.1.3.2 Lithophysae

Lithophysae are found in varying abundance in portions of the Topopah Spring Member of the Paintbrush Tuff outside of the proposed repository horizon. In addition, the thermal effects of these cavities on conductivity are difficult to measure because the void spaces, which are up to 5 cm or more in diameter, are large in relation to usual laboratory specimens. Tests on six samples of lithophysal Topopah Spring Member from Busted Butte are under way to provide thermal conductivity data for this rock type.

#### 2.4.2.2 Heat capacity

No measurements of the specific heat or heat capacity of tuffs have yet been made for the NNWSI Project. Instead, the product of heat capacity and density (volumetric heat capacity) has been calculated assuming a constant heat capacity ( $C_p$ ) of 0.84 J/gK for the silicate mineral assemblage, 4.18 J/gK for water, and 1.0 J/gK for air as shown in Equation 2-8.

$$(\rho C_p)_{\text{bulk}} = \rho_g (1-\rho) C_p (\text{silicates}) + \rho_{(H_2O)} \phi_s C_p (\text{water}), \quad (2-8)$$

where

$C_p$	= heat capacity (J/gK)
$\rho_{\text{bulk}}$	= bulk density ( $\text{g/cm}^3$ ) = $\rho_g (1-\phi) + \rho_{(\text{H}_2\text{O})} (\phi s)$
$\rho_g$	= grain density ( $\text{g/cm}^3$ )
$\rho_{(\text{H}_2\text{O})}$	= density of water = $1 \text{ g/cm}^3$
$s$	= saturation (volume fraction)
$\phi$	= porosity (volume fraction).

The calculated values of the volumetric heat capacity (Table 2-12) indicate a broad range that is strongly dependent on both porosity and the degree of saturation. A series of measurements of the heat capacity of tuffs from Yucca Mountain is planned to examine the validity of the assumed value of heat capacity of the silicate mineral assemblage (Section 8.3.1.15). Preliminary analysis suggests that the constant value of 0.84 J/gK is incorrect; the heat capacity of the mineral assemblage is in fact a function of temperature (Nimick and Schwartz, 1987).

The water present in the pores of tuffs from Yucca Mountain gives rise to a large endothermic reaction associated with volatilization of contained pore fluids at temperatures near the in situ boiling point of water. Variability in the in situ temperatures and pressures expected near a repository will cause variability in the importance of this volatilization to heat transfer calculations.

#### 2.4.2.3 Thermal expansion

This section summarizes the results of earlier studies of unconfined thermal expansion (Lappin, 1980a), as well as with the results of more-recent confined measurements. The newer data are consistent with previous results and describe both the predehydration behavior of zeolitic tuffs and the effects of increased fluid pressures on the dehydration temperatures of expandable clays (neither of which can be assessed adequately in unconfined tests). Current calculations suggest that temperatures in the Bullfrog and Tram Members and in most of the tuffaceous beds of the Calico Hills will not be high enough to cause dehydration (Johnstone et al., 1984). Comparison of the measured and calculated thermal expansion of zeolitic tuffs is difficult because of the lack of data for pure phases. Data for pure zeolite minerals are being collected to allow calculation of the thermal expansion of zeolitic tuffs.

Summarized in Table 2-13 are average linear thermal-expansion coefficients for material from the welded devitrified Tram and Bullfrog members of the Crater Flat Tuff, the densely welded Topopah Spring Member of the Paintbrush Tuff, and the highly zeolitized nonwelded to partially welded ash flows in the tuffaceous beds of Calico Hills and lower units. Because of the

CONSULTATION DRAFT

Table 2-12. Calculated volumetric heat capacity as a function of porosity and saturation<sup>a</sup>

Volumetric heat capacity (J/cm <sup>3</sup> K)				
grain density = 2.65 g/cm <sup>3</sup>			grain density = 2.38 g/cm <sup>3</sup>	
Porosity	Saturated	Dry	Saturated	Dry
0.0	2.22	2.22	2.01	2.01
0.1	2.43	2.01	2.22	1.80
0.2	2.59	1.76	2.43	1.59
0.3	2.80	1.55	2.64	1.38

<sup>a</sup>Source: Tillerson and Nimick (1984).

presence of variable amounts of hydrous phases, such as clays, zeolites, glass, and opaline silica, three temperature ranges must be defined for the thermal expansion behavior of the tuffs from Yucca Mountain: pretransition, transition, and post-transition. Transition behavior for samples containing significant amounts of the various hydrous phases (e.g., zeolitized tuffs) is likely to vary with the amount of expansion or contraction on heating and the temperature range over which dehydration takes place.

The Bullfrog and Tram members of the Crater Flat Tuff are devitrified welded tuffs, generally found below the water table. Because of the relatively uniform mineral composition, the expansion behavior of devitrified welded tuffs from below the water table is quite uniform, except for the effects of small fractions (generally less than 5 percent) of expandable clays (Waters and Carroll, 1981; Bish, 1981). The results of confined and unconfined tests are consistent and agree well with calculated behavior.

The Topopah Spring Member of the Paintbrush Tuff contains devitrified densely welded tuffs, generally found above the water table. The mineralogic composition of devitrified welded tuffs above the water table locally reflects past vapor-phase activity. This has resulted in the deposition of variable amounts of secondary feldspar and cristobalite, with locally important amounts of quartz, tridymite, and possibly expandable clay (Section 4.1.1.3). The thermal expansion of vapor-phase-altered tuffs changes above about 200°C because of the variable content of cristobalite, tridymite, and/or expandable clays. Even at high waste emplacement densities, temperatures approaching 200°C would occur only very close to waste canisters.

Thermal expansion data for zeolitized nonwelded to partially welded tuff layers were collected before the Topopah Spring Member was recommended as the repository horizon. The data are summarized here because of the possibility that these tuffs may be located within the region of elevated temperature

CONSULTATION DRAFT

Table 2-13. Summary of average thermal expansion coefficients for silicic tuffs from Yucca Mountain

Rock type	Units	Linear expansion coefficient ( $10^{-6}K^{-1}$ ) <sup>a</sup>		
		Pre-transition	Transition	Post-transition
Nonzeolitized/ welded, devitrified	Bullfrog and Tram Members	$8.3 \pm 1.4^b$ (25 to 100°C)	$-12 \pm 4^b$ (100 to 125°C)	$10.9 \pm 0.8$ (125 to 300°C)
Nonzeolitized/ densely welded, devitrified	Topopah Spring Member	TSw1 <sup>c</sup> 9.5 TSw2 $8.9 \pm 0.9$ (25 to 200°C)	$27.4(+27.1, -13.6)^{c,d}$ $28.7 \pm 11.4^d$ (200 to 300°C)	NA <sup>e</sup>
Zeolitized, nonwelded to partially welded	Calico Hills (also por- tions of Topopah Spring, Prow Pass, Bullfrog, Tram)	$6.7 \pm 3.7^b$ (25 to 100°C)	Variable $-29$ to $-56^f$ depending on mineralogy and degree of welding (100 to 150°C)	Variable $-4.5$ to $+4.4$ depending on miner- alogy and degree of welding. (150 to 300°C)
Vitric, welded	Topopah Spring Member	$5.2 \pm 1.1$ (25 to 150°C)	$3.5 \pm 4.9$ (150 to 250°C)	NA NA

<sup>a</sup>Data for TSw1, TSw2, and vitric welded material adapted from Nimick and Schwartz (1987).

<sup>b</sup>Confined expansion measurements (10 MPa confining pressure), all other measurements made under unconfined conditions. Accuracy of unconfined measurements  $\pm 1.0 \times 10^{-6}K^{-1}$  (Lappin, 1980a); accuracy of confined measurements  $\pm 1.5 \times 10^{-6}K^{-1}$  (Lappin and Nimick, 1985b).

<sup>c</sup>Nonlithophysal layers; transitional behavior measured only for 200 to 250°C. Nonsymmetrical standard deviation for data in transitional interval result from log-normal distribution of data. No standard deviation is available for 25 to 200°C because of change in statistical distribution of data between low-temperature intervals (25 to 50°C, 50 to 100°C) and high-temperature intervals (100 to 150°C, 150 to 200°C).

<sup>d</sup>Nonlinear transitional behavior of the Topopah Spring Member (200 to 350°C) results from the  $\alpha$  to  $\beta$  transformations of cristobalite and tridymite.

<sup>e</sup>NA = not applicable. These materials do not show post-transition behavior.

<sup>f</sup>Calculated coefficient based on measured unconfined expansion through 100°C and the measured, confined, predehydration expansion coefficient.

around a repository. Under unconfined conditions, thermal expansion behavior is more complex and variable than that of devitrified tuffs. Three distinct types of behavior have been noted (Lappin and Nimick, 1985a):

1. A linear contraction of 0.2 to 0.3 percent upon dehydration, to temperatures as high as 300°C, with a contraction of 0.2 percent generally occurring by about 150°C. This behavior is dominant in quartz- and feldspar-poor, heavily zeolitized tuffs.
2. A maximum linear contraction of 0.2 percent at temperatures near 150°C (unconfined), followed by expansion to nearly initial length on additional heating. This type of behavior appears to be most prominent in nonwelded or partially welded zeolitized tuffs from below the water table, which are richer in quartz and feldspar than analogous tuffs higher in the section.
3. A very small amount of contraction at temperatures near dehydration, followed by expansion to more than the initial length. This type of behavior is prominent in the few relatively thin, bedded, or reworked intervals identified in the stratigraphic section at Yucca Mountain.

In confined tests (confining pressure of 10 MPa, pore fluid pressure of 0.1 to 1.5 MPa) all zeolitized tuffs expand continuously, until the onset of dehydration, at rates ranging from 3 to 13 x 10<sup>-6</sup> K<sup>-1</sup> (Lappin and Nimick, 1985a). Detailed correlation of predehydration expansion with mineralogic composition is under way.

Comparison of replicate unconfined expansion runs made parallel and perpendicular to bedding in a devitrified, densely welded sample from the Grouse Canyon Member of the Belted Range Tuff indicates that there is no significant variation in the unconfined matrix thermal expansion behavior as a function of textural anisotropy or bedding (Lappin, 1980a).

#### 2.4.2.4 Density and porosity

Both density and porosity vary between the different tuff units at Yucca Mountain. In general, a higher degree of welding results in a lower porosity and a corresponding higher bulk density. Superimposed on this trend are mineralogic effects, reflected by grain density. Vitric tuffs have the lowest grain density, the zeolitic tuffs have a higher grain density, and the grain density of the devitrified tuffs is higher still (Lappin, 1980b).

In addition to the porosity discussed in the previous paragraph, additional porosity is present in portions of the Topopah Spring Member in the form of lithophysae. This additional porosity takes two forms: (1) lithophysal cavities and (2) an increased void space (relative to the surrounding matrix material) in the vapor-phase-altered material that usually encloses the large cavities (Price et al., 1985). Spengler and Chornack (1984) have documented the volume percentage of lithophysae as a function of depth in several drillholes at Yucca Mountain. The lithophysal cavities can contribute from 0 to 28 percent to the total porosity of localized portions of the

Topopah Spring Member. Within the nonlithophysal part of the Topopah Spring Member denoted as unit TSw2 in the thermal and mechanical stratigraphy, the lithophysal cavities contribute from 0 to 8.5 percent to the total porosity, with an average contribution of approximately 1 percent (Nimick and Schwartz, 1987).

#### 2.4.3 THERMAL PROPERTIES STRATIGRAPHY FOR YUCCA MOUNTAIN

A set of units, each of which has definable thermal and mechanical properties, has been described in the section on the stratigraphic framework for testing in the introduction to this chapter and defined in Figure 2-5. The recommended values for the grain density, porosity, thermal conductivity, volumetric heat capacity, and coefficient of thermal expansion for the thermal and mechanical units are given in Table 2-14. For most units, the volumetric heat capacity data was calculated from information provided in Table 2-12 and the bulk properties in Table 2-14. For units TSw1, TSw2, and TSw3, the heat capacities of the silicate mineral assemblages were assumed to be those given by Nimick and Schwartz (1987). For the lithophysal zones, lithophysal cavities (17 volume percent as determined by Price et al., 1985) are assumed to be dry. For units above the water table (assumed to be CHn3 and above) the saturation is assumed to be as given by Montazer and Wilson (1984) for temperatures below the boiling temperature.

#### 2.5 THERMAL AND THERMOMECHANICAL PROPERTIES--LARGE SCALE

This section provides an overview of the field tests in tuff that have provided information on the in situ values of thermal conductivity, heat capacity, and thermal expansion. To date, these field tests have been performed with the objective of observing thermal and hydrothermal phenomena in simulated nuclear waste repository environments. As such, the measurements of thermal properties generally have not been a direct goal of a test.

All field tests to date have been performed in tuffs in G-Tunnel. Four small-diameter heater tests have been completed, although the data from the most recently completed test have yet to be reduced and analyzed. In addition, the testing of the heated block (Section 2.3.2) included thermal-cycle testing from which thermal expansion behavior has been quantified.

Of the tests mentioned in the preceding paragraph, information on in situ thermal conductivity can be extracted from three of the heater tests. Small-scale cylindrical heaters were emplaced in drillholes in the Grouse Canyon Member and in tunnel bed 5 in G-Tunnel (Zimmerman, 1983; Johnstone et al., 1985). By comparing the temperatures and temperature gradients predicted by thermal modeling of these tests with the actual temperatures and gradients measured in situ, an assessment can be made of whether in situ thermal conductivity can be accurately predicted from laboratory values. Specific limitations or uncertainties inherent in such tests follow:

Table 2-14. Recommended values for thermal and physical properties of thermal/mechanical units

Unit <sup>b</sup>	Grain density (g/cm <sup>3</sup> )		Porosity		Thermal conductivity (W/mK)				Coefficient of thermal expansion (10 <sup>-6</sup> K <sup>-1</sup> )						Volumetric heat capacity, J/cm <sup>3</sup> K	
	Mean	St. dev.	Mean	St. dev.	Saturated <sup>a</sup>		Dry		Pretransition	Transition		Posttransition		Saturated <sup>k</sup>	Dry	
					Mean	St. dev.	Mean	St. dev.		Mean	T(°C)	Mean	T(°C)			Mean
TCw	2.51	0.04	0.11	0.04	2.03 <sup>c</sup>	0.20 <sup>c</sup>	1.76 <sup>c</sup>	0.29 <sup>c</sup>	8.8 <sup>d</sup>	25-200 <sup>d</sup>	NA <sup>e</sup>	NA	NA	NA	2.18	1.88
PTn	2.37	0.15	0.45	0.15	1.35	0.06	1.02	0.19	5.3 <sup>f</sup>	25-150 <sup>f</sup>	3.5 <sup>f</sup>	150-250 <sup>f</sup>	NA	NA	2.24	1.09
TSw1 <sup>g</sup>	2.54	0.04	0.14	0.04	2.03	0.20	1.76	0.29	11.8	25-200	51.8	200-250	NA	NA	2.09	1.98
TSw1 <sup>h</sup>	2.53	0.02	0.35 <sup>1</sup>	0.03	1.96	0.41	1.21	0.14	NA	NA	NA	NA	NA	1.87 <sup>i</sup>	1.38 <sup>i</sup>	
TSw2	2.55	0.03	0.12	0.03	2.29	0.17	1.88	0.24	8.8	25-200	24.0	200-300	NA	NA	2.16	2.17
TSw3	2.39	0.02	0.04	0.03	1.34	0.10	1.40	0.16	5.3	25-150	3.5	150-250	NA	NA	2.06	2.45
CHn1v	2.34	0.06	0.36	0.09	1.35	0.06	1.02	0.19	5.3 <sup>f</sup>	25-150 <sup>f</sup>	3.5 <sup>f</sup>	150-150 <sup>f</sup>	NA	NA	2.61	1.26
CHn1s	2.41	0.06	0.33	0.04	1.48	0.17	1.01	0.14	6.7	25-T <sub>b</sub> <sup>j</sup>	-56.0	T <sub>b</sub> -150	-4.5	150-300	2.61	1.36
CHn2	2.54	0.12	0.29	0.06	1.61	0.04	1.21	0.04	6.7 <sup>k</sup>	25-T <sub>b</sub> <sup>k</sup>	-56.0 <sup>k</sup>	T <sub>b</sub> -150 <sup>k</sup>	-4.5 <sup>k</sup>	150-300 <sup>k</sup>	2.62	1.51
CHn3	2.41	0.04	0.36	0.08	1.43 <sup>l</sup>	0.03 <sup>l</sup>	1.04 <sup>l</sup>	0.05 <sup>l</sup>	6.7 <sup>k</sup>	25-T <sub>b</sub> <sup>k</sup>	-56.0 <sup>k</sup>	T <sub>b</sub> -150 <sup>k</sup>	-4.5 <sup>k</sup>	150-300 <sup>k</sup>	2.66	1.30
PPw	2.58	0.04	0.24	0.07	2.00 <sup>m</sup>	0.27 <sup>m</sup>	1.35 <sup>m</sup>	0.30 <sup>m</sup>	8.3 <sup>m</sup>	25-T <sub>b</sub> <sup>m</sup>	-12.0 <sup>m</sup>	T <sub>b</sub> -125 <sup>m</sup>	10.9 <sup>m</sup>	>125 <sup>m</sup>	2.65	1.65
CFUn	2.43	0.07	0.30	0.08	1.43	0.03	1.04	0.06	6.7 <sup>k</sup>	25-T <sub>b</sub> <sup>k</sup>	-56.0 <sup>k</sup>	T <sub>b</sub> -150 <sup>k</sup>	-4.5 <sup>k</sup>	150-300 <sup>k</sup>	2.68	1.43
BFw	2.60	0.04	0.24	0.08	2.00	0.27	1.35	0.30	8.3	25-T <sub>b</sub> <sup>k</sup>	-12.0	T <sub>b</sub> -125	10.9	>125	2.66	1.66
CFMn1	2.41	0.06	0.25	0.06	1.43	0.00	1.11	0.07	6.7 <sup>k</sup>	25-T <sub>b</sub> <sup>k</sup>	-56.0 <sup>k</sup>	T <sub>b</sub> -150 <sup>k</sup>	-4.5 <sup>k</sup>	150-300 <sup>k</sup>	2.56	1.52
CFMn2	2.52	0.06	0.24	0.03	1.61	0.04 <sup>n</sup>	1.21 <sup>n</sup>	0.04 <sup>n</sup>	6.7 <sup>k</sup>	25-T <sub>b</sub> <sup>k</sup>	-56.0 <sup>k</sup>	T <sub>b</sub> -150 <sup>k</sup>	-4.5 <sup>k</sup>	150-300 <sup>k</sup>	2.61	1.61
CFMn3	2.44	0.07	0.27	0.03	1.46	NA	1.11	NA	6.7 <sup>k</sup>	25-T <sub>b</sub> <sup>k</sup>	-56.0 <sup>k</sup>	T <sub>b</sub> -150 <sup>k</sup>	-4.5 <sup>k</sup>	150-300 <sup>k</sup>	2.62	1.50
TRw	2.63	0.04	0.19	0.06	2.09	0.18	1.79	0.37	8.3 <sup>m</sup>	25-T <sub>b</sub> <sup>m</sup>	-12.0 <sup>m</sup>	T <sub>b</sub> -125 <sup>m</sup>	10.9 <sup>m</sup>	>125 <sup>m</sup>	2.58	1.79

<sup>a</sup>Thermal conductivity data for all units except TSw1 (nonlithophysal), TSw2, TSw3, and volumetric heat capacity data for PPw and underlying units are for a nominal saturation of 1.0, whereas volumetric heat capacity data are calculated using saturations from Montazer and Wilson (1984) for CHn3 and overlying units.

<sup>b</sup>See Figure 2-5 for definition of thermal/mechanical units.

<sup>c</sup>Assumed to be the same as correlative property for TSw1 (nonlithophysal).

<sup>d</sup>Assumed to be the same as correlative property for TSw2.

<sup>e</sup>NA = not applicable or no data.

<sup>f</sup>Assumed to be the same as correlative property for TSw3.

<sup>g</sup>Nonlithophysal layers within unit TSw1.

<sup>h</sup>Lithophysal layers within unit TSw1.

Note that, for lithophysal layers, the total porosity is  $\phi_M + \phi_A + \phi_L$ , where  $\phi_M$  is matrix porosity,  $\phi_A$  is porosity of vapor-phase-altered material,  $\phi_L$  is the volume percent lithophysal cavities, and M and A are volume fractions of matrix and vapor-phase-altered material, respectively. In order to calculate volumetric heat capacity,  $M = 0.55$ ,  $A = 0.29$ ,  $\phi_M = 0.08$  and  $\phi_A = 0.49$  (Price et al., 1985).

<sup>j</sup>T<sub>b</sub> = boiling point of water.

<sup>k</sup>Assumed to be the same as correlative property for CHn1s.

<sup>l</sup>Assumed to be the same as correlative property for CFUn.

<sup>m</sup>Assumed to be the same as correlative property for BFw.

<sup>n</sup>Assumed to be the same as correlative property for CHn2.

1. Variable and uncontrolled degrees of saturation may have existed in the rock mass containing the heater. Such variations would have affected thermal conductivity, amounts of fluid released, and fluid movements during heating.
2. Thermocouples spring-mounted on the heater could not be fully shielded from thermal radiation between the heater and the drillhole wall. As a result, these thermocouples can register a temperature as much as 20 Celsius degrees too high (Johnstone et al., 1985).

Direct measurement of the in situ thermal expansion of the rock mass has been accomplished in other rock types by means of standard extensometers (wire, rod or both) (Lappin et al., 1981). Laser strain interferometry has been attempted in G-Tunnel (Johnstone et al., 1985), but the lack of a suitably stable platform from which to make the measurement made the resulting data difficult to interpret. Deformations related to the thermal expansion of the heated block were measured with horizontal surface extensometers and multiple-point borehole extensometers (Zimmerman et al., 1985). Both types of instrumentation provided reliable data for the duration of the test.

Indirect observations of the thermal expansion behavior of the Grouse Canyon Member of the Belted Range Tuff have also been made with borehole stressmeters (Johnstone et al., 1985). Measurements of stress induced in the rock mass by heater operation were obtained using this instrumentation, from which inferences were drawn concerning in situ thermal expansion.

#### 2.5.1 THERMAL AND THERMOMECHANICAL PROPERTIES OF OTHER ROCKS

A number of in situ heater tests, similar to those conducted for the NNWSI Project, have been performed in other rock types. Of the thermal and thermomechanical properties discussed in Section 2.4, two are often obtained from in situ tests--thermal conductivity and thermal expansion. The data obtained from tests conducted in other jointed rocks (granitic rocks and basalt) are summarized in the following discussion.

To derive an in situ thermal conductivity for the Stripa granite, Jeffry et al. (1979) assumed that the heat capacity and density were known. Numerical calculations were then performed by varying the thermal conductivity until the predicted temperature field matched that observed during the heater test. This in situ thermal conductivity differed by less than 1 percent from the laboratory value. Jeffry et al. (1979) also matched temperature fields by allowing both the thermal conductivity and the thermal diffusivity (the ratio of the thermal conductivity to the product of density and heat capacity) to vary independently. With this two-parameter approach, in situ thermal conductivity differed from the laboratory value by approximately 5 percent.

Montan and Bradkin (1984) report the results of a similar two-parameter approach to the determination of the in situ thermal conductivity of the Climax granite. Their results indicated an in situ value approximately 11 percent higher than an average laboratory value, but within 3 percent of

one sample measured in the laboratory. Even though the laboratory samples did not come from the location where the heater test was performed, the agreement seems to be quite good.

Kim and McCabe (1984) provide a comparison between laboratory values of thermal conductivity and a best-fit rock mass thermal conductivity for basalt. The value for the rock mass (1.7 W/mK) is within the range for the laboratory data (1.6 to 2.2 W/mK); no discussion of the data is provided.

Hardin et al. (1982) describe the in situ testing of a large (8 m<sup>3</sup>) block of biotite gneiss. Field values of thermal conductivity, thermal diffusivity, or both, were derived by numerical modeling of the temperature field produced by the heaters in the block. No direct comparison of these in situ data with laboratory data was made.

Thermal expansion coefficients determined from in situ tests also compare well with corresponding laboratory values. The thermal expansion behavior observed in basalt agreed quite well with that predicted with a laboratory-determined thermal expansion coefficient (Gregory and Kim, 1981). Hardin et al. (1982) report that the thermal expansion coefficients derived from field measurements on biotite gneiss are consistent with laboratory-determined coefficients for other granitic rocks (Stripa and Climax granites). In contrast, Cook et al. (1983) found that the ratio of field-to-laboratory values for the thermal expansion coefficient of Stripa granite was approximately 0.68. This latter observation appears to conflict with the data from other rocks, but no error bands or experimental ranges are provided with which to analyze the discrepancy.

## 2.5.2 THERMAL AND THERMOMECHANICAL PROPERTIES OF ROCK AT THE SITE

### 2.5.2.1 Thermal conductivity

The in situ thermal conductivity of tuff has been determined during the G-Tunnel heated-block experiment. Measured values ranged from 1.53 to 1.63 W/mK over a temperature range of 18 to 80°C (Zimmerman et al., 1986). These values are consistent with data obtained in the laboratory.

In addition to the in situ values, an approach slightly different from that used in analyzing the in situ tests in Section 2.5.1 was used. Laboratory data for thermal conductivity and heat capacity were used in the calculation of the temperature fields to be expected in the tuff surrounding the heaters. A comparison of these predicted temperatures with those actually observed indicated that when laboratory data for the thermal properties were used in the calculations, the measured temperatures were within 6 percent of the predicted values in 2 tests (Zimmerman, 1983), whereas measured temperatures were 12 percent less than predicted values for a third heater test during the heating phase (Johnstone et al., 1985). The discrepancies in the last test were attributed to the modeling of the heat source and the water transport, because predicted and measured temperatures were almost identical during cooldown (Johnstone et al., 1985).

The results obtained to date in tuff suggest that little additional in situ testing of thermal conductivity is required for welded tuffs above the water table to determine the rock mass thermal conductivity for use in far-field or room-scale calculations. Additional evaluations will be made in tests conducted in the exploratory shaft to increase confidence in the values of thermal conductivity used in the heat transfer analyses for repository design (Section 8.3.1.15).

The effects of joints or fracture porosity on the in situ thermal conductivity of devitrified welded tuffs have been estimated, assuming a fracture porosity of 3 percent (Lappin et al., 1982). This assumption ignores the possibility of joint closure resulting from overburden pressures or from the thermal expansion of the rock and, therefore, is assumed to provide an estimate of the maximum change in thermal conductivity attributable to the presence of joints. In addition, in situ fracture porosity is expected to be much less than 3 percent. Although no direct data are available for the Topopah Spring Member, estimates of fracture porosity for units in the saturated zones by Erickson and Waddell (1985) for tuffs below the water table are on the order of  $10^{-4}$  to  $10^{-5}$ . For both other rock types (Section 2.5.1) and similar rocks from the NTS (Sections 2.5 and 2.1.1) effects of jointing on thermal conductivity were not discernible.

The thermal conductivity of the rock mass of the Topopah Spring Member will be examined in tests in the exploratory shaft facility (Section 8.3.1.15).

#### 2.5.2.2 Thermal expansion

The attempt to measure directly the thermal expansion of welded tuff in situ during the earliest heater test (Johnstone et al., 1985) was unsuccessful. However, the measurement of thermally induced stresses was at least partially successful. In this test, measured thermally induced stresses were approximately 40 percent of expectations on the basis of thermomechanical modeling using laboratory-derived expansion values.

Data taken during the thermal-cycle testing of the heated-block test yielded in situ values for the thermal expansion coefficients ranging from  $5.0$  to  $8.7 \times 10^{-6} \text{K}^{-1}$  (Zimmerman et al., 1985). This range compares favorably with the range in mean values from laboratory tests,  $6.4$  to  $8.0 \times 10^{-6} \text{K}^{-1}$  (Lappin and Nimick, 1985b).

The approximate equivalence of laboratory and rock mass thermal expansion coefficients determined for the Grouse Canyon Member of the Belted Range Tuff suggests that the discrepancy between predicted and measured thermal stresses observed by Johnstone et al. (1985) is attributable to differences between laboratory and in situ elastic moduli.

### 2.5.3 RELATIONSHIP BETWEEN INTACT ROCK AND LARGE-SCALE PROPERTIES

The results of the in situ heater tests in G-Tunnel described above indicate that the laboratory measured thermal conductivity can be used in successfully modeling temperatures observed in field tests. Thus, as a good approximation, the values of rock mass thermal conductivity are assumed to be the same as those for intact rock. The same approximation is made concerning heat capacity and the coefficient of linear expansion. The latter will be measured in situ in the exploratory shaft facility to examine the validity of extrapolating laboratory values to the rock mass.

### 2.6 EXISTING STRESS REGIME

Designing the Yucca Mountain repository will require knowledge of the magnitude, direction, and variability of the preconstruction in situ state of stress, excavation-induced stresses, and thermally induced stresses. The preconstruction state of stress is particularly vital to the determination of site suitability. Design parameters (such as room dimensions and pillar widths) can be varied to change the magnitude and direction of excavation-induced stresses. Similarly, parameters such as gross thermal loading, waste package dimensions, and emplacement orientations can be adjusted to modify thermally induced stresses. Because the preconstruction in situ stress field cannot be modified, the design analyses will treat the in situ stresses as an initialized stress state on which the excavation and thermal stresses must be superposed. The magnitude, direction, and variability of principal stresses are of importance in the analysis and design of stable underground openings as well as in the prediction of rock mass deformation for both long and short times and the resulting applications to performance assessment calculations. Subsurface openings must be designed to provide stability from construction through permanent closure.

This section reviews the current understanding of the state of stress at Yucca Mountain and its vicinity. Regional geologic studies, field measurements at Yucca Mountain and nearby Rainier Mesa, and finite-element calculations of the overburden-induced component of in situ stress are presented to summarize the state of knowledge.

Detailed results of in situ stress measurements in tuffs at Yucca Mountain or at Rainier Mesa are contained in several references (Hooker et al., 1971; Haimson et al., 1974; Ellis and Ege, 1976; Tyler and Vollendorf, 1975; Ellis and Magner, 1980; Warpinski et al., 1981; Zimmerman and Vollendorf, 1982; Stock et al., 1984). These references also discuss details of testing techniques and potential limitations and errors. Additional discussion of some of the results is provided in Chapter 1, along with information on regional geologic studies relevant to the stress state.

Two methods were used by most of the workers cited in the previous paragraph for measuring in situ stress: overcoring and hydraulic fracturing. With the overcoring technique (Hooker and Bickel, 1974), changes in strain are measured in a small borehole before, during, and after overcoring with a larger core barrel. As such, the rock around the overcored region is strain relieved. The complete state of stress can be calculated from such strain

relief measurements in three nonparallel drillholes by using the appropriate equations (Jaeger and Cook, 1979). Triaxial cells have been developed that (see for example, Leeman, 1964; Doe et al., 1981) allow the measurement of principal stresses by overcoring in a single hole. The advantage of the overcoring technique is that it allows for an estimation of the full stress tensor. A limitation of the method is that the deformation modulus of the rock must be known to obtain the stresses from the measurements.

For the hydraulic fracturing technique, the borehole is assumed to be parallel to a principal stress. First, a selected section of a borehole is sealed off with packers. Then, fluid pressure is increased within the sealed section until the rock at the borehole wall fractures. Theory predicts that at a high enough borehole pressure, the rock will fail in tension. For a borehole that parallels a principal stress direction, the fracture that forms at the borewall is generally perpendicular to the minimum horizontal stress, and the pressure required to hold the fracture open provides a reasonable estimate of the minimum horizontal stress (Stock et al., 1984). (If the borehole axis does not coincide with a principal stress, the testing will provide a measure of the stresses normal to the borehole rather than the principal stresses.) The maximum horizontal stress can be calculated if other properties can be acquired (Stock et al., 1984). Borehole televiewer or impression packers are required to determine the orientation of hydraulic fractures at the borehole wall and, hence, the orientation of the minimum stress acting normal to the borehole. It is possible, with the hydraulic fracturing technique, to make stress measurements anywhere that a borehole exists. A limitation to the technique is that the results may be difficult to interpret in heavily fractured or otherwise permeable rock.

It is apparent that both measurement techniques could be used at a particular site to minimize the limitations and to maximize the advantages of each technique. Overcoring can provide an indication of the validity of assuming that a borehole used for hydraulic fracturing is parallel to a principal stress. Hydraulic fracturing measures the in situ stress state on a larger scale than does overcoring. Satisfactory correlation has been observed between the measurement techniques when used together in the past (Miller, 1976; Doe et al., 1981; Haimson, 1981; Doe et al., 1983). However, Dischler and Kim (1985) point out that overcoring results from experiments on closely jointed rocks show great variability, making the stress measurements difficult to compare with those from other techniques. Both techniques generally assume an isotropic, elastic material. As discussed in Section 2.1, these two assumptions are probably reasonable for the intact tuffs at Yucca Mountain.

Numerical modeling (finite elements) has been used to estimate the overburden-induced component of in situ stress at Rainier Mesa. Using linear elastic behavior and isotropic material properties within each tuff layer, plane-strain approximations of the gravity-induced component (including surface topography) of the in situ stress agree rather well with in situ measurements (Holland and Bauer, 1984). Used in combination with in situ stress measurements, this technique will permit a better understanding of the contributions of each stress component. Furthermore, if applicable, this technique can assist in understanding the spatial variations in the state of in situ stress.

## 2.6.1 STRESS REGIME IN REGION OF THE SITE

### 2.6.1.1 Tectonic and geologic evidence

Tectonic and structural evidence for stress orientation at the NTS has been summarized by Carr (1974) and more recently by Stock et al. (1985). Synthesis of tectonic and structural data, combined with seismic data and limited stress and borehole deformation measurements, suggests that the minimum principal stress in the NTS region is horizontal and in a northwest to west-northwest direction. This is also reflected in the orientation of borehole breakouts in large-diameter test holes in Yucca Flat (Springer et al., 1984) and is consistent with regional stress trends summarized by Zoback and Zoback (1980). An analysis of regional geologic structures indicates that the stress state within the Great Basin, in which the NTS lies, has changed from crustal shortening to crustal extension in the last 20 to 30 million years (Section 1.3.2.3).

Seismicity studies during the 1970s included strain-release analysis of two small earthquakes at the NTS. One had a compressive axis of  $N.23^{\circ}E.$  and a corresponding extensional axis at  $N.67^{\circ}W.$  The compressive axis for the second event was approximately  $N.50^{\circ}E.$  (Fischer et al., 1972). A compilation of focal mechanisms for the NTS region by Stock et al. (1985) indicates that most movement is strike-slip along steeply dipping planes that strike north to northeast.

Fractures, interpreted to be tensile, in a playa at the NTS have strikes of approximately  $N.50^{\circ}E.$ , suggesting relative extension in a  $N.40^{\circ}W.$  direction (Carr, 1974). Dimensional changes of vertical boreholes in the alluvium of the playa, determined by borehole caliper, indicate an average direction of drillhole elongation of  $N.60^{\circ}W.$ , consistent with the relative extension in this direction (Carr, 1974; Stock et al., 1984).

### 2.6.1.2 Overcoring measurements

Limited stress measurements in tunnels in mesas at the NTS, made using overcore techniques, have been summarized (Ellis and Magner, 1980). In overcore measurements made at nine locations, the average bearing for the minimum principal stress was  $N.56^{\circ}W.$  for seven of the nine locations, which is in good agreement with the data of Carr (1974).

Overcore measurements in welded and nonwelded tuff at Rainier Mesa have provided results that indicate that in situ stress may exhibit considerable spatial variation. The differences may be attributed to the contrasting mechanical properties of the different tuffs (Warpinski et al., 1981). Rainier Mesa consists of many layers of tuff of varying thicknesses and properties. The welded tuff unit that was measured is relatively thin (13 m), has a relatively high Young's modulus and a low Poisson's ratio, and lies between nonwelded tuffs with low elastic moduli and higher Poisson's ratios. The layers are stacked, well bonded, and appear to be predominantly gravity loaded. The net result is a vertical compressional loading with an apparent tendency for the layers to extend laterally toward the free surface

of the mesa wall because of Poisson's effect. The nonwelded tuff units having the higher Poisson's ratio appear to deform readily toward the free surface, whereas the stiffer welded tufts resist the gravity-induced deformation and then are extended by the deforming nonwelded tufts (Ellis and Swolfs, 1983). This phenomenon is well illustrated by the distinctly low minimum horizontal stress measured in the welded tuff unit. This hypothesis is further supported by hydraulic fracturing measurements in adjoining welded and nonwelded tufts and by finite-element calculations.

#### 2.6.1.3 Hydraulic fracturing studies

G-Tunnel in Rainier Mesa has been the location of a number of hydraulic fracture studies. Tests in nonwelded tuff along the length of the tunnel have been reported by Smith et al. (1981). One result of these tests was the observation that the orientation of the fractures tended to tilt toward the edge of the mesa at test locations nearer to the sloping mesa walls. The trend or strike of the outermost fractures tended to be parallel with the mesa edge. This observation agrees with that made by Ellis and Magner (1980) regarding topographical influences on in situ stresses measured with the overcoring technique.

Vertical hydraulic fracture studies in Rainier Mesa (Warpinski et al., 1981) document the vertical variation in minimum stress, which has been correlated to the vertical variation in material properties. Minimum horizontal stresses tend to be lower in the welded tufts, which have high values of Young's modulus and low values of Poisson's ratio, and higher in the nonwelded tufts, which have lower Young's moduli and higher Poisson's ratios.

#### 2.6.1.4 Finite-element calculations

Using a two-dimensional finite-element model of Rainier Mesa, the stresses resulting from gravity loading and elasticity of the rocks have been calculated (Holland and Bauer, 1984; Bauer et al., 1985). The calculations assumed plane strain conditions and linear elastic material response. The material properties were assumed to be different for welded and nonwelded units. The ground surface was assumed to be a free surface, whereas the remaining boundaries were sufficiently far from the region of interest as to have no effect on the calculational results. These analyses, which incorporated topographical and stratigraphic effects but neglected tectonic and residual stresses, appear to account for the vertical variation in stresses reported by Warpinski et al. (1981).

## 2.6.2 STRESS REGIME AT THE SITE

### 2.6.2.1 Field observations

The preceding discussions have focused on observations and measurements of stress fields at the NTS as a whole and under Rainier Mesa. The evidence, which is discussed in greater detail in Chapter 1, suggests a dominating regional stress field in which the minimum principal stress is oriented approximately along the axis N.65°W. to N.70°W. (USGS, 1984). The maximum principal stress in the region is generally also horizontal indicating a strike-slip regime, whereas at Yucca Mountain the maximum stress axis is vertical as is discussed below. The mean value for the magnitude of the vertical stress, determined by the product of overburden, density, and gravitational acceleration is 7 MPa at 300 m depth. A discussion of ranges in this value is given in Section 6.1.2.2.2.

Hydraulic stress measurements and borehole televiwer observations in drillhole USW G-2 (Stock et al., 1985) indicate an orientation of N.60 to 65°W. for the direction of least horizontal stress and a minimum horizontal stress ( $S_h$ ) to vertical stress ( $S_v$ ) ratio of  $\leq 0.84$  at a depth of 295 m decreasing to 0.47 at 1,209 m (Figure 2-21). The inequality on the first ratio listed is based on discussion by Stock et al. (1984, 1985), which suggests that the values calculated for the minimum horizontal stress from the measurements may be greater than the actual values for this stress in the unsaturated zone.

In situ stress data from drillhole USW G-1 are also shown in Figure 2-21; in this drillhole, all data are from tests in the saturated zone. Ratios of  $S_h$  to  $S_v$  in drillhole USW G-1 are approximately 0.3 to 0.5, and are consistent with ratios for tests in the saturated zone in drillhole USW G-2. Televiwer observation of drillholes has indicated the presence of drilling-induced hydraulic fractures in the shallow parts of drillholes USW G-1 and USW G-2 (Stock et al., 1985). These fractures have orientations consistent with the orientations measured by hydraulic fracturing tests.

The magnitude of the maximum horizontal stress ( $S_H$ ) was estimated by Stock et al. (1985) to be approximately halfway between  $S_h$  and  $S_v$ . This conclusion was based on calculations from hydraulic fracturing data combined with observations of well bore spalling in drillholes USW G-1 and USW G-2. The relative magnitudes of the three principal stresses are consistent with a normal faulting regime (Stock et al., 1985), and differs from the strike-slip regime that is typical of the NTS region.

The possibility that movement on favorably oriented fault planes may occur under the existing stress regime has been mentioned by the USGS (1984) and Stock et al. (1985). Further discussion of this topic is presented in Section 1.3.2.3.

The in situ stress at Yucca Mountain has also been measured in drillholes UE-25p#1, USW GU-3, and USW G-3. Data from these tests are being reduced and analyzed. In addition, some data will be obtained during exploratory shaft activities (Section 8.3.1.15).

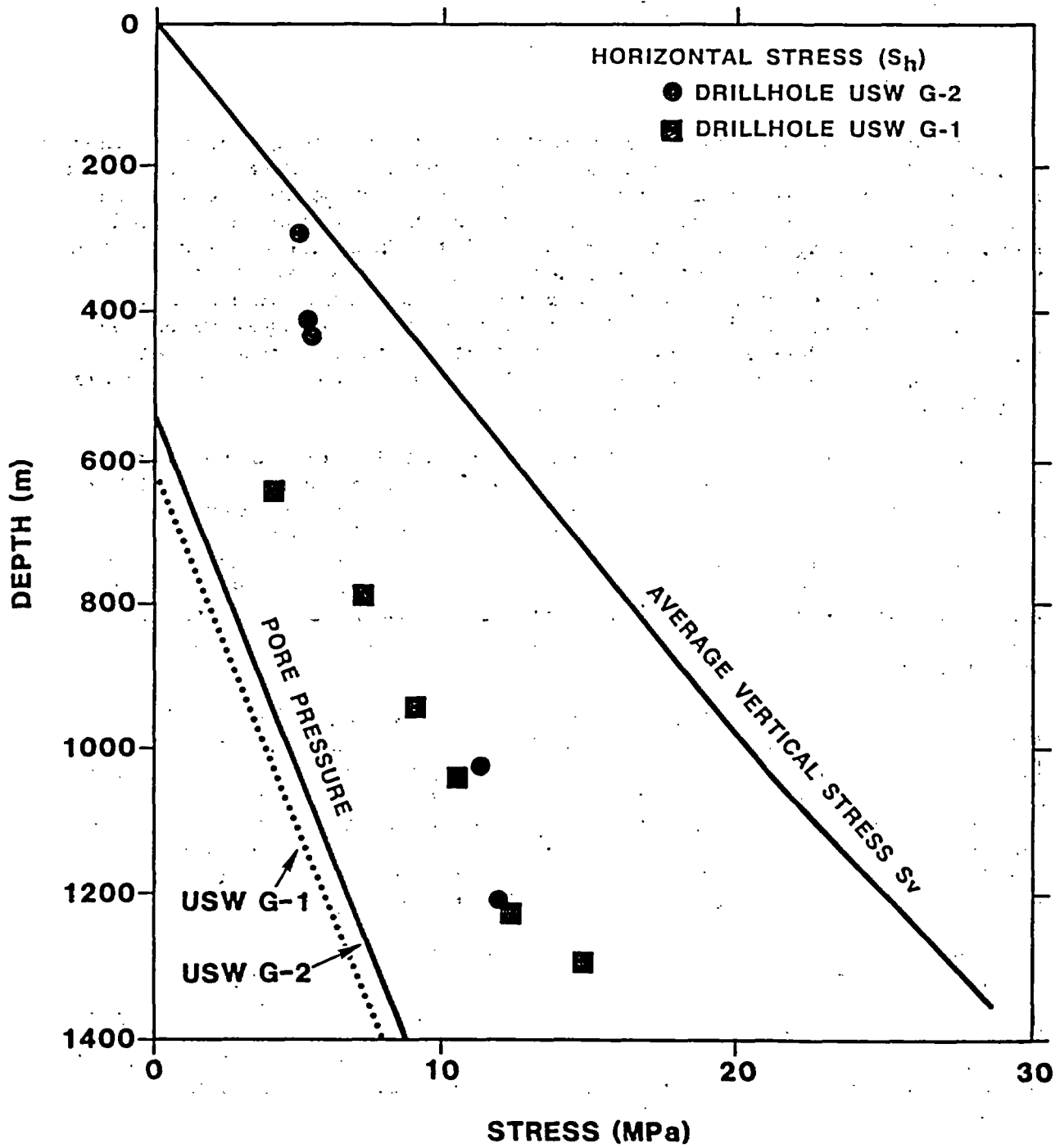


Figure 2-21. Least horizontal and vertical principal stress values and pore pressure plotted against depth. Modified from Stock et al. (1984).

### 2.6.2.2 Finite-element calculations

Finite-element calculations similar to those described in Section 2.6.1.4 for Rainier Mesa have been performed to estimate the gravity-induced component of in situ stress at Yucca Mountain (Bauer et al., 1985). At the 300-m depth range, gravity loading alone produced a ratio of  $S_h$  to  $S_v$  of approximately 0.3. Since the maximum value measure in drillhole USWVG-2 for this ratio was 0.8, the gravity load can account for at least 38 percent of the minimum horizontal stress and may account for more if the ratio from field data is actually less than 0.8. The remainder of the minimum horizontal stress comes from tectonic stresses, residual stresses, or both.

Another analytic calculation of the stress state at Yucca Mountain has been described by Swolfs and Savage (1985) who also conclude that gravity plays a major role in determining the in situ stresses. In addition, they suggest that the distribution of near-vertical fractures and faults causes transverse anisotropy in rock mass elastic properties, which in turn affects the relative stress magnitudes.

The two studies mentioned in the preceding paragraphs have attempted to provide a general understanding of stress distribution with depth at Yucca Mountain. Although the two studies took somewhat different approaches, both explained the limited available measurements. Neither modeling effort considered all the possible relevant parameters. Bauer et al. (1985) assumed that each tuff unit was isotropic, in contrast to the transverse anisotropy examined by Swolfs and Savage (1985). Swolfs and Savage (1985) did not consider the variation in elastic properties between differing lithologies. Bauer et al. (1985) found a model that incorporated variable elastic properties to be more successful at reproducing measured data at Rainier Mesa than a model using homogeneous properties. In addition, both studies assumed instantaneous gravity loading rather than the sequential loading imposed by normal depositional processes. This last deficiency may lead to results that differ from the theoretically correct calculated stresses (Goodman and Brown, 1963).

Nevertheless, finite-element calculations have the potential to be a useful tool in estimating the two- or three-dimensional distribution of in situ stresses for use in repository design or performance-assessment calculations. Care must be taken to understand the limitations of such an estimate and to incorporate measured data into the calculation to the degree possible.

## 2.7 SPECIAL GEOENGINEERING PROPERTIES

Two special geoenvironmental considerations are recognized to be of potential importance for evaluating the effects of waste emplacement in Yucca Mountain tuffs: thermally induced degradation of the rock mass and thermally induced dewatering (water migration). Both of these phenomena were hypothesized because of the varying porosity, permeability, and degree of saturation, coupled with the geologically instantaneous thermal loading. Additional phenomena or processes requiring study may be identified during site characterization. Performance assessment work will determine the sensitivity of repository performance to all identified processes.

Thermally induced degradation was considered because of its potential impact on the mechanical and transport properties of the rock mass. Conceptually, the high thermal expansion of water relative to that of most silicates conceivably could lead to very-near-field rock mass degradation. This degradation would result from high fluid pressures developed during heating, particularly if the hydro-thermomechanical state were such that localized high pressure could not be relieved.

The effects of thermally induced water migration were considered because the thermal and mechanical properties of tuff are affected by the state of saturation and because thermally driven dewatering might result in fluid fluxes into underground workings and thus might affect ventilation requirements. Thermally induced water migration is judged to be possible and will be evaluated in light of tests to be performed in the exploratory shaft facility (Section 4.2).

### 2.7.1 ROCK MASS DEGRADATION

The results of investigations performed to date to define the potential for, and the effects of, rock mass decrepitation and thermal dewatering are summarized in the following sections.

#### 2.7.1.1 Near-field decrepitation

Emplacing hot nuclear waste in relatively cold (25°C), partially saturated tuff produces a geologically instantaneous load on the rock-water system. Both the temperature and the temperature gradient change [in rock these temperature changes are interdependent (Johnson and Gangi, 1980)] with resulting development of thermal strains, stresses, or both. A number of phenomena, including mineral phase changes, dehydration, and mineral and water expansion, contribute to the reaction of the rock mass to the changes in the temperature field. The total effect has been quantified by numerous thermal expansion measurements (Lappin, 1980a). Each of these phenomena can promote intergranular thermal stresses resulting from the differential thermal expansion of adjacent minerals. However, in tuff thermal cracking per se is expected to be minimal (as in other materials) because of the fine grain size of tuff (Kuszyk and Bradt, 1973; Kingery et al., 1976; Bauer and Handin, 1983).

## CONSULTATION DRAFT

A nonuniform temperature change (temperature gradient) will generate a stress field in a solid whenever differential thermal expansion or contraction cannot proceed freely. With a uniform temperature change, the effects are constrained by the stress field present (in part determined by the temperature gradient), whereas the effects resulting from a temperature gradient are influenced by the intrinsic rock properties. (Rock properties like Young's modulus could be altered by the introduction of thermal cracks.) These two types of temperature change are clearly interdependent.

The potential for fluid-induced fracturing resulting from temperature increases in welded tuff below the water table (Bullfrog and Tram members) has been investigated in a series of calculations simulating waste emplacement (Eaton et al., 1981). The results can be applied to assess the potential for thermally induced degradation of the partially saturated Topopah Spring Member.

To bound the potential effects, three assumptions were made that led to the calculation of maximum fluid pressures. First, a rigid matrix was assumed, so that thermal expansion of the silicate framework and the contained porosity were ignored. Second, the calculation did not treat the capillary movement of water or dehydration at temperatures below the boiling point of water. Finally, fully saturated conditions were considered, making analytical results conservative in that the highest possible fluid pressures were calculated.

The effects of fracture spacing, fracture orientation, and thermal loading on pore fluid pressures were evaluated. The results showed that in unfractured rock the maximum fluid pressures will occur within a few days of waste emplacement. The calculated pore pressures decreased significantly with an increasing number of fractures in the host rock. In a partially saturated, heavily fractured rock such as the Topopah Spring Member, thermally induced pore pressures would be expected to be low. Thus, the potential for thermally induced degradation of the Topopah Spring Member should be small.

An experiment was conducted in which the amount of thermal decrepitation resulting from the rapid heating of unconfined, fully saturated samples of Topopah Spring Member from ambient temperature to 225°C was quantified by measuring the relative changes of the moisture content between pre- and post-thermal treatment measurements (Nimick, 1987). No measureable changes in the moisture content were observed. It was concluded that (1) if new void spaces (cracks) were induced in the rock, they were of insufficient magnitude to be measured and (2) if new cracks were induced, they did not act to enhance interconnectivity to previously isolated void space. From these conclusions it was further speculated that, when the saturated rock was heated, no anomalously high pore pressures from water trapped in voids (on the order of the tensile strength of grain boundaries as a maximum) were generated. This means that either all pore spaces were initially well interconnected or high temperatures facilitated fluid flow (by decreasing water viscosity and opening preexisting cracks), or both. This experiment and analysis together imply that changes in microstructure resulting from realistic thermal loading do not occur, and thus alteration of mechanical and transport properties (thermal degradation) in the very-near-field is not predicted. The effects of elevated temperature on the mechanical properties

of intact Topopah Spring Member will be measured, as mentioned in Sections 2.1.2.2 and 2.1.2.3.1.3, and discussed in more detail in Section 8.3.1.15.1.

Expected stratigraphic variations in the potential for rock mass degradation can be qualitatively assessed and extended on the basis of the results of work performed to date. Increases in thermal conductivity should decrease the potential for degradation at any given thermal loading because very-near-field temperatures and thermal gradients decrease when thermal conductivity increases. Partial saturation of the rock mass should decrease the degradation potential because it would provide additional free volume for fluid expansion. Increasing fracture frequency should decrease the degradation potential because the path lengths to be traversed by the fluid to achieve pressure release would be shorter. Finally, decreasing the thermal loading of a repository should decrease the degradation potential because the volume of rock that experiences sufficiently rapid heating will be smaller.

Because of these considerations, the degradation of tuffs in general is considered improbable. Degradation of the Topopah Spring Member is considered extremely improbable because of the high fracture frequency (Section 1.3.2.2) and partial saturation (65 percent) (Montazer and Wilson, 1984). In addition, no evidence of degradation has been observed in the walls of heater holes in three heater tests conducted in G-Tunnel in both welded (two tests) and nonwelded tuff. No additional tests are planned specifically for obtaining data on thermal degradation, but the response of the Topopah Spring Member to elevated temperatures will be observed during exploratory shaft facility testing.

## 2.7.2 THERMALLY INDUCED WATER MIGRATION

Formation of convection cells of liquid water is not expected to occur in a partially saturated host rock above the water table because of the lack of global continuity of the liquid phase. The thermal gradients produced by the emplaced waste allow the possibility of vapor convective cells to be produced. Fractures in partially saturated systems are considered to be generally unsaturated because water they might contain is drawn into the rock matrix by capillarity (Montazer and Wilson, 1984). The fractures therefore have relatively high vapor conductivity and exert a strong effect on both moisture movement and convective heat transfer. The discussion in the following two paragraphs pertains to a conceptual model for thermally induced moisture movement in a continuum.

Water movement is generally recognized to occur because of a vaporization-condensation mechanism (Gurr et al., 1952; Somerton, 1982). As the boiling point is reached in the partially saturated rock matrix, liquid water vaporizes and tends to move down the temperature gradient away from the emplaced waste. The phase change produces a gas pressure that drives vapor away from the location of boiling. Vapor moves in the direction of a potential gradient that is a function of static pressure and temperature. Gas pressure might also drive the movement of liquid water away from the emplaced waste although it is anticipated to be a smaller flux than the vapor transport (Gurr et al., 1952). Vapor will condense at the leading edge of the

dewatered region around the borehole, causing a locally increased level of saturation.

The gas pressure equilibrates rapidly with the flow of displaced liquid water. A dewatered region around the emplacement borehole develops that expands with time, and produces a gradient in the liquid saturation. The liquid potential is a function of saturation as well as temperature and static pressure. The saturation gradient tends to drive liquid water toward the emplaced waste. Even in the simplest form of this conceptual model, the magnitudes and directions of the liquid and vapor fluxes depend on many parameters including the permeability of the medium, in situ saturation, the hydraulic characteristics of the unsaturated matrix, and the specific heat source.

Pruess et al. (1984) formulated numerical models of the thermal migration problem in fractured tuff, using both an explicit representation of idealized discrete fractures, and an equivalent continuum approach that included some of the effects of fractures. The results of this work show that thermally induced water migration will produce a saturation front profile that is qualitatively similar to the one shown in Figure 2-22. This figure was generated using a model of an infinite linear array of waste containers in a partially saturated, fractured porous medium, simulated by an equivalent continuum. The front moves outward from the container array with time until the heat can no longer support the vaporization of water.

The velocity of the evaporative front, as well as the volume of the dewatered region, will depend on the saturation of the host rock, the degree of fracturing, the relative permeabilities of the liquid and vapor, the waste emplacement scheme (vertical or horizontal), and the type of waste emplaced. Although the waste emplacement scheme will affect the temperature field and moisture movement, the liquid water velocity for any of the schemes is expected to be small, on the order of  $10^{-6}$  to  $10^{-10}$  m/s (Mondy et al., 1983). As the rock cools with time, water begins to condense and move back into the dewatered region under the influence of the saturation gradient.

The effect of fractures, as demonstrated in the explicit, discrete fracture model of Pruess et al. (1984), is to attract much of the vapor mobilized from the boiling region, and conduct it outward to a region of condensation. The liquid condensate is then drawn into the matrix by capillary action, and tends to flow down the saturation gradient back toward the boiling region. The vapor flux exceeds the liquid return flux, so the dewatered region expands around the borehole. If the fracture characteristics are adjusted to permit liquid movement in the fractures, then the saturation gradient drives liquid back toward the boiling region along the fractures. A vapor-liquid counterflow develops, which accounts for much of the heat flow away from the borehole. Movement of the boiling front in the matrix is accordingly reduced.

Preliminary design specifications associated with the work of Pruess et al. (1984) indicate that a dried-out, dewatered region forms around the waste emplacement holes in less than a year, so that the possibility for liquid transport of radionuclides is apparently reduced. The majority of mass transport of water at early time after emplacement is expected to occur in

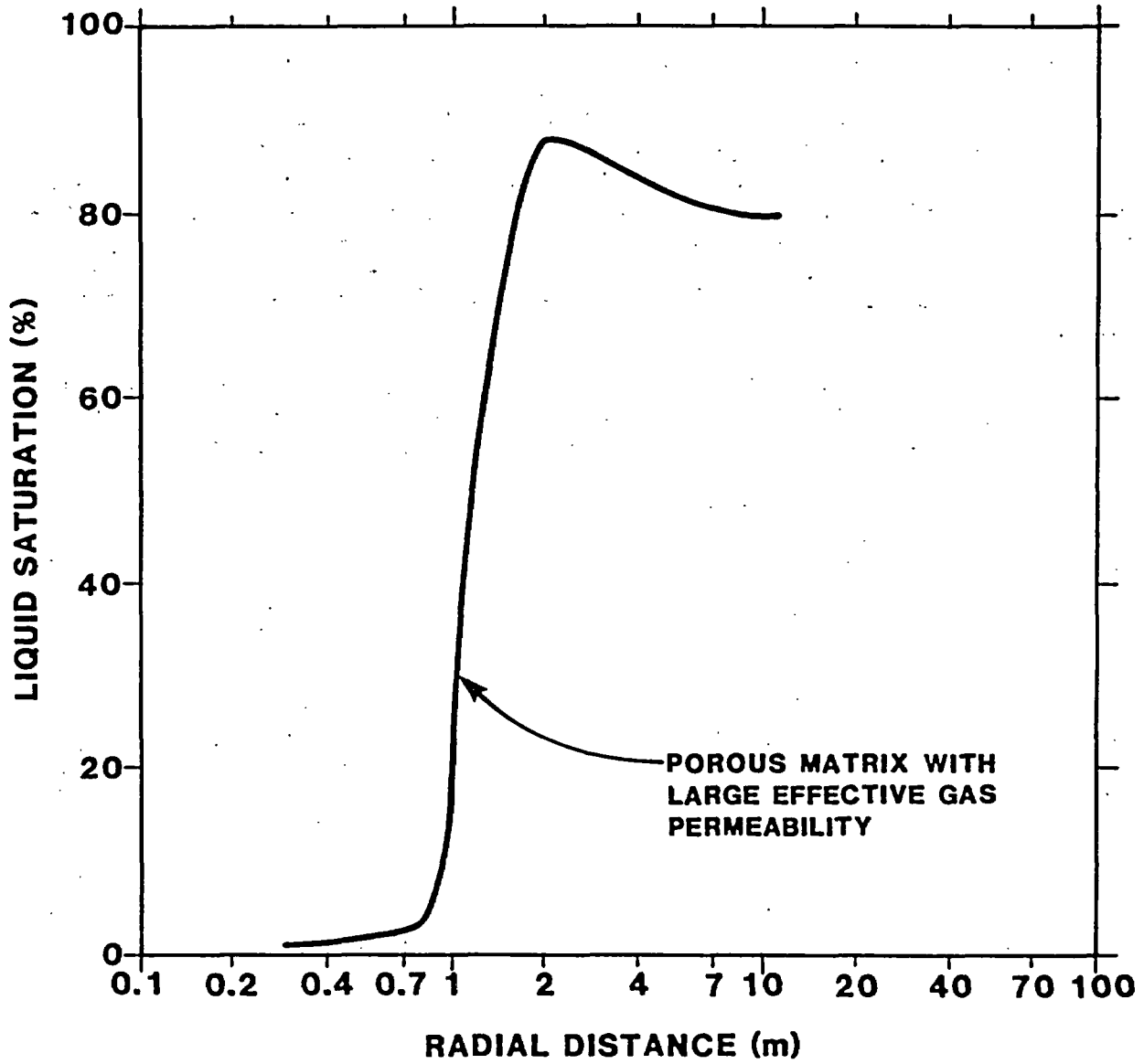


Figure 2-22. Simulated liquid saturation profile near a container in tuff ( $t = 160$  days, initial saturation = 80 percent). Modified from Pruess et al. (1984).

## CONSULTATION DRAFT

the vapor phase. Heated vapor will be introduced into the drifts, and ventilation requirements must be considered.

Field experiments in granite and tuff indicate that water movement is an induced response that can be expected upon heating a rock mass. In many instances, water has entered heater and instrumentation holes, thereby affecting instrumentation longevity as well as the temperatures resulting from simulated waste emplacement (Carlsson, 1978; Lappin et al., 1981; Johnstone et al., 1985). In tests in the Eleana argillite and in the water migration experiment carried out in G-Tunnel above the water table, most, if not all, the water entering the instrumentation and heater areas was pore fluid removed from the surrounding rock mass as a result of heating. An in situ heater experiment carried out in the G-Tunnel underground facility (Johnstone et al., 1985) yielded amounts of water that, as shown in Figure 2-23, are in qualitative agreement with predictions by an evaporation-front model in which water vapor moves in response to local gradients in the partial pressure of water in air. The results showed that the convection of the water vapor and capillary forces in the matrix were important factors in the transport of water in a low permeability material, such as densely welded tuff.

No detailed numerical modeling of the thermally induced water migration occurring in these experiments has been done at this time. The test results indicate a dried-out zone occurring around the heaters, consistent with generic modeling results (Pruess et al., 1984). The modeling results of Pruess et al. (1984) have not shown the potential for water movement into the heater hole, probably because of the one-dimensional geometry. In situ experiments are inherently at least two-dimensional because the heater does not approximate an infinite line source. Detailed two-dimensional modeling must be done to more fully evaluate the results.

Two small-diameter heater experiments also were performed in the G-Tunnel underground facility (Zimmerman, 1983) in which a 10.2-cm-diameter heater was placed successively in two vertical 12.7-cm-diameter boreholes for heating periods of about 30 days. The first test was conducted in welded tuff, and the second in nonwelded tuff. Only small amounts of liquid water (less than 2.5-cm deep) were detected in the bottom of the borehole (and that occurred only at the start of the test). Once the rock wall temperatures exceeded 94°C (the boiling temperature at ambient pressure in G-Tunnel), convective water transport mechanisms appeared to dominate. This was evidenced by the presence of vapor in the warmer air around the heater and condensate in the cooler region at the bottom of the boreholes. Differences between the two experiments in the quantities of water collected in cooler regions of the borehole suggest that some vapor may have moved through the fractures in the welded tuff.

Additional evaluations of water migration phenomena were made as part of the recently completed heated-block test, again carried out in G-Tunnel (Zimmerman et al., 1984). Those measurements were intended primarily to evaluate changes in local saturations or pore pressures upon heating. Documentation of the saturations as a function of temperature is provided by Zimmerman et al. (1985). The moisture content as a function of temperature was monitored at one location for more than 8 months using a neutron moisture probe. The moisture content began to decrease at approximately 80°C and

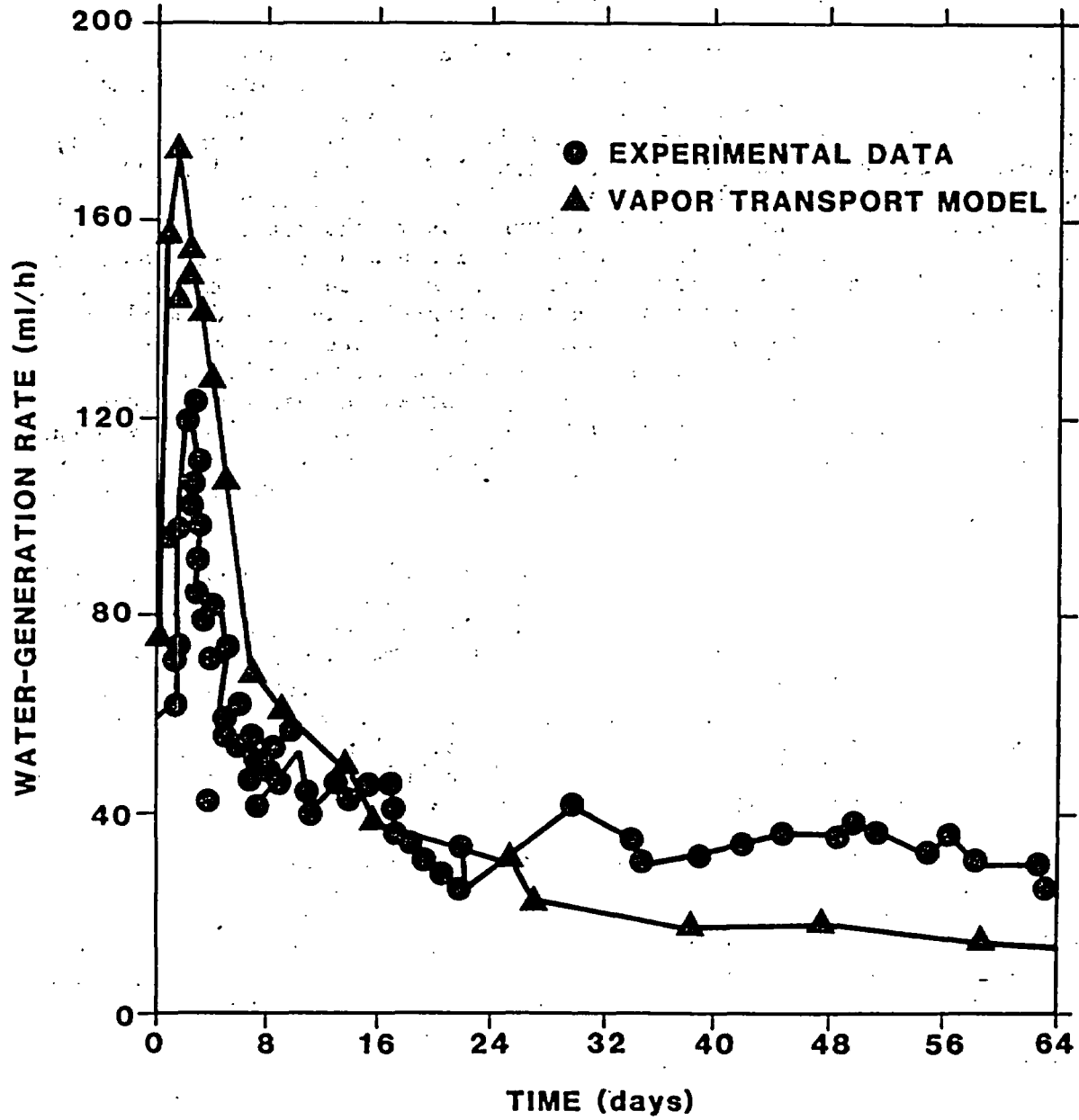


Figure 2-23. Comparison of measured and calculated water inflow rates in tuff water migration/heater experiment. Modified from Figure 31 of Johnstone et al. (1985).

## CONSULTATION DRAFT

continued to decrease to the measurement limit of 15 percent saturation, attained at a temperature of approximately 150°C. When coupled with the temperature measurements, these results should aid in understanding thermally induced flow and its effect on material properties (primarily thermal conductivity).

From the results of heated-borehole experiments in a granitic rock mass monitored for nearly 2 yr, it was concluded that the induced temperature field caused stress in the rock mass that closed fractures and cracks (Nelson and Rachiele, 1982). The water contained in the openings was forced to migrate as pore and crack space was reduced. When the heat was turned off, the cracks ceased closing, and the flow of water into the instrumented boreholes was reduced or stopped. It should be noted that in a partially saturated, fractured rock mass like the Topopah Spring Member, the fractures are expected generally to be in a condition of very low saturation because of the strong capillary forces of the matrix (Montazer and Wilson, 1984). Therefore, the closing of fractures by thermal strain should not be a significant cause of water migration in the Topopah Spring Member.

Additional evaluations of thermally induced water migration phenomena are planned as part of laboratory testing (Section 8.3.4.2). Thermally induced water migration phenomena will also be observed in association with in situ testing in the exploratory shaft facility. These tests are intended to examine both the mechanisms of thermally induced water movement and the effect of thermal dewatering on the thermal and mechanical properties of the rock mass.

### 2.7.3 GEOENGINEERING PROPERTIES OF SURFACE MATERIALS

Ongoing studies to select a site for the major surface facilities of a repository at Yucca Mountain are concentrating on locations in which the surface material is alluvium (Neal, 1985). A general description of this material is provided in Chapter 1. A more site-specific description is given in this section, along with the available geoenvironmental data pertinent to the design of the surface facilities.

#### 2.7.3.1 Lithologic description of alluvium

Limited preliminary investigations, consisting of surface observations and exploratory borings, were completed in six areas selected as potential sites for central surface facilities (Neal, 1985). Preliminary stratigraphic information has been developed from the exploratory boreholes. The total depth of the alluvium at the proposed location of the central surface facilities (designated site 3 by Neal (1985)) is about 90 ft (27.4 m); however, because the bedrock surface is sloping, the thickness of alluvium may be more or less than this value, depending on the final location of surface structures.

In general, the alluvium is a light tan-to-gray, silty-to-sandy gravel, with numerous blocky cobbles and boulders. These rock particles, which are

derived from nearby bedrock sources, consist mostly of welded or partly welded volcanic ash-flow tuffs. Test pits excavated at several of the sites studied showed well-developed soil horizons in the upper portions of the alluvium. The top 1 or 2 ft (0.3 or 0.6 m) (A and B horizons) are loose and fine grained; this soil will be removed during construction. The underlying material typically is partly cemented with calcite (caliche) to a depth of about 8 ft (2.4 m). Below a depth of 8 ft (2.4 m), the soil is not appreciably cemented or may be cemented only locally. Figure 2-24 provides a description of the material observed in test pit SFS-3, located at the site proposed for the surface facilities.

### 2.7.3.2 Physical properties of alluvium

The physical properties of alluvium that have been measured are index properties and compaction characteristics. The techniques for the measurements are in accord with American Society for Testing and Materials (ASTM) procedures, as discussed by Ho et al. (1986).

Three samples were obtained from the lower two horizons shown in Figure 2-24 and the minus 3-in. fraction was subjected to sieve analysis; the results are shown in Figure 2-25. Most of the material is sandy gravel, with up to 7 percent silt. However, considering the mode of deposition of desert alluvial deposits, considerable variation in grain size and gradation characteristics is possible, both laterally and vertically.

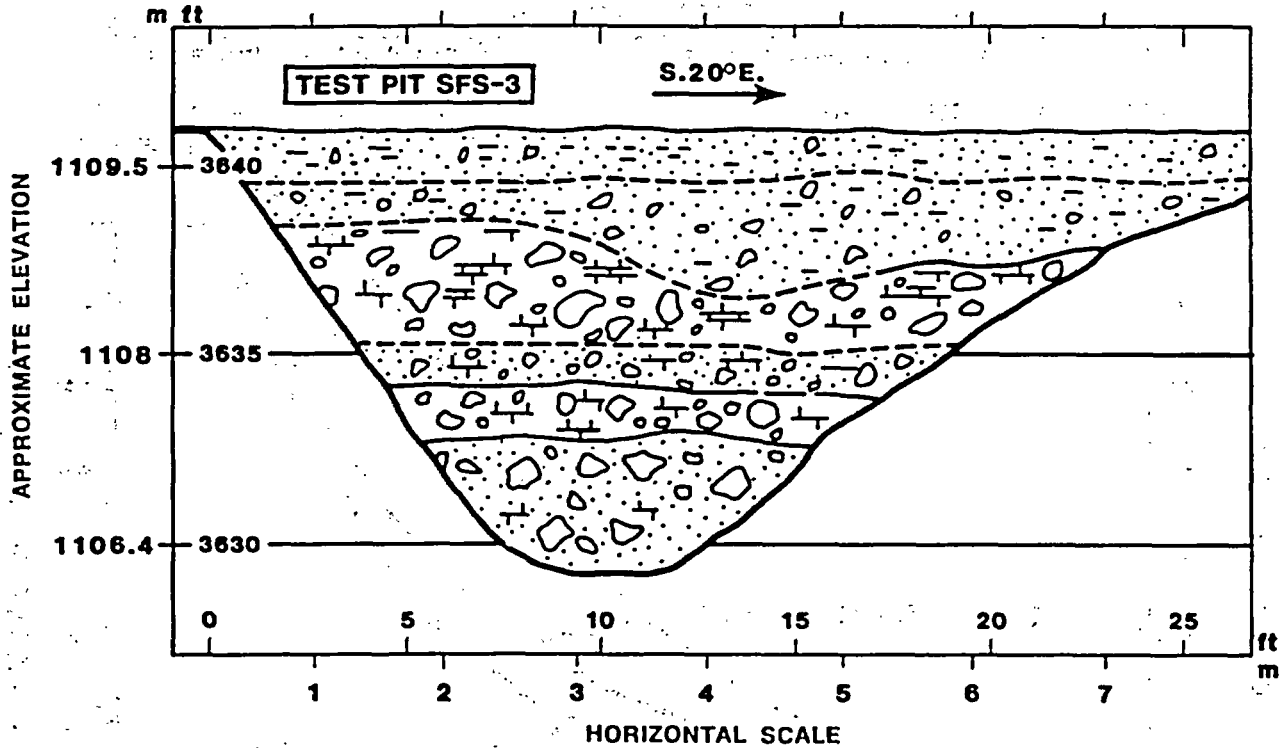
The specific gravity of the alluvium samples appears to vary somewhat with grain size. The specific gravity of larger particles (retained on #4 sieve) averaged about 2.35, whereas the average specific gravity of the finer particles was about 2.50. The lower specific gravity of the larger particles may result from the presence of noninterconnected void spaces in the larger particles, which is common for these rock types (ash-fall and ash-flow tuffs). The average specific gravity is given as 2.43.

In situ densities, which were measured by the sand-cone method (ASTM D1557, Method D (ASTM, 1978)) and nuclear density tests, range from 101 to nearly 112 lb/ft<sup>3</sup> (1.62 to 1.79 g/cm<sup>3</sup>), for samples from test pit SFS-3. These densities were found to be about 93.5 to 100 percent of the maximum dry density.

Compaction test results for the soils sampled from test pit SFS-3 show appreciable variation. The maximum dry density ranges from 108 to 114 lb/ft<sup>3</sup> (1.73 to 1.83 g/cm<sup>3</sup>). The corresponding optimum moisture contents are 14.7 and 12.0 percent, respectively.

The requirements for performing sand cone and compaction tests precludes consideration of the larger particles (greater than 0.75 in.), which if included would increase the measured densities. Similarly, the presence of cobbles and boulders in the soil matrix affects the results of nuclear density tests. Thus, the reported results are more indicative of the soil matrix materials than the entire soil profile (including the cobbles and boulders). Evaluation of the density of the entire soil profile would have

CONSULTATION DRAFT



DEPTH (ft)	SAMPLE NUMBER	DESCRIPTION
0--4	B-1	SAND, LIGHT BROWN, FINE-GRAINED, SILTY, WITH SOME GRAVEL, COBBLES, AND BOULDERS; UNCEMENTED, FIRM, NONBEDDED, BOTTOM CONTACT UNDULATORY. BETWEEN 0 AND 1.5 FEET: LOOSE; LESS GRAVEL (A&B SOIL HORIZONS).
~4-8	B-2	GRAVEL, LIGHT GREY TO TAN, WITH FINE SAND, VOLCANIC COBBLES, AND BOULDERS TO 20 INCHES IN DIAMETER; HARD, WELL CEMENTED WITH CALICHE, BOULDERS BREAK APART ON EXCAVATION; BEDDING INDISTINCT; GRAVELS MOSTLY SUBANGULAR. BETWEEN 6 AND 7 FEET: BROWNISH GRAVELLY SAND, POORLY BEDDED; LAMINA OF WHITE CALICHE MARKS PROMINENT BEDDING PLANE AT 7 FEET.
8-12	B-3	GRAVEL, LIGHT BROWN TO TAN, WITH FINE SAND, COBBLES AND BOULDERS TO 20 INCHES DIAMETER; DENSE, SLIGHTLY CEMENTED WITH CALICHE; BEDDING INDISTINCT.

Figure 2-24. Geologic log of test pit SFS-3. Modified from Ho et al. (1986). Samples described were bulk samples from sand cone and nuclear density tests.

CONSULTATION DRAFT

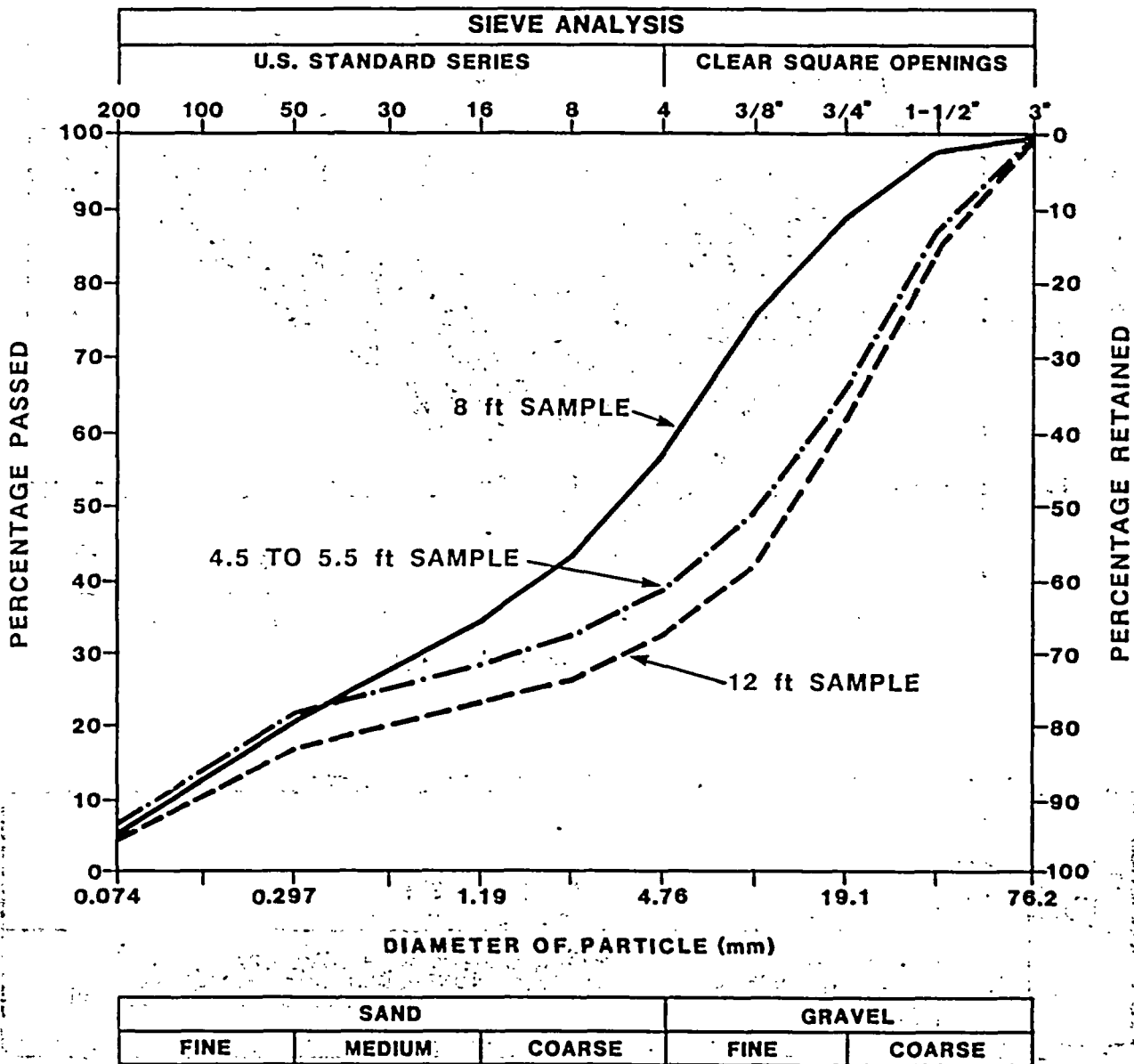


Figure 2-25. Gradation curves of samples from test pit SFS-3 at 4.5 to 5.5, 8, and 12-ft depths. Modified from Ho et al. (1986).

required large-scale, nonstandard, density testing that was judged to be unnecessary.

All soils studied were found to be dry. At test pit SFS-3, the average measured natural moisture content was 7.2 percent.

### 2.7.3.3 Engineering properties of alluvium

No direct measurements or tests of engineering properties of site soils have been completed. However, conservative estimates can be made through standard techniques based on the results of the index property tests, knowledge of the general behavior of the identified soils, and the Unified Soil Classification System. The engineering properties given here apply to uncemented soils below the zone of loose topsoil.

For engineering design purposes, the granular soils can be assumed to be cohesionless. They are assumed to behave like an elastic solid so that settlement will occur more or less simultaneously with the applied loads. Because the soils are predominantly in a dense to very dense state, settlement is expected to be small. Elastic settlement under various loadings can be calculated either from Young's modulus and Poisson's ratio or from the modulus of subgrade reaction. The engineering properties and measured physical properties are summarized in Table 2-15.

## 2.8 EXCAVATION CHARACTERISTICS OF THE ROCK MASS

This section reviews the excavation characteristics of, or experiences in tuff, with respect to the dimensions of mined openings, support requirements for these openings, excavation methods, damage to the rock resulting from excavation, and water inflow. In addition, the effect on geoenvironmental properties of damage resulting from excavation is discussed, and potential effects on performance are reviewed. The data for this evaluation come from observations and measurements made on cores from each of the horizons considered in Yucca Mountain for waste emplacement, coupled with data from the mined openings in G-Tunnel. Additional evaluations will be made in the exploratory shaft facility in both the upper and lower breakout rooms and in the planned sequential drift mining evaluations.

### 2.8.1 EXCAVATION CHARACTERISTICS OF SIMILAR ROCKS

Excavation characteristics of other rock masses are considered explicitly in the extensive data base used to develop and evaluate both of the rock mass classification techniques discussed in the following section. Therefore, no explicit list of the characteristics of other formations is provided here.

Table 2-15. Summary of physical and engineering properties of alluvium<sup>a</sup>

PHYSICAL PROPERTY <sup>b</sup>	
Soil classification	GP and GM present <sup>c</sup>
Natural moisture content	5.1-9.2%
In situ density	101-112 pcf (1.62-1.79 g/cm <sup>3</sup> )
Percent of maximum dry density	93.5-100%
Specific gravity of soil solids	2.43
Void ratio	0.37
ENGINEERING PROPERTY <sup>d</sup>	
Young's modulus	10,000-20,000 psi (0.7-1.4 GPa)
Poisson's ratio	0.30-0.35
Modulus of subgrade reaction	200-300 pci (5,536-8,304 g/cm <sup>3</sup> )
Cohesion	0
Angle of internal friction	33-37°C
Allowable bearing pressure <sup>e</sup>	6 ksf (0.3 MPa)

<sup>a</sup>Source: Ho et al. (1986).

<sup>b</sup>Values and ranges of physical properties are from samples taken from test pit SFS-3.

<sup>c</sup>GP classification is poorly graded gravels, gravel-sand mixtures, and little or no fines. GM classification is silty gravels, and gravel-sandsilt mixtures, which may be poorly graded.

<sup>d</sup>Estimated from index properties.

<sup>e</sup>For footings wider than 4 ft, subject to verification that settlement will be tolerable in the case of very large structures.

## 2.8.2 EXCAVATION CHARACTERISTICS OF ROCK AT THE SITE

### 2.8.2.1 G-Tunnel experience

For definition of the mining methods to be used in the repository, the most applicable data come from experience gained in the development of G-Tunnel at the NTS. G-Tunnel experience in the Grouse Canyon Member and planned excavations in Yucca Mountain are similar in many ways:

1. Overburden loadings, opening dimensions (up to 5-m span), and excavation methods will be similar.

## CONSULTATION DRAFT

2. The degrees of saturation are similar for geoengineering purposes (0.65 in the Topopah Spring Member (Montazer and Wilson, 1984) versus 0.6 to 0.9 in the Grouse Canyon Member (Zimmerman et al., 1984b)), however, for hydrologic purposes these differences may be significant.
3. The thermal, mechanical, and bulk properties of the tuffs are similar (Table 2-16).
4. The degree and nature of fracturing are similar (Langkopf and Gnirk, 1986).

Because of these similarities, the data obtained from tests and observations in G-Tunnel can be used in conceptual and preliminary design and analysis for a repository in the Topopah Spring Member at Yucca Mountain.

In 1961, the development of G-Tunnel was started, and since that time about 3,500 m of drift have been excavated into the tunnel beds (informal units of nonwelded to moderately welded tuffs in Rainier Mesa). These beds are similar to the tuffaceous beds of Calico Hills in Yucca Mountain and are substantially weaker than the welded Topopah Spring Member, yet they have remained stable with minimal support for more than 20 yr. Currently a mechanical mining machine (Alpine miner) is being used to excavate the tunnel bed tuff. No formal investigations have been performed to quantify the damage to the rock produced by this mining technique, but an examination of the ribs and roof reveals very little visible damage. In the initial few hundred meters of excavation, steel sets and lagging were used for support. Since then, roof bolts and wire mesh have been used successfully to stabilize the openings.

As part of the NNWSI Project, about 130 m of drift have been excavated in the welded tuff of the Grouse Canyon Member of the Belted Range Tuff, which is similar to the nonlithophysal portion of the Topopah Spring Member at Yucca Mountain. In general the welded tuff in G-Tunnel was excavated using controlled drilling and blasting techniques. An examination of the ribs and roof appeared to indicate more damage to the finished rock surfaces in the welded tuff than occurred during excavation of the portions of G-Tunnel in the tunnel beds, a series of nonwelded tuffs underlying the Grouse Canyon Member. However, since the Grouse Canyon Member is more highly fractured than the nonwelded material, it is more difficult to assess whether damage to finished rock surfaces is the result of the mining technique. A mechanical miner was used successfully to cut the welded tuff and to level the floors, although relatively rapid wear of the picks attached to the rotating drum was noted. The spans of G-Tunnel openings in the welded material (Figures 2-2 and 2-3) range from 3.4 to 5 m. The experiment drift identified is 5 m wide and 5 m high, approximately the dimensions being considered for repository drifts. At one time during the excavation of the extensometer drift, miners were unavailable to install roof supports immediately after seven blasting rounds had been shot. This left a 14 m length of roof unsupported for 1 to 2 months. During this time no deterioration of roof material was evident. Following this hiatus, roof bolts and wire mesh were installed successfully in the roof. A nearly vertical fault with 1 m of vertical displacement was encountered during mining activities in the welded Grouse Canyon Member in G-Tunnel. The conclusion drawn by Tibbs (1985) is

CONSULTATION DRAFT

Table 2-16. Comparison of properties of Topopah Spring and Grouse Canyon members

Property	G-Tunnel Grouse Canyon Member	Yucca Mountain Topopah Spring Member
Matrix porosity ( $^{00}/0$ )	6-24 <sup>a</sup>	6-19 <sup>a</sup>
Grain density (g/cm <sup>3</sup> )	2.57-2.63 <sup>b</sup>	2.51-2.58 <sup>b</sup>
Saturation	0.6-0.9 <sup>a</sup>	0.65 <sup>c</sup>
Saturated thermal conductivity (W/mK)	1.6-2.0 <sup>a</sup>	2.1-2.5 <sup>a</sup>
Dry thermal conductivity (W/mK)	1.0-1.6 <sup>b</sup>	1.5-2.1 <sup>b</sup>
Coefficient of linear thermal expansion ( $10^{-6} K^{-1}$ )	7.8-10.6 <sup>a</sup>	7.3-14.1 <sup>a</sup>
Young's modulus (GPa)	22-28 <sup>a</sup>	24-38 <sup>a</sup>
Poisson's ratio	0.16-0.32 <sup>a</sup>	0.12-0.32 <sup>a</sup>
Unconfined compressive strength (MPa)	64-142 <sup>a</sup>	55-287 <sup>a</sup>

<sup>a</sup>Zimmerman et al. (1984b).

<sup>b</sup>Nimick and Lappin (1985).

<sup>c</sup>Montazer and Wilson (1984).

that crossing the fault did not result in the need for special ground support in excess of the standard methods used in the drift where no faulting occurred.

#### 2.8.2.2 Rock mass classification of Yucca Mountain tuffs

Rock-mass classification systems have been used to assess the excavation characteristics and support requirements for mined openings in Yucca Mountain. Two rock mass classification systems were used: the Norwegian Geotechnical Institute (NGI) system proposed by Barton et al. (1974a) and the South African Council for Scientific and Industrial Research Geomechanics (CSIR) system proposed by Bieniawski (1976). Both systems use data on rock

quality, as determined from core observations, and information on joint characteristics such as the number of joint sets, the nature of joint surfaces, and the ground-water conditions in the joints. In addition, the NGI system considers in situ stress conditions, and the CSIR system includes information on the orientation of structural features and the strength of the rock. These classification systems are mainly used for single tunnels but have been applied to multiple underground openings with pillar dimensions of about 15 m with extraction ratios of 25 to 50 percent. A summary of evaluations of the tuff units studied by the NNWSI Project is presented in the following discussion.

Before the recommendation of a repository horizon was made, several Yucca Mountain stratigraphic units were classified by these systems. These included the nonlithophysal Topopah Spring Member, the upper ash flow of the tuffaceous beds of the Calico Hills, the welded devitrified portion of the Bullfrog Member, and the welded devitrified portion of the Tram Member. The tunnel beds and the welded portion of the Grouse Canyon Member in G-Tunnel also were rated for comparison (Tillerson and Nimick, 1984). The classifications have been updated since the unit evaluation study based on additional information on the units from Yucca Mountain (Langkopf and Gnirk, 1986).

Comparative ratings for the Topopah Spring Member and the two units from G-Tunnel are presented graphically in Figure 2-26. The scales for the two classification systems have been correlated according to Bieniawski (1976). The ratings are taken from Langkopf and Gnirk (1986). In general the ratings for the three units are similar. This observation, combined with the long-term stability of G-Tunnel with minimum support, suggests that an excavation in the Topopah Spring Member would be stable for long periods of time without extensive support.

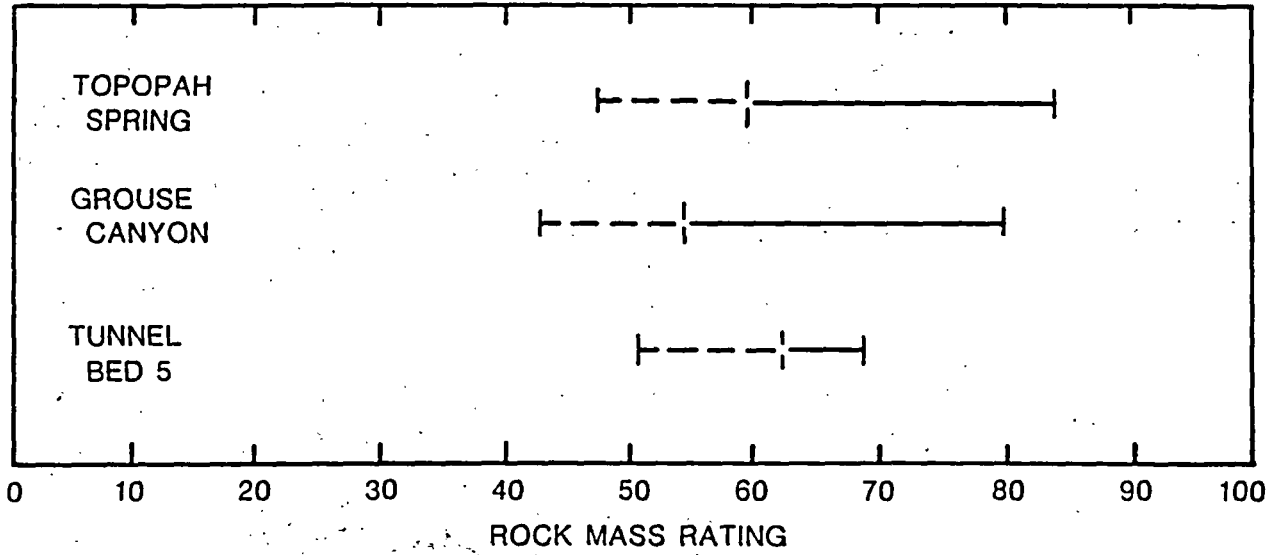
### 2.8.2.3 Estimated support requirements based on rock mass classification

The Norwegian Geotechnical Institute Rock Mass classification system is based upon approximately 200 case histories of tunnels (including 2 cases in tuff) (Barton et al., 1974b). This method was used to develop preliminary estimates of support requirements for excavations in tuff at Yucca Mountain and in G-Tunnel (Table 2-17). Despite the variation in rock mass classification for the various units, the support estimates indicate that either untensioned grouted rock bolts with shotcrete or tensioned grouted rock bolts with shotcrete should suffice in most instances. These estimates are based both on an assumed span width of 5 m and on an excavation support ratio (ESR) consistent with permanent support similar to that required for underground power stations, major road and railway tunnels, and civil defense chambers, which somewhat exceed the support required for a permanent mine opening. For the tunnel beds and the Grouse Canyon Member, the actual support requirements are at the lower end of the range of estimated support requirements. Actual support for these members consists of tensioned rock bolts (grouted) and wire mesh, without shotcrete being necessary.

More detailed studies and evaluations of requirements for permanent support systems will be made in the exploratory shaft facility. Additional

CONSULTATION DRAFT

PLOT OF CSIR CLASSIFICATION RATINGS FOR SELECTED NTS TUFF MEMBERS



--- PORTION OF OVERALL RANGE THAT CAN BE ELIMINATED IF THE DRIFTS CAN BE ORIENTED "VERY FAVORABLY" WITH RESPECT TO THE JOINTS

PLOT OF NGI CLASSIFICATION RATINGS FOR SELECTED NTS TUFF MEMBERS

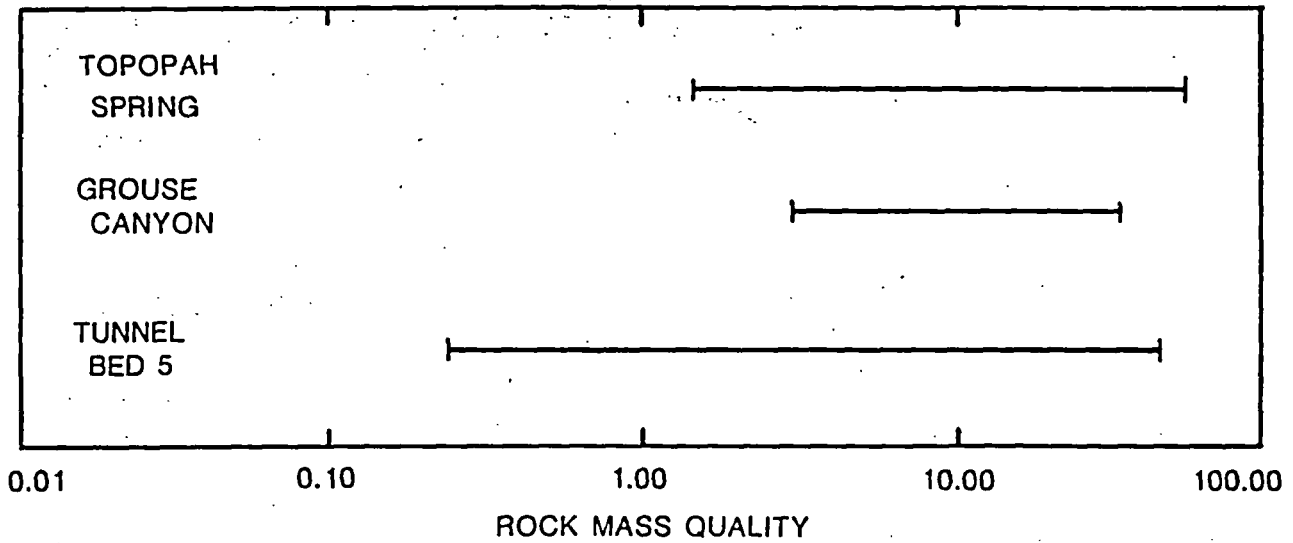


Figure 2-26. Rock mass classification values for various tuff units. Modified from Lankopf and Gnirk (1986).

CONSULTATION DRAFT

Table 2-17. Estimated support requirements based on the Norwegian Geotechnical Institute (NGI) Rock Mass Classification System

Unit	Location	Classification value (Q)	Suggested support requirements
Nonlithophysal Topopah Spring Member	Yucca Mountain	53.3 to 1.46	(a), (b)
Tunnel bed 5	G-Tunnel	46.5 to 0.24	(c), (a), (b)
Welded Grouse Canyon Member	G-Tunnel	34.0 to 3.08	(c), (a), (b)

<sup>a</sup>Untensioned grouted rock bolts with unreinforced shotcrete.

<sup>b</sup>Tensioned grouted rock bolts with wire mesh-reinforced shotcrete.

<sup>c</sup>No support requirements.

discussion of support considerations in the design process is provided in Section 6.2.6.3.6.

#### 2.8.2.4 Estimates of ground-water inflow

As expected above the water table, there is no spatially continuous flow of water into any of the drifts in G-Tunnel. An unmeasured but presumed small quantity is removed by the ventilation system. Observed water flow is limited to seepage from saturated faults or fractured zones oriented more or less vertically. The quantities of water are estimated to be approximately 15 gal/d (Fernandez and Freshley, 1984) and are removed by routine pumping of a small sump area.

It is expected that ground-water inflow in the Topopah Spring Member in Yucca Mountain will be even less than that at G-Tunnel and that dewatering requirements will be minimal. This conclusion is based on the lower degree of saturation in the Topopah Spring Member, on the lack of significant inflow during the drilling of drillholes through the unsaturated zone at Yucca Mountain, and on the lesser precipitation and smaller frequency of snow cover on Yucca Mountain as compared with Rainier Mesa.

#### 2.8.2.5. Excavation methods

The conclusions that are drawn from the observations made in G-Tunnel as related to repository design in the Topopah Spring Member are as follows:

1. Controlled drilling and blasting mining techniques can be used successfully for excavating welded tuff.
2. Because the welded tuff was cut successfully (during floor leveling) with a mechanical mining machine, tunnel-boring machines and mechanical miners could be used.

#### 2.8.3 CHANGES IN GEOENGINEERING PROPERTIES RESULTING FROM EXCAVATION

Underground excavation causes changes in rock mass properties in the vicinity of the excavation. The changes result from stress changes caused by the removal of material and also from fracturing induced by the excavation process. Few studies distinguish between these two mechanisms. Excavation-induced stress changes may either open or close preexisting fractures, depending on fracture orientations relative to the underground opening and to the preexisting in situ stresses. Kelsall et al. (1982) point out that stress relief resulting from excavation primarily will open preexisting fractures, whereas the excavation process will cause additional fractures. The effect of each of these on rock permeability (and, by inference, on the geoengineering properties sensitive to fracture aperture) is approximately equal if controlled blasting is the excavation technique (Kelsall et al., 1982).

Three excavation methods for the repository have been considered:

1. Drilling and blasting.
2. Mechanical mining.
3. Tunnel-boring.

The mechanical fracturing induced is different for the three different methods of excavation.

Fracturing induced by drilling and blasting may extend up to 3 m ahead of and around the opening (Svanholm et al., 1977); major disturbance is generally limited to within 1 m or less of the tunnel wall (Kelsall et al., 1982). The fracturing induced in more competent and uniform rock will extend a shorter distance away from the charge. Careful planning, careful shothole spacing, and proper selection of the charge-and-firing sequence can minimize the thickness of the zone of increased fracturing.

Mechanical mining machines cause fracturing for a distance of only several centimeters into the rock (Agapito et al., 1984). Slow, deep, and straight cuts with the mechanical miner minimize the specific energy of the process and also the collateral fracturing.

## CONSULTATION DRAFT

Tunnel-boring machines using disk cutters create a zone of increased fracturing in rock up to 30 cm thick (Nishida, 1982). Optimization of the specific energy for the specific in situ circumstances reduces the collateral fracturing.

Regardless of the excavation technique used, a zone of increased fracturing will exist in which rock properties will differ from those in the surrounding rock mass. This zone will be more intensely fractured than the remainder of the rock and may have reduced saturations resulting from the ventilation of the adjacent openings. The characterization of this zone is one of the goals of some tests planned for the exploratory shaft (Section 8.3.1.15).

The mechanical properties of the rock in the zone of increased fracturing, especially the strength and deformation modulus, will be reduced from values in the surrounding rock. The magnitude of the reduction will depend on the extent of fracturing in the zone. Section 2.3.3 discusses the qualitative effects of fracturing on mechanical properties.

The volumetric heat capacity in the zone of increased fracturing will be lower than rock mass values because of the higher porosity and the lower water content (Section 2.4.2.2). The coefficient of thermal expansion will be lowered by the presence of more fractures, but the deviation from the thermal expansion coefficient of the rock mass will decrease as the fractures are closed by expansion during the initial portion of the temperature rise around a repository.

The presence of excavated openings will change the distribution of stresses in the vicinity of the openings. The importance of this stress change in affecting geoenvironmental properties depends primarily on the magnitude and the direction of the resultant deviatoric stress. Factors that may affect the resultant deviatoric stress include opening size and shape, the in situ stress field and its anisotropy, and the spatial distribution of fractures. The effects of these factors are discussed in Chapter 6.

## 2.9 SUMMARY

### 2.9.1 SUMMARY OF SIGNIFICANT RESULTS

This section summarizes the important results from Sections 2.1 through 2.8. Individual sections should be consulted for additional details.

#### 2.9.1.1 Geoenvironmental properties

The development of the data base of geoenvironmental properties for use in technical decisions related to a repository at Yucca Mountain is well under way. At present, the data base consists primarily of the results of laboratory tests on core samples, but it is enhanced by initial results from field observations and tests being made in G-Tunnel at Rainier Mesa. The selection

## CONSULTATION DRAFT

of the Topopah Spring Member as the target horizon for the repository was based mostly on the average thermal and mechanical properties (for each of the four horizons considered) defined from approximately 600 bulk-property measurements, 75 thermal conductivity tests, 95 thermal expansion tests, 35 mineralogic-petrologic analyses, 60 mechanical tests on jointed-rock samples, and 190 unconfined and 50 mechanical-property triaxial tests. Definition of the properties to be expected in the candidate repository horizons relied on combining the measured thermal and mechanical property data with the corresponding bulk properties (porosity and grain density) to produce average thermal and mechanical properties for thermal and mechanical units. The thermal and mechanical units can be defined in the exploration holes drilled to date, although individual layers vary in thickness and, in places, do not coincide with identified lithologic tuff units. The preliminary values of geoenvironmental properties for the thermal and mechanical units to be used in design and performance assessment work have been summarized in Tables 2-7, 2-9, and 2-14.

Studies of the mechanical properties of intact samples from Yucca Mountain indicate that observed variations between the four horizons studied for horizon selection depend mainly on porosity. Preliminary assessments have been performed of the effects of water, temperature, confining and fluid pressure, loading time, lithophysae, and anisotropy. Additional testing is being focused almost entirely on the Topopah Spring Member. Large-scale laboratory tests (sample diameters up to 30 cm) have been performed to evaluate lithophysae effects, and similar testing is under way to examine parameter effects (temperature, confining pressure, strain rate, saturation, and sample size) on mechanical properties. Assessment of the lateral variability of properties will rely partly on material from the lateral boreholes or drifts planned for the exploratory shaft facility.

Studies of the mechanical properties of discontinuities (e.g., joints, bedding planes, and faults) have focused on the mechanical properties of simulated joints precut in samples of tuffs from the Grouse Canyon and the Prow Pass members. These results are included in this report because of the physical and mechanical similarities of these units to the Topopah Spring Member. Variations in the mechanical properties of simulated joints resulting from the effects of displacement rate, water saturation, and time-dependent behavior have been quantified for use in predicting the mechanical response of the rock mass. Testing is under way to determine the properties of natural and artificial joints in samples of the Topopah Spring Member. In addition to providing data on the selected horizon, such testing will enable an evaluation of the application of results from other welded, devitrified tuff to the Topopah Spring Member. The type, spacing, orientation, and properties of discontinuities at the repository level will be characterized in the exploratory shaft facility.

To date there has been no large-scale testing of the tuffs from Yucca Mountain. The heated-block test performed in G-Tunnel has provided some data for the rock mass modulus of deformation. These data can be used with the laboratory results for the Grouse Canyon Member to estimate how much the intact rock Young's moduli of Yucca Mountain units need to be reduced to describe the rock mass. Currently, it is estimated that the in situ modulus of deformation will be about half the Young's modulus measured in the

## CONSULTATION DRAFT

laboratory. The pressurized-slot tests fielded in G-Tunnel will provide additional data on the in situ modulus of deformation.

When underground access to the Topopah Spring Member becomes available, large-scale in situ tests will be performed to measure directly rock mass mechanical properties and to evaluate whether rock mass response can be predicted using numerical analysis codes. These tests will be designed and positioned to be representative of the rock mass, including discontinuities. Plate-bearing tests, strength tests, and the Yucca Mountain heated-block measurement will emphasize properties evaluations. Shaft and drift deformation monitoring during excavation along with the canister-scale heater test will assist in the design approach by evaluating the construction and thermal effects of waste emplacement on a larger scale than in the properties tests.

The thermal conductivities of saturated and dehydrated samples are variable and show dependence on variations in porosity and grain density (mineralogy). Studies indicate that the effects of layering (fabric anisotropy) on the thermal conductivity of welded and nonwelded tuffs are negligible. It appears that the effects on conductivity of air-filled lithophysae that occur within the Topopah Spring Member can be modeled as additional air-filled porosity. However, the distribution of these voids remains poorly defined, and the above assertion requires further confirmation. The presence of fractures is expected to have a negligible effect on in situ rock mass thermal conductivity.

The calculated values of volumetric heat capacity for the tuff strongly depend on porosity and degree of saturation and somewhat depend on mineralogy (grain density). A series of measurements of the heat capacity of some of the thermal and mechanical units at Yucca Mountain is planned to provide confirmation of the calculated values.

The laboratory measurements of the thermal expansion of samples from Yucca Mountain indicate that because of the presence of variable amounts of hydrous phases, three temperature ranges must be defined for the thermal-expansion behavior of Yucca Mountain tuffs: pretransitional, transitional, and posttransitional. Studies indicate that the effects of bedding and textural anisotropy on matrix thermal expansion behavior of densely welded tuffs are negligible. The presence of thermally induced or preexisting fractures is expected to reduce thermally induced rock mass stresses to below those predicted using thermal and mechanical properties measured in the laboratory, primarily because of the lower elastic moduli in the field.

An examination of in situ stress at the NTS and at Yucca Mountain indicates that measurements at Yucca Mountain are consistent with other measurements in the region. Measurements and calculations have provided reasonable bounds on the magnitudes of in situ stresses at Yucca Mountain.

For a repository in the Topopah Spring Member, analyses predict that the partial saturation, relatively low porosity, and the presence of prevalent fractures preclude thermally induced decrepitation of the rock mass. Laboratory tests of thermally induced water migration will be made to estimate its effect on ventilation requirements in a repository and on the effective thermal conductivity of the rock mass. In addition, these tests will provide a better understanding of the mechanisms and magnitude of water movement in

## CONSULTATION DRAFT

tuff subjected to a changing temperature field. Observations of thermally induced water migration will also be made in engineered barrier system design tests planned for the exploratory shaft facility.

Because tuffs at Yucca Mountain and Rainier Mesa are similar, G-Tunnel experience indicates that controlled-blasting techniques can be used to excavate the welded tuff. In addition, roof bolts and wire mesh should be sufficient to stabilize the openings. Control of water flow should not be a significant factor in the repository design. The excavation characteristics of tuffs from Yucca Mountain have been evaluated by using several empirical approaches with borehole and core sample data. These empirical correlations suggest that no unusual support systems will be required during the excavation of the exploratory shaft or the repository in the Topopah Spring Member. Confidence in the predictions was gained by applying them to the nonwelded tuffs in tunnel bed 5 and the welded tuffs in the Grouse Canyon Member at Rainier Mesa.

### 2.9.1.2 Relationship of data to performance objectives

The data required to analyze the performance objectives have been identified through the definition of information needs. These information needs and their relationship to specific performance objectives are discussed in Section 8.2. The data in Chapter 2 that apply to performance objectives are presented in Section 2.9.3. The performance objectives to which the analysis of geoenvironmental data contribute are briefly discussed in this section.

Performance objectives for the geologic operations area are described in 10 CFR Part 60. Those objectives to which information in Chapter 2 are most relevant are discussed in the following paragraphs.

Part (b) of 10 CFR 60.111 (retrievability of waste) is the performance objective for which geoenvironmental data provide the most information. To satisfy this objective, the NNWSI Project position is that all underground openings, including waste emplacement holes, drifts, and access ramps from the surface must remain stable through the retrievability period (Flores, 1986). For emplacement drillholes, there must be reasonable assurance that the walls will not deteriorate to an extent that would preclude removal of waste containers. The data summarized in this chapter demonstrate that both mechanical and thermal properties of the Topopah Spring Member are similar to correlative properties of the Grouse Canyon Member where, even at high temperatures, heater tests have not resulted in any damage to the heater-hole walls (Zimmerman, 1983).

A similar statement can be made about drifts in the Topopah Spring Member. G-Tunnel, which penetrates tuffs similar to the Topopah Spring Member, has required minimal support over its lifetime and has remained a stable opening. The additional factor of the elevated temperatures expected in the Topopah Spring Member, as a result of waste emplacement, must be treated with thermal and mechanical calculations such as those discussed in Chapter 6.

## CONSULTATION DRAFT

The data in Chapter 2 also may be used in an assessment of the performance objective for particular barriers after permanent closure (10 CFR 60.113). The analysis of the mechanical stability of the emplacement hole and of the expected environment (e.g., moisture content and temperature) must demonstrate that the waste package portion of the engineered barrier system will isolate the waste for the specified time (10 CFR 60.113(a)(1)(ii)(A)) and that radionuclide release rates from the engineered barrier system will be less than or equal to the limits specified in 10 CFR 60.113(a)(1)(ii)(B).

The conceptual models representing tuffs at Yucca Mountain were described briefly in the introduction to this chapter and are discussed in more detail in Chapter 6. All the data necessary to implement the models have been identified and either have been obtained or are part of the test program discussed in Chapter 8. Specific items that are either data or boundary conditions for which information is incomplete are presented in the following paragraphs.

The data summarized in Chapter 2 are insufficient for complete site characterization in the following specific areas:

1. The effects of the parameters (temperature, confining pressure, strain rate, saturation, and sample size) on the mechanical properties of welded, devitrified Topopah Spring Member.
2. The measurement of properties of joints in the Topopah Spring Member.
3. The confirmation that data obtained to date are representative of material to be characterized during underground testing in the exploratory shaft.
4. In situ measurement of geoenvironmental properties including thermal and mechanical rock mass properties, fracture properties, and in situ stress.

The data discussed in this chapter are of good quality (i.e., were obtained following detailed test procedures and using calibrated instruments under controlled test conditions); the experimental uncertainties are approximately 10 percent for thermal properties and 3 percent for mechanical properties. The data still to be gathered should be of at least comparable quality. Section 8.6 discusses quality assurance as related to test procedures to be used in future data collection.

### 2.9.1.3 Preliminary evaluation of data uncertainty

The test programs for rock characteristics (Sections 8.3.1.4 and 8.3.1.5) express data needs in terms of qualitative ranges of acceptable uncertainty at a specified confidence level. This type of confidence level analysis is not provided in Chapter 2 because it would be premature. The availability of samples and the scope of testing have been limited before site characterization, in such a way that sampling uncertainty is still high, and confidence requirements expressed in the aforementioned test programs

have not been reached. However, the requirements have been structured with respect to the available data such that (1) the requirements have already been attained (based on preliminary data) for a number of parameters, including bulk physical properties (porosity, grain density, and in situ bulk density), Poisson's ratio, and heat capacity (inferred from geochemistry), or (2) the requirements are probably attainable. But if certain requirements are unattainable because of sampling uncertainty then the requirements can be relaxed as part of performance assessment.

### 2.9.2 RELATION TO DESIGN

The information discussed in the preceding sections of Chapter 2 applies directly to the design process. The strength of the rock allows the calculation of factors of safety through comparison with the stress field around openings. The stress field, in turn, is a function of the preexisting stresses and of the stresses induced in the rock by the presence of the openings and of the heat produced by the waste canisters. The location, size, and orientation of openings will be a function of the stress field and of the expected mechanical behavior of the rock mass. The thermal field generated by a repository is a function of the preexisting temperatures and of the thermal conductivity and heat capacity of the rock. The allowable thermal loading and the distribution of the waste within the repository will be a function of the thermal properties and the predicted thermomechanical response of the rock mass. All these relationships between rock properties and the design of a repository are discussed in more detail in Chapter 6.

The rock properties are also relevant to the design of waste containers appropriate for waste emplacement in tuff. Thermal conductivity, heat capacity, and bulk density are the parameters that determine the rate at which heat is removed from the vicinity of the waste container; thus they affect the temperatures to which the containers will be subjected. The mechanical response (deformation modulus for an elastic medium) and the coefficient of thermal expansion help to determine the thermal stresses that will occur in the rock surrounding the waste container, so that the borehole stability can be estimated. Knowledge about thermally induced water migration behavior provides information on the expected chemical environment to which waste container materials will be subjected. These topics are presented in more detail in Chapter 7.

### 2.9.3 IDENTIFICATION OF INFORMATION NEEDS

This section provides a synopsis of information needs for which data in Chapter 2 are relevant. Geoengineering data pertinent to each listed information need are also provided. Table 2-18 is a summary of the information discussed in Chapter 2. A complete listing of information needs and investigations, including those for which geoengineering data are not pertinent, is provided in Section 8.2. Individual information needs and investigations and the strategies to be used in acquiring the necessary data are discussed in Section 8.3.

Table 2-18. Relationship of geoen지니어ing data to issues, information needs and investigations  
(page 1 of 3)

Information need or investigation	Description	Pertinent geoen지니어ing data	Relevant section of Chapter 2
1.1.1	Site information needed to calculate the releases of radionuclides to the accessible environment (Section 8.3.5.13.1)	Porosity	2.4.3
1.6.1	Site information and design concepts needed to identify the fastest path of likely radionuclide travel and to calculate the ground-water travel time along that path (Section 8.3.5.12.1)	Porosity	2.4.3
1.6.5	Boundaries of the disturbed zone (Section 8.3.5.12.5)	Effect of excavation methods on rock properties.	2.8.3
1.7	Determination that the subsurface conditions encountered and the changes in those conditions during construction and waste emplacement operations are within the limits, assumed in the licensing review [10 CFR 60.43(b), 60.74, 60.140(a)(1) and 60.141(b)] (Section 8.3.5.16)	Ambient stress conditions Porosity Density Thermal conductivity Heat capacity Thermal expansion Compressive strength Tensile strength Elastic moduli Joint properties	2.6 2.4.3 2.4.3 2.4.2.1, 2.5.2 2.4.2.2, 2.5.2 2.4.2.3, 2.5.2 2.1.2.3.1, 2.3.2, 2.3.3 2.1.2.3.2, 2.3.3 2.1.2.2, 2.3.2, 2.3.3 2.2
1.11.1	Site characterization information needed for design (Section 8.3.2.2.1)	All properties in Chapter 2	2.1-2.8
1.11.6	Predicted thermal and thermomechanical response of the host rock surrounding strata, and ground-water system (Section 8.3.2.2.6)	Ambient stress conditions Porosity Density Thermal conductivity Heat capacity Thermal expansion Compressive strength Tensile strength Elastic moduli Joint properties Thermally induced water migration	2.6 2.4.3 2.4.3 2.4.2.1, 2.5.2 2.4.2.2, 2.5.2 2.4.2.3, 2.5.2 2.1.2.3.1, 2.3.2, 2.3.3 2.1.2.3.2, 2.3.3 2.1.2.2, 2.3.2, 2.3.3 2.2 2.7.2

Table 2-18. Relationship of geoengineering data to issues, information needs and investigations  
(page 2 of 3)

Information need or investigation	Description	Pertinent geoengineering data	Relevant section of Chapter 2
8.3.1.2.2	Description of the unsaturated zone hydrologic system at the site	Porosity	2.4.3
8.3.1.2.3	Description of the saturated zone hydrologic system at the site	Porosity	2.4.3
8.3.1.3.4	Radionuclide retardation by sorption processes along flow paths to the accessible environment	Dry bulk density	2.4.3
8.3.1.3.6	Radionuclide retardation by dispersive/diffusive/advective transport processes along flow paths to the accessible environment	Porosity	2.4.3
8.3.1.15.1	Spatial distribution of thermal and mechanical properties	Thermal conductivity Thermal expansion Heat capacity Compressive strength Elastic moduli Joint properties Tensile strength	2.4.2.1, 2.5.2 2.4.2.3, 2.5.2 2.4.2.2, 2.5.2 2.1.2.3.1, 2.3.2, 2.3.3 2.1.2.2, 2.3.2, 2.3.3 2.2 2.1.2.3.2, 2.3.3
8.3.1.15.2	Spatial distribution of ambient stress and thermal conditions	Ambient stress conditions	2.6
8.3.1.6.4	Potential effects of erosion on the hydrologic and geochemical characteristics at Yucca Mountain	All of Chapter 2	2.1-2.8
8.3.1.8.5	Potential effects of igneous and tectonic activity on rock characteristics	All of Chapter 2	2.1-2.8
8.3.1.9.3	Potential effects of exploiting natural resources on hydrologic, geochemical, and rock characteristics	All of Chapter 2	2.1-2.8
2.4.1	Site and design data required to support retrieval (Section 8.3.5.2.1)	Thermal conductivity Thermal expansion Heat capacity	2.4.2.1, 2.5.2 2.4.2.3, 2.5.2 2.4.2.2, 2.5.2

Table 2-18. Relationship of geoenvironmental data to issues, information needs and investigations  
(page 3 of 3)

Information need or investigation	Description	Pertinent geoenvironmental data	Relevant section of Chapter 2
		Joint properties	2.2
		Compressive strength	2.1.2.3.1, 2.3.2, 2.3.3
		Tensile strength	2.1.2.3.2, 2.3.3
		Elastic moduli	2.1.2.2, 2.3.2, 2.3.3
2.7.1	Site information needed for design (Radiological protection)(Section 8.3.2.3.1)	All of Chapter 2	2.1-2.8
4.2.1	Site and performance assessment information needed for design (Section 8.3.2.4.1)	All of Chapter 2	2.1-2.8
4.4.1	Site and performance assessment information needed for design (Section 8.3.2.5.1)	All of Chapter 2	2.1-2.8
8.3.1.14.2	Soil and bedrock properties of potential locations of surface facilities	Geoenvironmental properties of surface materials	2.7.3
8.3.1.15.1	Spatial distribution of thermal and mechanical properties	Thermal conductivity	2.4.2.1, 2.5.2
		Heat capacity	2.4.2.2, 2.5.2
		Thermal expansion	2.4.2.3, 2.5.2
		Compressive strength	2.1.2.3.1, 2.3.2, 2.3.3
		Elastic moduli	2.1.2.2, 2.3.2, 2.3.3
		Joint properties	2.2
		Tensile strength	2.1.2.3.2, 2.3.3
8.3.1.15.2	Spatial distribution of ambient stress and thermal conditions	Ambient stress conditions	2.6

2-117

CONSULTATION DRAFT

A general list of geoengineering information needed to complete site characterization was given in Section 2.9.1. The remainder of this section sets preliminary priorities on the geoengineering information required. These priorities are based on the discussion in Chapter 6.

The data needs discussed in Sections 6.3 and 6.4 show that data on the mechanical properties of fractures in the Topopah Spring Member are the most important deficiency in the existing data base. These properties are an important part of the mechanical behavior of the rock mass, as well as a factor in decisions about the size, shape, and orientation of the mined openings of a repository.

Detailed knowledge of in situ stress at Yucca Mountain and its spatial variation is also lacking. This information is also important in the design process and plays a large role in determining the suitability of the site in terms of seismic and tectonic stability.

A third area where more data are required is that of the mechanical properties of the matrix of the Topopah Spring Member. Specifically, more information is needed on the effects of parameter variation (temperature, pressure, saturation state, and sample size) on the mechanical properties so that these properties can be estimated for the varying conditions expected during the life of a repository. Also, the mechanical properties of lithophysae-rich Topopah Spring Member must be better understood so that the volume of usable material can be better defined and so that allowance can be made in the design process for the presence of such material within the repository horizon.

#### 2.9.4 RELATION TO REGULATORY GUIDE 4.17

The following discussion is based upon an examination of NRC Regulatory Guide 4.17 (Revision 1), Part A, Section 2 (NRC, 1987). The discussion is intended to identify requirements from this document that do not apply to geoengineering properties for the Yucca Mountain site.

Regulatory Guide 4.17 requires that an analysis of elastic and inelastic behavior be included in the section on the mechanical properties of the rock matrix (NRC, 1987). As discussed in Section 2.1.2.3.1.4 of this report, inelastic deformation of the matrix of the Topopah Spring Member is considered unlikely at Yucca Mountain. Additional experimental work is ongoing to examine the validity of this position, as discussed in Section 8.3.1.15.

A description of special geoengineering properties is required to be present in a site characterization plan. Of the examples of such properties listed in NRC Regulatory Guide 4.17 (NRC, 1987), brine migration is not relevant to the Yucca Mountain site. Section 2.7.1 has predicted that thermal degradation and thermally induced water migration will not be significant. The latter conclusion is being examined in more detail during in situ testing in the exploratory shaft.

---

***Nuclear Waste Policy Act  
(Section 113)***

---

REFERENCES

***Consultation Draft***



***Site Characterization  
Plan***

***Yucca Mountain Site, Nevada Research  
and Development Area, Nevada***

---

***Volume I***

---

***January 1988***

---

***U.S. Department of Energy  
Office of Civilian Radioactive Waste Management  
Washington, DC 20585***

---

---

---

---

---

---

## CONSULTATION DRAFT

### REFERENCES FOR CHAPTER 2

- ASTM (American Society for Testing and Materials), 1966. True Specific Gravity of Refractory Material by Water Immersion, Standard Test Method, Reapproved 1976, ASTM C 135-66, Philadelphia, Penn.
- ASTM (American Society for Testing and Materials), 1971. Linear Thermal Expansion of Rigid Solids With a Vitreous Silica Dilatometer, Standard Test Method, ASTM E 228-71, Philadelphia, Penn.
- ASTM (American Standard Test Methods), 1978. Moisture-Density Relations of Soils and Soil-Aggregate Mixtures Using 10-lb (4.54-kg) Rammer and 18-in. (457 mm) Drop, Standard Test Methods, ANSI/ASTM D 1557-78, pp. 270-276.
- ASTM (American Society for Testing and Materials), 1979a. True Specific Gravity of Refractory Materials by Gas-Comparison Pycnometer, Standard Test Method, ASTM C 604-79, Philadelphia, Penn.
- ASTM (American Society for Testing and Materials), 1979b. Unconfined Compressive Strength of Intact Rock Core Specimens, Standard Test Method, ANSI/ASTM D 2938-79, Philadelphia, Penn.
- ASTM (American Society for Testing and Materials), 1980a. Triaxial Compressive Strength of Undrained Rock Core Specimens Without Pore Pressure Measurements, Standard Test Method, ASTM D 2664-80, Philadelphia, Penn.
- ASTM (American Society for Testing and Materials), 1980b. Elastic Moduli of Intact Rock Core Specimens in Uniaxial Compression, Standard Test Method, ANSI/ASTM D 3148-80, Philadelphia, Penn.
- ASTM (American Society for Testing and Materials), 1981a. Density of Soil and Soil-Aggregate in Place by Nuclear Methods (Shallow Depth), ASTM D 2922-81, Philadelphia, Penn.
- ASTM (American Society for Testing and Materials), 1981b. Splitting Tensile Strength of Intact Rock Core Specimens, Standard Test Method, ASTM D 3967-81, Philadelphia, Penn.

CONSULTATION DRAFT

- ASTM (American Society for Testing and Materials), 1982. Density of Soil in Place by the Sand-Cone Method, ASTM D 1556-82, Philadelphia, Penn.
- ASTM (American Society for Testing and Materials), 1983a. Absorption and Bulk Specific Gravity of Natural Building Stone, Standard Test Method; ASTM C 97-83, Philadelphia, Penn.
- ASTM (American Society for Testing and Materials), 1983b. Laboratory Determination of Pulse Velocities and Ultrasonic Elastic Constants of Rock, Standard Test Method, ASTM D 2845-83, Philadelphia, Penn.
- ASTM (American Society for Testing and Materials), 1983c. Bulk Specific Gravity and Density of Compacted Bituminous Mixtures Using Paraffin-Coated Specimens, Standard Test Method, ASTM D 1188-83, Philadelphia, Penn.
- ASTM (American Society for Testing and Materials), 1984. Thermal Conductivity of Refractory Brick, Standard Test Method, ASTM C 202-84, Philadelphia, Penn.
- Agapito, J. F. T., H. N. Maleki, J. R. Aggson, and L. A. Weakly, 1984. "Impact of Excavation Technique on Strength of Oil Shale Pillars," International Journal of Mining Engineers, Vol. 2, pp. 93-105.
- Bandis, S., A. C. Lumsden, and N. R. Barton, 1981. "Experimental Studies of Scale Effects on the Shear Behavior of Rock Joints," International Journal of Rock Mechanics, Mining Science, and Geomechanical Abstracts, Vol. 18, pp. 1-21.
- Barton, N., 1973. "Review of New Shear-Strength Criterion for Rock Joints," Engineering Geology, Vol. 7, pp. 287-332.
- Barton, N., R. Lien, and J. Lunde, 1974a. Analysis of Rock Mass Quality and Support Practice in Tunneling and a Guide for Estimating Support Requirements, Internal Report 54206, Norwegian Geotechnical Institute, Oslo, Norway.
- Barton, N., R. Lien, and J. Lunde, 1974b. "Engineering Classification of Rock Masses for the Design of Tunnel Support," Rock Mechanics, Vol. 6, No. 4, pp. 189-236.

- Bauer, S. J., and J. Handin, 1983. "Thermal Expansion and Cracking of Three Confined, Water-Saturated Rocks to 800 deg. C," Rock Mechanics and Rock Engineering, Vol. 16, pp. 181-198.
- Bauer, S. J., J. F. Holland, and D. K. Parrish, 1985. "Implications About In Situ Stress at Yucca Mountain," Proceedings of the 26th U.S. Symposium on Rock Mechanics, Vol II, Rapid City, North Dakota, pp. 1113-1120.
- Bieniawski, Z. T., 1976. "Rock Mass Classifications in Rock Engineering," in Proceedings of the Symposium on Exploration for Rock Engineering, Johannesburg, 1-5 November 1976, Z. T. Bieniawski (ed.), Vol. 1; A. A. Balkema, Cape Town, South Africa, pp. 97-106.
- Bieniawski, Z. T., and W. L. Van Heerden, 1975. "The Significance of In Situ Tests on Large Rock Specimens," International Journal of Rock Mechanics, Mining Science, and Geomechanical Abstracts, Vol. 12, Pergamon Press, Great Britain, pp. 101-113.
- Bish, D. L., 1981. Detailed Mineralogical Characterization of the Bullfrog and Tram Members in USW-G1, with Emphasis on Clay Mineralogy, LA-9021-MS, Los Alamos National Laboratory, Los Alamos, N. Mex.
- Blacic, J., and R. Andersen, 1983. Methodology for Determining Time-Dependent Mechanical Properties of Tuff Subjected to Near-Field Repository Conditions, LA-9322-MS, Los Alamos National Laboratory, Los Alamos, N. Mex.
- Blacic, J. D., J. Carter, P. Halleck, P. Johnson, T. Shankland, R. Andersen, K. Spicochi, and A. Heller, 1982. Effects of Long-Term Exposure of Tuffs to High-Level Nuclear Waste Repository Conditions, LA-9174-PR, Los Alamos National Laboratory, Los Alamos, N. Mex.
- Blanford, M. L., 1982. Heated Block Test Conceptual Design Calculations, SAND81-1841. Sandia National Laboratories, Albuquerque, N. Mex.
- Board, M. P., M. L. Wilson, and M. D. Voegelé, 1987. Laboratory Determination of the Mechanical, Ultrasonic and Hydrologic Properties of Welded Tuff from the Grouse Canyon Heated Block Site, SAND86-7130, Science Applications International Corp.,

Las Vegas, N. Mex.

Broxton, D. E., D. T. Vaniman, F. Caporuscio, B. Arney, and G. Heiken, 1982. Detailed Petrographic Descriptions and Microprobe Data for Drill Holes USW-G2 and UE25b-1H, Yucca Mountain, Nevada; LA-9324-MS, Los Alamos National Laboratory, Los Alamos, N. Mex.

Byerlee, J., 1978. "Friction of Rocks," Pageoph (Pure and Applied Geophysics), Vol. 116, pp. 615-626.

Carlsson, H., 1978. A Pilot Heater Test in the Stripa Granite, Swedish-American Cooperative Program on Radioactive Waste Storage in Mined Caverns in Crystalline Rock, Technical Project Report No. 6, LBL-7086, Lawrence Berkeley Laboratory, Berkeley, Calif.

Carr, W. J., 1974. Summary of Tectonic and Structural Evidence for Stress Orientation at the Nevada Test Site, USGS-OFR-74-176; Open-File Report, U.S. Geological Survey, Denver, Colo.

Chen, E. P., 1987. A Computational Model for Jointed Media with Orthogonal Sets of Joints, SAND86-1122, Sandia National Laboratories, Albuquerque, N. Mex.

Cook, N. G. W., P. A. Witherspoon, E. L. Wilson, and L. R. Myer, 1983. "Progress with Thermomechanical Investigations of the Stripa Site," Proceedings of the Workshop on the Geological Disposal of Radioactive Waste In Situ Experiments in Granite, Stockholm, Sweden, October 25-27, 1983, pp. 19-31.

Costin, L. S., 1983. "A Microcrack Model for the Deformation and Failure of Brittle Rock," Journal of Geophysical Research, Vol. 88, No. B11, pp. 9485-9492.

Dieterich, J. H., 1978. "Time-Dependent Friction and the Mechanics of Stick-Slip," Pageoph (Pure and Applied Geophysics), Vol. 116, pp. 790-806.

Dischler, S. A., and K. Kim, 1985. "Determination of Rock Mass Deformation Modulus during Hydraulic Fracturing," Proceedings of the 26th U.S. Symposium on Rock Mechanics, Rapid City, South Dakota, June 26-28, 1985, E. Ashworth (ed.), A. A. Balkema, Boston, Mass., pp. 363-373.

- Doe, T., K. Ingevald, L. Strindell, B. Haimson, and H. Carlsson, 1981. "Hydraulic Fracturing and Overcoring Stress Measurements in a Deep Borehole at the Stripa Test Mine, Sweden," Proceedings of the 22nd U.S. Symposium on Rock Mechanics, Massachusetts Institute of Technology, Cambridge, Mass., pp. 373-378.
- Doe, T. W., K. Ingevald, L. Strindell, B. Leijon, W. Hustrulid, E. Majer, and H. Carlsson, 1983. In Situ Stress Measurements at the Stripa Mine, Sweden, LBL-15009, Lawrence Berkeley Laboratory, Berkeley, Calif.
- Eaton, R. R., D. E. Larson, and C. M. Korbin, 1981. "Sensitivity of Calculated Pore-Fluid Pressure to Repository Fracture Geometry," Scientific Basis for Nuclear Waste Management, J. G. Moore (ed.), Vol. 3, Plenum Press, New York, pp. 591-598.
- Ellis, W. L., and J. R. Ege, 1976. Determination of In Situ Stress in U12g Tunnel, Rainier Mesa, Nevada Test Site, Nevada, USGS-474-219, U.S. Geological Survey, Denver, Colo.
- Ellis, W. L., and J. E. Magner, 1980. Compilation of Results of Three-Dimensional Stress Determinations Made in Rainier and Aqueduct Mesas, Nevada Test Site, Nevada, USGS-OFR-80-1098, Open-File Report, U.S. Geological Survey, Reston, Va.
- Ellis, W. L., and H. S. Swolfs, 1983. Preliminary Assessment of In Situ Geomechanical Characteristics in Drill Hole USW G-1, Yucca Mountain, Nevada, USGS-OFR-83-401, Open-File Report, U.S. Geological Survey, Denver, Colo.
- Erickson, J. R., and R. K. Waddell, 1985. Identification and Characterization of Hydrologic Properties of Fractured Tuff Using Hydraulic and Tracer Tests--Test Well USW H-4, Yucca Mountain, Nye County, Nevada, USGS-WRI-85-4066, Water-Resources Investigations Report, U.S. Geological Survey, Denver, Colo.
- Fernandez, J. A., and M. D. Freshley, 1984. Repository Sealing Concepts for the Nevada Nuclear Waste Storage Investigations Project, SAND83-1778, Sandia National Laboratories, Albuquerque, N. Mex.

CONSULTATION DRAFT

- Fischer, F. G., P. J. Papanek, and R. M. Hamilton, 1972. The Massachusetts Mountain Earthquake of 5 August 1971 and Its Aftershocks, Nevada Test Site, USGS-474-149, U.S. Geological Survey, Denver, Colo., 20 p.
- Flores, R. J., 1986. Retrievability: Strategy for Compliance Demonstration, SAND84-2242, Sandia National Laboratories, Albuquerque, N. Mex.
- Goodman, L. E., and C. B. Brown, 1963. "Dead Load Stresses and the Instability of Slopes," Journal of the Soil Mechanics and Foundations Divisions, Proceedings of the American Society of Civil Engineers, May 1963, pp. 103-134.
- Goodman, R. E., 1980. Introduction to Rock Mechanics, John Wiley & Sons, Inc., New York.
- Gregory, E. C., and K. Kim, 1981. "Preliminary Results from the Full-Scale Heater Tests at the Near-Surface Test Facility," Proceedings of the 22nd U.S. Symposium on Rock Mechanics, Massachusetts Institute of Technology, Cambridge, Mass., pp. 137-142.
- Gurr, C. G., T. J. Marshall, and J. T. Hutton, 1952. "Movement of Water in Soil Due to a Temperature Gradient," Soil Science, Vol. 74, No. 5, pp. 335-345.
- Guzowski, R. V., F. B. Nimick, M. D. Siegel, and N. C. Finley, 1983. Repository Site Data Report for Tuff: Yucca Mountain, Nevada, NUREG/CR-2937, SAND82-2105, U.S. Nuclear Regulatory Commission, Washington, D.C.
- Haimson, B. C., 1981. "Confirmation of Hydrofracturing Results Through Comparisons with Other Stress Measurements," Proceedings of the 22nd U.S. Symposium on Rock Mechanics, Massachusetts Institute of Technology, Cambridge, Mass., pp. 379-385.
- Haimson, B. C., J. Lacombe, A. H. Jones, and S. J. Green, 1974. "Deep Stress Measurements in Tuff at the Nevada Test Site," Advances in Rock Mechanics, Vol. II, Part A, National Academy of Science, Washington, D.C. pp. 557-561.

CONSULTATION DRAFT

- Hardin, J., R. V. Hager, M. Friedman, and J. N. Feather, 1963. "Experimental Deformation of Sedimentary Rocks Under Confining Pressure: Pore Pressure Tests," Bulletin of the American Association of Petroleum Geologists, Vol. 47, No. 5, pp. 717-755.
- Hardin, E., N. Barton, M. Voegele, M. Board, R. Lingle, H. Pratt, and W. Ubbes, 1982. "Measuring the Thermomechanical and Transport Properties of a Rockmass Using the Heated Block Test," 23rd U.S. Symposium of Rock Mechanics, pp. 802-813.
- Hardin, E. L., M. D. Voegele, M. P. Board, and H. R. Pratt, 1985. "Development of a Test Series to Determine In Situ Thermomechanical and Transport Properties," in Measurement of Rock Properties at Elevated Pressures and Temperatures, H. J. Pincus and E. R. Hoskins (eds.), ASTM STP 869, American Society for Testing and Materials, Philadelphia, Penn., pp. 128-153.
- Hart, R. D., P. A. Cundall, and M. L. Cramer, 1985. "Analysis of a Loading Test on a Large Basalt Block," Proceeding of the 26th Symposium on Rock Mechanics, Rapid City, S.D., pp. 759-768.
- Heuze, E. H., and A. Salem, 1977. "Rock Deformability Measured In Situ, Problems and Solutions," Field Measurements in Rock Mechanics, International Symposium, Zurich, Switzerland, April 4-6, 1977, Vol. 1, pp. 375-387.
- Heuze, F. E., 1980. "Scale Effects in the Determination of Rock Mass Strength and Deformability," Rock Mechanics, Vol. 12, pp. 167-192.
- Heuze, F. E., and B. Amadei, 1985. "The NX-Borehole Jack: A Lesson in Trials and Errors," International Journal on Rock Mechanics, Mining Science, and Geomechanical Abstracts, Vol. 22, No. 2, pp. 105-112.
- Heuze, F. E., W. C. Patrick, R. V. De la Cruz, and C. F. Voss, 1981. In Situ Geomechanics, Climax Granite, Nevada Test Site, UCRL-53076, Lawrence Livermore National Laboratory, Livermore, Calif.

CONSULTATION DRAFT

- Ho, D. M., R. L. Sayre and C. L. Wu, 1986. Suitability of Natural Soils for Foundations for Surface Facilities at the Prospective Yucca Mountain Nuclear Waste Repository, SAND85-7107, Sandia National Laboratories, Albuquerque, N. Mex.
- Holland, J., and S. J. Bauer, 1984. Calculation of Overburden-Induced Stresses at Rainier Mesa, Nevada, SAND84-1592A, Sandia National Laboratories, Albuquerque, N. Mex.
- Hooker, V. E., and D. L. Bickel, 1974. Overcoring Equipment and Techniques Used in Rock Stress Determination, U.S. Bureau of Mines Information Circular 8618, Washington, D.C.
- Hooker, V. E., J. R. Aggson, and D. L. Bickel, 1971. Report on In Situ Determination of Stresses, Rainier Mesa, Nevada Test Site, U.S. Bureau of Mines Report, Denver Mining Research Center, Denver, Colo.
- Hubbert, M. K., and D. G. Willis, 1957. "Mechanics of Hydraulic Fracturing," Journal of Petroleum Technology, Vol. 210, pp. 153-168.
- Hustrulid, W. A., 1976. "An Analysis of the Goodman Jack," 17th U.S. Symposium on Rock Mechanics, Snowbird, Utah, Paper 4B10, pp. 4B10-4 to 4B10-8
- ISRM (International Society for Rock Mechanics), 1978. "Suggested Methods for Determining Tensile Strength of Rock Materials," International Journal of Rock Mechanics, Mining Science, and Geomechanical Abstracts, Vol. 15, pp. 99-103.
- ISRM (International Society for Rock Mechanics), 1979a. "Suggested Methods for Determining the Uniaxial Compressive Strength and Deformability of Rock Materials," International Journal of Rock Mechanics, Mining Science, and Geomechanical Abstracts, Vol. 16, pp. 135-140.
- ISRM (International Society for Rock Mechanics), 1979b. "Suggested Methods for Determining Water Content, Porosity, Density, Absorption and Related Properties and Swelling and Slake-Durability Index Properties," International Journal of Rock Mechanics, Mining Science, and Geomechanical Abstracts, Vol. 16, pp. 141-156.

CONSULTATION DRAFT

- Jaeger, J. G., and N. G. W. Cook, 1979. Fundamentals of Rock Mechanics, Chapman and Hall, London, pp. 60, 390-391, 405.
- Jeffry, J. A., T. Chan, N. G. W. Cook, and P. A. Witherspoon, 1979. Determination of In-Situ Thermal Properties of Stripa Granite from Temperature Measurements in the Full-Scale Heater Experiments: Method and Preliminary Results; Swedish-American Cooperative Program on Radioactive Waste Storage in Mined Caverns in Crystalline Rock, Technical Information Report No. 24, LBL-8423, Lawrence Berkeley Laboratory, Berkeley, Calif.
- Johnson, B., and A. F. Gangi, 1980. "Thermal Cracking of Nonuniformly Heated Thick-Walled Cylinders of Westerly Granite," Proceedings of the 21st U.S. Symposium of Rock Mechanics, University of Rolla, pp. 197-206.
- Johnstone, J. K., R. R. Peters, and P. F. Gnirk, 1984. Unit Evaluation at Yucca Mountain, Nevada Test Site: Summary Report and Recommendation, SAND83-0372, Sandia National Laboratories, Albuquerque, N. Mex.
- Johnstone, J. K., G. R. Hadley, and D. R. Waymire, 1985. In Situ Tuff Water Migration/Heater Experiment: Final Report, SAND81-1918, Sandia National Laboratories, Albuquerque, N. Mex.
- Kelsall, P. C., J. B. Case, and C. R. Chabannes, 1982. A Preliminary Evaluation of the Rock Mass Disturbance Resulting From Shaft, Tunnel, or Borehole Excavation, ONWI-411, Office of Nuclear Waste Isolation, Columbus, Ohio.
- Kim, K., and W. M. McCabe, 1984. "Geomechanics Characterization of a Proposed Nuclear Waste Repository Site in Basalt," Proceedings of the 25th U.S. Symposium on Rock Mechanics, Evanston, Ill., pp. 1126-1135.
- Kingery, W. D., H. K. Bowen, and D. R. Uhlmann, 1976. Introduction to Ceramics, Second Edition, John Wiley & Sons, New York, p. 608.
- Kovari, K., A. Tisa, H. H. Einstein, and J. A. Franklin, 1983. "Suggested Methods for Determining the Strength of Rock Materials in Triaxial Compression: Revised Version," International Journal of Rock Mechanics, Mining Science, and Geomechanical Abstracts, Vol. 20, No. 6, pp. 283-290.

CONSULTATION DRAFT

- Kuszyk, J. A., and R. C. Bradt, 1973. "Influence of Grain Size on Effects of Thermal Expansion Anisotropy in MgTi<sub>2</sub>O<sub>5</sub>," Journal of the American Ceramic Society, Vol. 56, No. 8, pp. 420-423.
- Lama, R. D., and V. S. Vutukuri, 1978. Handbook on Mechanical Properties of Rocks - Testing Techniques and Results - Volume II, Trans Tech Publications, Clausthal, Germany, pp. 231-236.
- Langkopf, B. S., and P. R. Gnirk, 1986. Rock-Mass Classification of Candidate Repository Units at Yucca Mountain, Nye County, Nevada, SAND82-2034, Sandia National Laboratories, Albuquerque, N. Mex.
- Lanigan, D. C., M. L. Cramer, and K. Kim, 1983. "Determination of Rock Mass Deformation Modulus in Closely Jointed Columbia River Basalt," EOS, Transactions American Geophysical Union, Vol. 64, No. 9, p. 87.
- Lappin, A. R., 1980a. Preliminary Thermal Expansion Screening Data for Tuffs, SAND78-1147, Sandia National Laboratories, Albuquerque, N. Mex.
- Lappin, A. R., 1980b. Thermal Conductivity of Silicic Tuffs: Predictive Formalism and Comparisons with Preliminary Experimental Results, SAND80-0769, Sandia National Laboratories, Albuquerque, N. Mex.
- Lappin, A. R., and F. B. Nimick, 1985a. Bulk and Thermal Properties of the Functional Tuffaceous Beds in Holes USW G-1, UE-25a 1, and USW G-2, Yucca Mountain, Nevada, SAND82-1434, Sandia National Laboratories, Albuquerque, N. Mex.
- Lappin, A. R., and F. B. Nimick, 1985b. Thermal Properties of the Grouse Canyon Member of the Belted Range Tuff and of Tunnel Bed 5, G-Tunnel, Nevada Test Site, SAND82-2203, Sandia National Laboratories, Albuquerque, N. Mex.
- Lappin, A. R., R. K. Thomas, and D. F. McVey, 1981. Eleana Near-Surface Heater Experiment Final Report, SAND80-2137, Sandia National Laboratories, Albuquerque, N. Mex.

## CONSULTATION DRAFT

- Lappin, A. R., R. G. VanBuskirk, D. O. Enniss, S. W. Butters, F. M. Prater, C. B. Muller, and J. L. Bergosh, 1982. Thermal Conductivity, Bulk Properties, and Thermal Stratigraphy of Silicic Tuffs from the Upper Portion of Hole USW-G1, Yucca Mountain, Nye County, Nevada, SAND81-1873, Sandia National Laboratories, Albuquerque, N. Mex.
- Leeman, E. R., 1964. "The Measurement of Stress in Rock. Part II: Borehole Rock Stress Measuring Instruments," Journal of the South African Institute of Mining and Metallurgy, pp. 82-114.
- McWilliams, J. R., 1966. "The Role of Microstructure in the Physical Properties of Rocks," Testing Techniques for Rock Mechanics, ASTM STP 402, American Society for Testing and Materials, pp. 175-189.
- Miller, C. H., 1976. A Method for Stress Determination in N, E, and T Tunnels, Nevada Test Site, by Hydraulic Fracturing, with a Comparison of Overcoring Methods, USGS-474-222, U.S. Geological Survey, Denver, Colo.
- Mondy, L. A., R. K. Wilson, and N. E. Bixler, 1983. Comparison of Waste Emplacement Configurations for a Nuclear Waste Repository in Tuff, IV. Thermo-Hydrological Analysis, SAND83-0757, Sandia National Laboratories, Albuquerque, N. Mex.
- Montan D. N., and W. E. Bradkin, 1984. Heater Test 1, Climax Stock Granite, Nevada, UCRL-53496, Lawrence Livermore National Laboratory, Livermore, Calif.
- Montazer, P., and W. E. Wilson, 1984. Conceptual Hydrologic Model of Flow in the Unsaturated Zone, Yucca Mountain, Nevada, USGS-WRI-84-4345, Water-Resources Investigations Report, U.S. Geological Survey, Lakewood, Colo.
- Morrow, C., and J. Byerlee, 1984. "Frictional Sliding and Fracture Behavior of Some Nevada Test Site Tuffs," Rock Mechanics in Productivity and Protection, Proceedings of the 25th Symposium on Rock Mechanics, Evanston, Illinois, June 25-27, 1984, Chapter 49, pp. 467-474.

CONSULTATION DRAFT

- Morrow, C. A., L. Q. Shi, and J. D. Byerlee, 1982. "Strain Hardening and Strength of Clay-Rich Fault Gouges," Journal of Geophysical Research, Vol. 87, No. B8, pp. 6771-6780.
- Moss, M., J. A. Koski, and G. M. Haseman, 1982a. Measurement of Thermal Conductivity by the Comparative Method, SAND82-0109, Sandia National Laboratories, Albuquerque, N. Mex.
- Moss, M., J. A. Koski, G. M. Haseman, and T. V. Tormey, 1982b. The Effects of Composition, Porosity, Bedding Plane Orientation, Water Content, and a Joint on the Thermal Conductivity of Tuff, SAND82-1164, Sandia National Laboratories, Albuquerque, N. Mex.
- NRC (U.S. Nuclear Regulatory Commission), 1987. Standard Format and Content of Site Characterization Plans for High-Level-Waste Geological Repositories, Regulatory Guide 4.17, Washington, D.C.
- Neal, J. T., 1985. Location Recommendation for Surface Facilities for the Prospective Yucca Mountain Waste Repository, SAND84-2015, Sandia National Laboratories, Albuquerque, N. Mex.
- Nelson, P. H., and R. Rachiele, 1982. "Water Migration Induced by Thermal Loading of a Granitic Rock Mass," International Journal of Rock Mechanics, Mineral Sciences and Geomechanical Abstracts, Vol. 19, No. 6, pp. 353-359.
- Nimick, F. B. (comp.), 1987. Technical Correspondence in Support of the Site Characterization Plan, SAND87-0115, Sandia National Laboratories, Albuquerque, N. Mex.
- Nimick, F. B., and A. R. Lappin, 1985. Thermal Conductivity of Silicic Tuffs from Yucca Mountain and Rainier Mesa, Nye County, Nevada, SAND83-1711/1J, Sandia National Laboratories, Albuquerque, N. Mex.
- Nimick, F. B., and B. M. Schwartz, 1987. Bulk, Thermal, and Mechanical Properties of the Topopah Spring Member of the Paintbrush Tuff, Yucca Mountain, Nevada, SAND85-0762, Sandia National Laboratories, Albuquerque, N. Mex.

- Nimick, F. B., R. H. Price, R. G. Van Buskirk, and J. R. Goodell, 1985. Uniaxial and Triaxial Compression Test Series on Topopah Spring Tuff from USW G-4, Yucca Mountain, Nevada, SAND84-1101, Sandia National Laboratories, Albuquerque, N. Mex.
- Nishida, T., 1982. "Excavation of an Inclined Tunnel by Tunnel-Boring Machine," Tunnelling '82, M. J. Jones (ed.), pp. 145-152.
- Olsson, W. A., 1982. Effects of Elevated Temperature and Pore Pressure on the Mechanical Behavior of Bullfrog Tuff, SAND81-1664, Sandia National Laboratories, Albuquerque, N. Mex.
- Olsson, W. A., 1987. Rock Joint Compliance Studies, SAND86-0177, Sandia National Laboratories, Albuquerque, N. Mex.
- Olsson, W. A., and A. K. Jones, 1980. Rock Mechanics Properties of Volcanic Tuffs from the Nevada Test Site, SAND80-1453, Sandia National Laboratories, Albuquerque, N. Mex.
- Ortiz, T. S., R. L. Williams, F. B. Nimick, B. C. Whittet, and D. L. South, 1985. A Three-Dimensional Model of Reference Thermal/Mechanical and Hydrological Stratigraphy at Yucca Mountain, Southern Nevada, SAND84-1076, Sandia National Laboratories, Albuquerque, N. Mex.
- Paterson, M. S., 1978. Experimental Rock Deformation - The Brittle Field, Springer-Verlag, New York, pp. 90-92, 99-111.
- Patton, F. D., 1966. "Multiple Modes of Shear Failure in Rock," Proceedings of the First Congress of the International Society of Rock Mechanics, pp. 509-513.
- Pratt, H. R., A. D. Black, W. S. Brown, and W. F. Brace, 1972. "The Effect of Specimen Size on the Mechanical Properties of Unjointed Diorite," International Journal of Rock Mechanics and Mining Science, Vol. 9, pp. 513-529.
- Price, R. H., 1983. Analysis of Rock Mechanics Properties of Volcanic Tuff Units from Yucca Mountain, Nevada Test Site, SAND82-1315, Sandia National Laboratories, Albuquerque, N. Mex.

CONSULTATION DRAFT

- Price, R. H., 1986. Effects of Sample Size on the Mechanical Behavior of Topopah Spring Tuff, SAND85-0709, Sandia National Laboratories, Albuquerque, N. Mex.
- Price, R. H., and S. J. Bauer, 1985. "Analysis of the Elastic and Strength Properties of Yucca Mountain Tuff, Nevada," Proceedings of the 26th U.S. Symposium on Rock Mechanics, pp. 89-96.
- Price, R. H., and A. K. Jones, 1982. Uniaxial and Triaxial Compression Test Series on Calico Hills Tuff, SAND82-1314, Sandia National Laboratories, Albuquerque, N. Mex.
- Price, R. H., and K. G. Nimick, 1982. Uniaxial Compression Test Series on Tram Tuff, SAND82-1055, Sandia National Laboratories, Albuquerque, N. Mex.
- Price, R. H., A. K. Jones, and K. G. Nimick, 1982a. Uniaxial Compression Test Series on Bullfrog Tuff, SAND82-0481, Sandia National Laboratories, Albuquerque, N. Mex.
- Price, R. H., K. G. Nimick, and J. A. Zirzow, 1982b. Uniaxial and Triaxial Compression Test Series on Topopah Spring Tuff, SAND82-1723, Sandia National Laboratories, Albuquerque, N. Mex.
- Price, R. H., S. J. Spence, and A. K. Jones, 1984. Uniaxial Compression Test Series on Topopah Spring Tuff from USW GU-3, Yucca Mountain, Southern Nevada, SAND83-1646, Sandia National Laboratories, Albuquerque, N. Mex.
- Price, R. H., F. B. Nimick, J. R. Connolly, K. Keil, B. M. Schwartz, and S. J. Spence, 1985. Preliminary Characterization of the Petrologic, Bulk, and Mechanical Properties of a Lithophysal Zone Within the Topopah Spring Member of the Paintbrush Tuff, SAND84-0860, Sandia National Laboratories, Albuquerque, N. Mex.
- Price, R. H., J. R. Connolly, and K. Keil, 1987. Petrologic and Mechanical Properties of Outcrop Samples of the Welded, Devitrified Topopah Spring Member of the Paintbrush Tuff, SAND86-1131, Sandia National Laboratories, Albuquerque, N. Mex.

CONSULTATION DRAFT

- Pruess, K., Y. W. Tsang, and J. S. Y. Wang, 1984. Numerical Studies of Fluid and Heat Flow Near High-Level Nuclear Waste Packages Emplaced in Partially Saturated Fractured Tuff, LBL-18552, Lawrence Berkeley Laboratory, Berkeley, Calif.
- Richardson, A. M., W. Hustrulid, S. Brown, and W. Ubbes, 1985. "In-Situ Load-Deformation Characterization of the CSM/OCRD Jointed Test Block," Proceedings of the 26th U.S. Symposium on Rock Mechanics, Rapid City, South Dakota, June 26-28, 1985, pp. 777-784.
- Rocha, M., 1970. "New Techniques in Deformability Testing of In Situ Rock Masses," Determination of the In-Situ Modulus of Deformation of Rock, ASTM, ASTM STP 477, American Society for Testing and Materials, Philadelphia, Penn., pp. 39-57.
- Scott, R. B. and M. Castellanos, 1984. Stratigraphic and Structural Relations of Volcanic Rocks in Drill Holes USW GU-3 and USW G-3, Yucca Mountain, Nye County, Nevada, USGS-OFR-84-491, Open-File Report, U.S. Geological Survey, Denver, Colo.
- Shimamoto, T., and J. M. Logan, 1981. "Effects of Simulated Clay Gouges on the Sliding Behavior of Tennessee Sandstone," Tectonophysics, Vol. 75, pp. 243-255.
- Smith, C., W. C. Vollendorf, and W. E. Warren, 1981. In-Situ Stress from Hydraulic Fracture Measurements in G-Tunnel, Nevada Test Site, SAND80-1138, Sandia National Laboratories, Albuquerque, N. Mex.
- Somerton, W. H., 1982. "Porous Rock-Fluid Systems at Elevated Temperatures and Pressures," Recent Trends in Hydrogeology, T. N. Narasimhan (ed.), Geological Society of America Special Paper 189, pp. 183-197.
- Spengler, R. W., and M. P. Chornack, 1984. Stratigraphic and Structural Characteristics of Volcanic Rocks in Core Hole USW G-4, Yucca Mountain, Nye County, Nevada, with a section on geophysical logs by D. C. Muller and J. E. Kibler, USGS-OFR-84-789, Open-File Report, U.S. Geological Survey, Denver, Colo.

CONSULTATION DRAFT

- Springer, J. E., R. K. Thorpe, and H. L. McKague, 1984. Borehole Elongation and Its Relation to Tectonic Stress at the Nevada Test Site, UCRL-53528, Lawrence Livermore National Laboratory, Livermore, Calif.
- Stock, J. M., J. H. Healy, and S. H. Hickman, 1984. Report on Televiwer Log and Stress Measurements in Core Hole USW G-2, Nevada Test Site, October-November 1982, USGS-OFR-84-172, U.S. Geological Survey, Menlo Park, Calif.
- Stock, J. M., J. H. Healy, S. H. Hickman, and M. D. Zoback, 1985. "Hydraulic Fracturing Stress Measurements at Yucca Mountain, Nevada, and Relationship to the Regional Stress Field," Journal of Geophysical Research, Vol. 90, No. B10, pp. 8691-8706.
- Sun, Z., C. Gerrard, and O. Stephansson, 1985. "Rock Joint Compliance Tests for Compression and Shear Loads," International Journal of Rock Mechanics, Mining Science, and Geomechanical Abstracts, Vol. 22, No. 4, pp. 197-213.
- Svanholm, B. O., P. A. Persson, and B. Larsson, 1977. "Smooth Blasting for Reliable Underground Openings," Proceedings of the First International Symposium Storage in Excavated Rock Caverns, Stockholm, 5-8 September 1977, M. Bergman (ed.), Vol. 3, pp. 573-579.
- Swolfs, H. S., and W. Z. Savage, 1985. "Topography, Stresses, and Stability at Yucca Mountain, Nevada," Proceedings of the 26th Symposium on Rock Mechanics, Rapid City, S.D., pp. 1121-1129.
- Teufel, L. W., 1981. Frictional Properties of Jointed Welded Tuff, SAND81-0212, Sandia National Laboratories, Albuquerque, N. Mex.
- Teufel, L. W., and J. M. Logan, 1978. "Effect of Displacement Rate on the Real Area of Contact and Temperatures Generated During Frictional Sliding of Tennessee Sandstone," Pageoph (Pure and Applied Geophysics), Vol. 116, pp. 840-865.
- Thomas, R. K., 1982. A Continuum Description for Jointed Media, SAND81-2615, Sandia National Laboratories, Albuquerque, N. Mex.

CONSULTATION DRAFT

- Tibbs, H., 1985. Letter from H. Tibbs (F&S) to J. J. D'Lugosz (DOE/NVO), September 23, 1985; regarding mining experience through faulted welded tuff beds in U12G Tunnel "Rock Mechanics" drift.
- Tillerson, J. R., and F. B. Nimick, 1984. Geoengineering Properties of Potential Repository Units at Yucca Mountain, Southern Nevada, SAND84-0221, Sandia National Laboratories, Albuquerque, N. Mex.
- Tyler, L. D., and W. C. Vollendorf, 1975. Physical Observations and Mapping of Cracks Resulting from Hydraulic Fracturing In Situ Stress Measurements, Paper SPE-5542, Society of Petroleum Engineers of American Institute of Mechanical Engineers, Dallas, Tex.
- USGS (U.S. Geological Survey) (comp.), 1984. A Summary of Geologic Studies through January 1, 1983, of a Potential High-Level Radioactive Waste Repository Site at Yucca Mountain, Southern Nye County, Nevada, USGS-OFR-84-792, Open-File Report, U.S. Geological Survey, Menlo Park, Calif.
- Van Buskirk, R., D. Enniss, and J. Schutz, 1985. "Measurement of Thermal Conductivity and Thermal Expansion at Elevated Temperatures and Pressures," Measurement of Rock Properties at Elevated Pressures and Temperatures, H. J. Pincus and E. R. Hoskins (eds.), ASTM STP 869, American Society for Testing and Materials, pp. 108-127.
- Warpinski, N. R., D. A. Northrop, R. A. Schmidt, W. C. Vollendorf, and S. J. Finley, 1981. The Formation Interface Fracturing Experiment: An In Situ Investigation of Hydraulic Fracture Behavior Near a Material Property Interface, SAND81-0938, Sandia National Laboratories, Albuquerque, N. Mex.
- Waters, A. C., and P. R. Carroll (eds.) 1981. Preliminary Stratigraphic and Petrologic Characterization of Core Samples from USW-G1, Yucca Mountain, Nevada, LA-8840-MS, Los Alamos National Laboratory, Los Alamos, N. Mex.
- Zimmerman, R. M., 1983. "First Phase of Small Diameter Heater Experiments in Tuff," in Proceedings of the 24th U.S. Symposium on Rock Mechanics, June 1983, pp. 271-282.

## CONSULTATION DRAFT

Zimmerman, R. M., and W. C. Vollendorf, 1982. Geotechnical Field Measurements, G-Tunnel, Nevada Test Site, SAND81-1971, Sandia National Laboratories, Albuquerque, N. Mex.

Zimmerman, R. M., M. P. Board, E. L. Hardin, and M. D. Voegele, 1984a. "Ambient Temperature Testing of the G-Tunnel Heated Block," Proceedings of the 25th U.S. Rock Mechanics Symposium, 1984, Northwest University Society of Mining Engineers, pp. 281-295.

Zimmerman, R. M., F. B. Nimick, and M. P. Board, 1984b. "Geoengineering Characterization of Welded Tuffs from Laboratory and Field Investigations," Proceedings of the Material Resources Society Annual Meeting, Boston, Massachusetts, November, 1984.

Zimmerman, R. M., M. L. Wilson, M. P. Board, M. E. Hall, and R. L. Schuch, 1985. "Thermal Cycle Testing of the G-Tunnel Heated Block," Proceedings of the 26th U.S. Symposium on Rock Mechanics, Rapid City, S.D., E. Ashworth (ed.), A. A. Balkema, Boston, Mass., pp. 749-758.

Zimmerman, R. M., R. L. Schuch, D. S. Mason, M. L. Wilson, M. E. Hall, M. P. Board, R. P. Bellman, M. L. Blanford, 1986. Final Report: G-Tunnel Heated Block Experiment, SAND84-2620, Sandia National Laboratories, Albuquerque, N. Mex.

Zoback, M. L., and M. D. Zoback, 1980. "State of Stress in the Conterminous United States," Journal of Geophysical Research, Vol. 85, No. B11, pp. 6113-6156.

### CODES AND REGULATIONS

10 CFR Part 60 (Code of Federal Regulations), 1987. Title 10, "Energy," Part 60, "Disposal of High-Level Radioactive Wastes in Geologic Repositories," U.S. Government Printing Office, Washington, D.C.

The following number is for OCRWM Records Management purposes only and should not be used when ordering this publication.

Accession Number: NNI.880104.0001